eman ta zabal zazu

Universidad del País Vasco
Euskal Herriko Unibertsitatea

Different approaches to obtain poly(lactic acid) based compounds for semidurable applications

PhD Thesis

Jon Anakabe Onaindia

Donostia-San Sebastián 2017

Thesis supervisors: PhD Aitor Arbelaiz Garmendia

PhD Ane Miren Zaldua Huici

(c)2017 JON ANAKABE ONAINDIA

Eskerrak / Acknowledgements

Hasteko, eskerrik asko Leartiker eta Lea Artibai Ikastetxeko lankide guztiei. Tesia burutzea proposatu zenidaten sasoian norbaitek gaur gauden lekura iritsiko ginela esan izan baligu gehienok ez genuke sineztu izango. Baina hemen gaude. Eta irrikaz nago nora arte helduko garen jakiteko ta batez be bide hori elkarrekin egiteko. Eskerrik asko zuen pazientziagatik, kanpoan egonaldiak egin eta tesian zentratzeko astia erraztu izanagatik, eta beti aurrera egiteko indarrak ematearren. Tesi hau, azken urteotan eman ditugun pauso handien artean beste pausotxu bat izan daitela.

Eskerrik asko Joana Kano eta Maite Intxaustiri, master ikasketak eta tesiaren lehen pausu haietan zuen laguntasuna eta babesa oso garrantzitsua izan zelako niretzat.

Eskertu nahi ditut baita ere Arantxa Eceiza eta berak zuzentzen duen "Materiale + Teknologia" (EHU-UPV, Donostia) ikerketa taldeko kide guztiak. Baita Material Berriztagarrien Ingeniaritza Masterra burutzean ikaskide izan nituen lagunak ere, orduan lortu baitnuen benetan tesian egin nahi nuena zehaztea.

Eskerrik asko baita Teresa Guraya eta berak zuzentzen duen EMERG (EHU-UPV, Bilbao) taldeko kideei, batez ere Maider Iturrondobeitia eta Julen Ibarretxeri. Zuengandik jasotako hurbiltasuna eta laguntzarako jarrera asko estimatzen dizuet.

I would also like to thank Proffesor Luc Avérous for his kindness from the very first time we met and his attitude when I showed my interest to make a stage in the ICPEES at the University of Strasbourg. It was a great pleasure to meet all the researches, share experiences with them and to spend 4 months in such a beautiful city. Thanks to all the people in the team, specially to Marie Reulier, Patricia Chavez, Thierry Dintzer, Thibaud Debuissy, Salima Nedjari and Amparo Quero, merci beaucoup pour tout!!

Esker bereziak eman nahi dizkiet tesi honetako lana zuzentzen, burutzen, idazten, argitaratzen eta neke gabe ni laguntzen aritu zareten Ane Miren Zaldua eta Aitor Arbelaizi. Zuen irizpide kritikorako gaitasuna eta behar izan zaituztedan bakoitzean jasotako erantzun azkar eta motibatzailea izan dira tesi honen ardatza neretzako. Zuekin batera eskertu nahi nuke ezagutu nuen unetik bidea erraztu, Masterrerako ateak ireki eta tesiaren lehen urtean gidatu ninduen Iñaki Mondragon zena. Faltan zaitugu Iñaki; zuk irekitako bideak aurrera darrai. Eskerrik asko hiruoi zuen laguntza ezinbestekoa izan delako tesi hau bukaeraraino burutu ahal izateko.

Eskerrik asko familia, bikote eta lagun guztioi beti nire ondoan zaudetelako. Oso kontziente naiz inguratzen nauen aberastasunaz. Mosu erraldoi berezi bana betidanik nire bizi-erreferentzia eta “itsasargi” ditudan bi arreba zoragarriei.

Azkenik, ilusio handia egiten dit gurasoak eskertzeko aukera hau izateak, eta aldi berean lan honen ekarpen umila beraiei eskaintzeak. Eskerrik asko aita ta ama, lan hau zuena ere bada.

Marije Onaindia eta Jeronimo Anakaberi.

Ulertu beharrik gabe nigan sinesteko ahalmena duzuelako.

Laburpena

1.1.Sarrera

XX. mende hasierarekin batera baliabide fosilen erabilera neurrigabea hasi zen elektrizitatea, beroa eta garraiorako erregaiak ekoizteko eta baita produktu kimikoak sintetizatzeko ere. Tamalez, ustiapen horrek gogor eragin du baliabide fosilen agortzean eta ingurumenean arazo larriak sortu ditu, mundu mailako berotze orokorra kasu. Ondorioz, petrolioa bezalako karbono zaharrean oinarritzen diren hornidurak biomasako iturri berriztagarriez ordezkatzea XXI. mendeko gizartearen jasangarritasuna bermatzeko gakoa bihurtu da. Produktu kimikoak ekoizteko gaur egungo prozesaketa sistemak oso eraginkorrak bihurtu dira hamarkada ugaritan burututako inbertsioen ondorioz. Beraz, arrakastatsu izateko, prozesaketa biologiko berriek epe laburrean berdindu beharko lituzkete pareko eraginkortasun eta produktibitate mailak. Ingurumena zaintzeko politika berriek eta teknologiaren garapenek biomasaren erabilpena eta metodo biologikoen aplikazioa bideragarri ezezik oso erakargarri bihurtu dituzte [1].

Polimero termoplastikoak erabilera anitzekoak dira, mundu osora hedatuta daude eta inguratzen gaituen alor ia guztietan aurkitzen dituzte erabilpenak. Honen arrazoiak, batik bat, ondorengoak dira: prezio baxua, dentsitate baxua izatea (energia aurreztea), tenperatura baxuetan prozesagarriak izatea eta berez dituzten propietateak kasuko aplikazioei egokitzeko bideragarritasuna. Egungo gizartea eta bizi kalitatea ezinezkoak lirateke kontsumo altuko produktuak plastikoz eginak ez baleude. 1950etik 2010era urtean 1.65 milioi tona erabiltzetik 255.5 milioi tona kontsumitzera pasatu gara, eta are gehiago, plastikoen erabilpenak urtero % 3-4ko igoera jasango duela espero da ondorengo urteotan [2]. Honekin lotuta, India eta Txina bezalako lurralde biztanletsuek jasandako industrializazio azkarrak ekoiztutako material plastikoen bolumenaren haztea bizkortzea eragin du. Dena den, petroliotik eratorritako plastikoen karbono oinatz maila altuak eragin zuzena du mundu mailan gertatzen ari den berotze orokorrean. Plastikoen erabilerak dakarren arazo hau aurrez ezagunak ziren zabortegi eta itsasoko kutsadurari gehitu zaie.

Testuinguru honetan, egungo plastikoek baino karbono oinatz maila baxuagoa duten plastikoen ekoizpenak interesa sortu izan du 80. hamarkadaz geroztik. Beraz, iturri berriztagarrietatik ekoitzi daitezkeen edo/eta izaera biodegradagarria duten plastikoak sakonki ikertuak izan dira berauen propietateak hobetzeko asmoz, egungo plastiko petrokimikoen alternatiba bideragarri bezala aurkezteko helburuarekin. Honela polilaktida (PLA edota poli(azido laktikoa)) etorkizun oparoko biopolimero bezala identifikatu da. Dena den, 1932an Carothers-ek lehenengoz ekoiztu eta bigarren mundu gudaren ostean DuPont enpresak garatu zuen arren, plastiko honen erabilpenak medikuntzarako sutura-hari bioabsorbagarrietara murriztu ziren 80. hamarkada arte. 1989an Cargill familiak PLA-ren potentzialean sinetsi eta beronen ekoizpen industriala eta komertzializazioaren alde apustu egin zuen. PLA iturri berriztagarrietatik ekoiztu ahal izateak eta izaera konpostagarria izateak bizi-zikloa ixtea ahalbidetu zuen.

Hala ere,PLA-k aurkezten duen hauskortasunak eta erresistentzia termomekaniko baxuak bizi iraupen ertain eta luzeko aplikazioetan PLA erabili ahal izatea sakon mugatu du.

1.2.Tesiaren helburua

Tesi honen helburua PLA-ren propietate mugatzaileak gainditu ditzaketen formulazio berriak garatu eta aztertzea izan da. Lortutako formulazioen bizi-iraupena aurreikusi da,

iraupen ertain eta luzeko aplikazioetan formulazio berriak erabili ahal daitezkeen estimatzeko.

1.3.Tesiaren estruktura

Tesi hau idazteko orduan ondorengo estruktura jarraitu da. Tesiaren aurreneko atalean motibazio eta helburuak definitu dira eta 2. atalean berrikuspen bibliografiko zabala burutu da.

3. Atalean PLA eta PMMA-z burututako nahasketa fisiko eta erreaktiboak aztertu dira. Polimetil metakrilatoa (PMMA) propietate fisiko eta kimiko onak dituen polimero sintetikoa da. Literatura zientifiko gutxi dago PLA/PMMA nahasketei buruz eta gehiengoa disoluzio bidez prestatutako nahasketetan oinarritzen da [3–7]. Dena den, egoera urtuan prestatutako PLA/PMMA nahasketei buruz bi lan ere aurki daitezke, baina bietan adierazten diren emaitzak kontrajarriak dirudite. Samuel-ek extrusio bidez prestatutako PLA/PMMA nahasketak nahaskorrak zirela ikusi zuen [8]. Aldiz, prozesaketa era berdina erabiliz Le et al. ikertzaileek sistema ez-nahaskorra eta ko-jarraiak diren faseak identifikatu zituzten SEM bidez. [9] 3. atalean bi torlojuko extrusorea erabiliz prestatutako PLA/PMMA nahasketa ezberdinen prestaketa eta karakterizazioa azaltzen da, literaturan ageri diren beste ikerketekin alderatzeaz gain. PLA eta PMMA proportzio ezberdinetan nahastu ostean, sistema hauen fase estruktura, morfologia, propietate termikoak eta propietate mekanikoak aztertu ziren. Talde kontribuzio metodoa Small eta Van Krevelen-ek proposatutako bi metodoen arabera aplikatuz, prestatutako nahasketen solubilitate parametroak kalkulatu ziren. Datu hauekin, Flory-Huggins interakzio parametroaren estimazioa burutu zen ondoren. Informazio teoriko eta esperimentala bateratuz, nahaskortasuna, fase estruktura eta propietateen arteko erlazioa bilatzeko azterketa egin zen.

PLA/PMMA sistemen nahaskortasuna prozesaketa metodo eta parametroen (tenperatura eta torlojuen bira abiadura) menpekoa eta polimeroen pisu molekularraren araberakoa dela ondorioztatu zen. DSC eta DMA emaitzetan lortutako beira trantsizio tenperatura sistemaren konposizioarekiko aldatzen dela ikusi zen, bi polimeroen molekulen arteko elkarreragina iradokiz eta nahasgarritasun partziala adieraziz. SEM bidezko mikrografiek bi fase bananduren existentzia erakutsi zuten, kasu guztietan 400 nm baino txikiagoak ziren dispertsaturiko fasea fase jarraian homogeneoki banatuak agertzen zirelarik. Beraz, gure lanean erabilitako PLA eta PMMA graduak ez dira guztiz nahasgarriak guk erabilitako

nahaste baldintzetan behinik behin. Nahasketa ezberdinen beira trantsizio tenperaturaren eboluzioa Gordon-Taylor ekuazioarekin zuzen doitu zen k=0.24 balioa aplikatuz, honek PLA eta PMMA-ren arteko interakzioa ahula dela iradoki zuelarik. FTIR bidez lortutako emaitzekin bat zetorren ondorio hau. Flory-Huggins interakzio parametroari dagokionez, estimatutako baloreek PLA/PMMA sistemek nahasgarriak izan behar luketela adierazi zuten, ikuspuntu termodinamikotik behinik behin. Dena den, PLA/PMMA sistemen nahasketa difusio mailaren araberako prozesua zela zirudien. Hots, nahasketa baldintzen arabera eta aukeratutako polimero graduen pisu molekularraren arabera guztiz edo partzialki nahaskorrak diren nahasketak lor daitezkeela. Propietate makromekanikoei dagokienez, nahasketa bakoitzean gehiengoa suposatzen zuen materialaren antzeko talka erresistentzia erakutsi zuten. PMMA-ren presentzia %50etik gorako zuten nahasketek beste nahasketek baino talka erresistentzi hobea erakutsi zuten, fase inbertsioaren ondorioz, ziurrenik.

Aztertutako nahasketen artean, PLA/PMMA 80/20 (%et) nahasketak egonkortasun termiko, trakzio erresistentzi eta modulu elastikorik altuena erakutsi zuen. Dena den, talka erresistentzia baxua eta interfase atxikidura urria ikusi ziren sisteman ageri ziren fase bien artean. Horregatik, poli(estireno-co-glizidil metakrilatoa) (P(S-co-GMA)) kopolimero erreaktiboak nahasketa honen erreologia, fase morfologia, egonkortasun termikoa, propietate mekanikoak eta talka erresistentzian duen eragina aztertu zen. Izan ere, epoxi taldedun sustantziekin prozesaketa erreaktiboa burutzeak PLA-n oinarritutako sistema batzuen bateragarritasuna hobetzen duela aurrez argitaratua izan da [10,11]. PLAren kate-bukaerako karboxilo eta hidroxilo taldeek epoxiarekin erreakzionatzeak polimero kateen adarkatzea eta ondorioz propietate mekaniko batzuen hobetzea eragin dezake [12,13]. Gainera, glizidil metakrilatoan oinarritutako kopolimeroak sistema ez-nahaskorren interfase atxikidura hobetzeko bateratzaile erreaktibo bezala erabiliak izan dira aurrez, esaterako PLA/PCL [14], PLA/ABS [15], PLA/SEBS [16], PLA/PBSA [17] sistemetan. Poli(estireno-co-glizidil metakrilatoa)ren erabilera aztertutako sistemaren hauskortasuna hobetzeko bide aparta zela ikusi zen, trakzio erresistentzia eta moduluan galerarik pairatu gabe. Nahasketa fisikoen antzera, bi fase ageri ziren SEM-eko emaitzetan. Baina kopolimero erreaktiboaren gehitzeak interfase atxikimendua hobetzen zuela agerikoa zen, sistemaren elongazio gaitasuna eta talka erresistentzia izugarri hobetuz. PLA/PMMA sistemari 3pph kopolimero gehitu ostean hauste deformazioa %1300 eta talka erresistentzia %60 altuagoak ziren, PLA hutsarekin alderatuz, beti ere trakzio erresistentzia eta moduluan galerarik gabe. Maila honetako

propietate hobetze orokorrik ez da lortu izan plastifikatzaile edota talka modifikatzaileak PLA-ri gehituz.

4. atalean PLAren kristalizazio zinetika eraldatu da plastifikatzaile eta nukleatzaileak bateraturik erabiliz. Injekzio bidezko moldeaketa polimeroen prozesaketa bide ezagunenetako bat da, batez ere plastikozko produktu iraunkor eta erdi-iraunkorrak ekoizteko. Prozesaketa bide honek injekzio ziklo denbora laburrak behar ditu ekonomikoki bideragarri izateko. Suberaketa edo "annealing" prozesua aurrez egoera amorfoan ekoitzitako produktuak bigarren pausu horretan kristaltzeko aukera bat den arren, prozesu horretan produktuak uzkurtu eta desitxuratu egin daitezke, fase kristalduaren bilakaera medio. Horregatik, tesiaren atal honetan azkar kristaltzen duen PLA oinarridun nahasketen ikerketa deskribatzen da, produktu kristalduak suberaketa ekidinez lortzeko bide bat aztertze asmoz. Beste lan batzuek aztertu zuten aurretiaz plastifikatzaile eta nukleatzaileen erabilpen bateratua PLA-n, eta aukera honek kristaltze zinetikan duen eraginaren baliagarritasuna frogatu zuten [18–25]. Dena den, literaturan aurki daitezkeen emaitzak ez dira erraz konparagarriak, pisu molekular eta D-azido laktiko eduki ezberdineko PLA-k ageri baitira ikerketa lan bakoitzean. Lan honetan plastifikatutako %0,5 eta %4 D-azido laktikodun bi PLA ezberdinen kristalizazio isotermoa aztertu da, urtze tenperaturatik kristaltze tenperatura ezberdinetara hoztu ostean eta nukleatzaile ezberdinak erabiliz. Plastifikatzaile modura dioctil adipatoa erabili da (DOA), PLA-rentzat plastifikatzaile eraginkorra dela frogatu dena [26]. Plastifikatutako PLA matrizeak talkoa, etilen bis(estearamida) EBS eta PDLA-rekin nukleatu dira. Emaitzen arabera, plastifikatzaile eta nukleatzaileen erabilera bateratua PLAren kristaltze zinetika azkartzeko oso bide eraginkorra dela frogatu da. L-azido laktiko kontzentrazio altuena zuen PLA-k kristaltze zinetika azkarrenak erakutsi zituen. Beraz, korrelazio handiagoa frogatu zen kristaltze zinetika eta L-azido laktiko kontzentrazioaren artean nukleatzaile edo tenperaturarekiko baino. Nukleatzaileen artean eraginkorrena talkoa izan zen. Talkoz nukleatutako L-azido laktiko eduki altuena zuen PLA plastifikatuak minutu bat baino gutxiagoko erdi-kristaltze denborak aurkeztu zituen, konposatu hauek PLA kristalduzko produktuak prozesatzeko oso interesgarri direla frogatuz. Halaber, presioa igotzeak kristaltze abiadura nabarmen igotzen duela ikusi zen PVT saiakeretan. Ondorioz, injekzio bidezko moldeaketa kasuetan, DSC bidez lortutako denborak baino are laburragoetan kristalduko lukete nahasketek. Kristaltze abiadura azkarrenak 90 eta 100 ºC bitartean ikusi ziren, edozein nukleatzaile erabilita ere. Avrami berretzailea $n \approx 2.7\text{-}3.0$ ingurukoa zen nahasketa guztietan, nukleatzailea eta kristaltze tenperatura edozein izanda

ere, esferuliten hazkuntza tridimentsionala iradokiz. WAXS difraktogramek α eta α' kristal formen koexistentzia agerian jarri zuten. Aztertutako parametro ezberdinen artean fusio tenperatura altuenarengan L-azido laktikoaren purutasunak bakarrik eragiten duela ikusi zen. Aldiz, lortutako kristaltze mailan eta batez ere fusio tenperatura baxuenarengan aukeratutako kristaltze tenperatura eta nukleatzaile motak nabarmenki eragiten du.

5. atalean PLA-n oinarritutako nahasketen bizi-iraupenaren estimazioa burutu da. PLA-n oinarritutako nahasketen erabilpena zehazteko beharrezkoa da material hauen zahartzea aztertzea beronen propietateetan eragin zuzena duelako. Iraunkortasunari dagokionez, PLAren portaera zahartze mekanismo ugariren menpe dago [27–31]. Gainera, orokorrean mekanismo ezberdinak aldi berean pairatzen ditu materialak, degradazio mekanismo konplexuak eraginez [32]. Bizi-iraupen aurreikuspenek zahartze bizkortuak burutzea eskatzen dute. Zahartze tenperatura ezberdinetara lortutako emaitzekin denbora-tenperatura gainjartzeak burutu daitezke, eta horretarako ISO 2578 [33] jarraibidea errespetatu da tesi lan honetan. Arau honen helburua plastikoen erresistentzia termikoaren mugak zehaztea da eta metodoa trakzio erresistentzia edo hauste deformazio baloreak zuzenean Arrhenius erako ekuazioetara zuzenean doitzean oinarritzen da. Lehenengo, zahartze tenperatura bakoitzeko, hautatutako propietatearen balioa denboraren logaritmoaren aurka grafikatzen behar da. Arauan azaltzen diren gomendapenei jarraiki, gure kasuan propietate bakoitzean hasierako balioaren %50era erortzea hautatu genuen bukaera irizpide legez. Puntu hauek zahartze tenperatura bakoitzean hauste denborak zehazten dituzte.

Atal honetan aurreko ataletan garatutako bi nahasketaren bizi-iraupena aurreikusi nahi izan da. Bi materialen laginei, aurrez tenperatura ezberdinetan zahartutakoak, trakzio saiakerak burutu zitzaizkien giro tenperaturan. Honela, zahartzearen eragina neurtu ahal izan zen propietate mekanikoetan.

Lortutako emaitzen arabera ondoriozta daiteke formulazio hauek ez direla aproposak aplikazio iraunkor estrukturaletarako, esaterako automozio edota etxetresna elektrikoetarako, 8-12 urteko bizi-iraupena bermatu beharra dagoelako. Ostera, erabilgarriak dirudite mugikorren karkasa, ordenagailuen teklatua eta era honetako aplikazio erdi-iraunkorretarako, 3-4 urteko bizi-iraupena duten produktuak ekoizteko alegia. Kasu hauetan PLA/PMMA nahasketak zahartze egonkortasun hobea izango luke PLA kristalduak baino 60 ºC-tik beherako aplikazioei dagokienez. Aplikazioaren arabera produktuak epe laburrean 60 ºC-tik gorako egoerak pairatu beharko lituzkeen kasuan, bestalde, PLA kristaldua aukera hobea litzake, beira trantsiziotik gora portaera hobea daukalako.

1.4.Erreferentziak

[1] D.R. Dodds, R.A. Gross, Chemicals from Biomass, Science. 318 (2007) 1250–1251. doi:10.1126/science.1146356.

[2] R. Narayan, Carbon footprint of bioplastics using biocarbon content analysis and life-cycle assessment, MRS Bull. 36 (2011) 716–721.

[3] G. Zhang, J. Zhang, S. Wang, D. Shen, Miscibility and phase structure of binary blends of polylactide and poly (methyl methacrylate), J. Polym. Sci. Part B Polym. Phys. 41 (2003) 23–30.

[4] S.-H. Li, E.M. Woo, Immiscibility–miscibility phase transitions in blends of poly (L-lactide) with poly (methyl methacrylate), Polym. Int. 57 (2008) 1242–1251.

[5] J.L. Eguiburu, J.J. Iruin, M.J. Fernandez-Berridi, J. San Roman, Blends of amorphous and crystalline polylactides with poly (methyl methacrylate) and poly (methyl acrylate): a miscibility study, Polymer. 39 (1998) 6891–6897.

[6] S. Hirota, T. Sato, Y. Tominaga, S. Asai, M. Sumita, The effect of high-pressure carbon dioxide treatment on the crystallization behavior and mechanical properties of poly (l-lactic acid)/poly (methyl methacrylate) blends, Polymer. 47 (2006) 3954–3960.

[7] B. Imre, K. Renner, B. Pukánszky, Interactions, structure and properties in poly (lactic acid)/thermoplastic polymer blends, Express Polym. Lett. 8 (2014) 2–14.

[8] C. Samuel, J.-M. Raquez, P. Dubois, PLLA/PMMA blends: A shear-induced miscibility with tunable morphologies and properties?, Polymer. 54 (2013) 3931–3939. doi:10.1016/j.polymer.2013.05.021.

[9] K.-P. Le, R. Lehman, J. Remmert, K. Vanness, P.M.L. Ward, J.D. Idol, Multiphase blends from poly (L-lactide) and poly (methyl mathacrylate), J. Biomater. Sci. Polym. Ed. 17 (2006) 121–137.

[10] S. Sun, M. Zhang, H. Zhang, X. Zhang, Polylactide toughening with epoxy-functionalized grafted acrylonitrile–butadiene–styrene particles, J. Appl. Polym. Sci. 122 (2011) 2992–2999. doi:10.1002/app.34111.

[11] Racha Al-Itry, Abderrahim Maazouz, Improvement in melt strengthening of Poly (lactic acid) through reactive blending with poly (butylene adipate-co-terephthalate) (PBAT) and epoxy-functionalized chains, in: Strassbourg, 2011.

[12] M. Mihai, M.A. Huneault, B.D. Favis, Rheology and extrusion foaming of chain-branched poly (lactic acid), Polym. Eng. Sci. 50 (2010) 629–642.

[13] A. Jaszkiewicz, A.K. Bledzki, R. van der Meer, P. Franciszczak, A. Meljon, How does a chain-extended polylactide behave?: a comprehensive analysis of the material, structural and mechanical properties, Polym. Bull. 71 (2014) 1675–1690.

[14] N.A.I. Wei Kit Chee, Impact Toughness and Ductility Enhancement of Biodegradable Poly(lactic acid)/Poly(ε-caprolactone) Blends via Addition of Glycidyl Methacrylate, Adv. Mater. Sci. Eng. 2013 (2013). doi:10.1155/2013/976373.

[15] M.Y. Jo, Y.J. Ryu, J.H. Ko, J.-S. Yoon, Effects of compatibilizers on the mechanical properties of ABS/PLA composites, J. Appl. Polym. Sci. 125 (2012) E231–E238.

[16] K. Hashima, S. Nishitsuji, T. Inoue, Structure-properties of super-tough PLA alloy with excellent heat resistance, Polymer. 51 (2010) 3934–3939.

[17] V. Ojijo, S.S. Ray, Super toughened biodegradable polylactide blends with non-linear copolymer interfacial architecture obtained via facile in-situ reactive compatibilization, Polymer. 80 (2015) 1–17. doi:10.1016/j.polymer.2015.10.038.

[18] H. Li, M.A. Huneault, Effect of nucleation and plasticization on the crystallization of poly (lactic acid), Polymer. 48 (2007) 6855–6866.

[19] H.W. Xiao, P. Li, X. Ren, T. Jiang, J.-T. Yeh, Isothermal crystallization kinetics and crystal structure of poly (lactic acid): Effect of triphenyl phosphate and talc, J. Appl. Polym. Sci. 118 (2010) 3558–3569.

[20] M. Pluta, Morphology and properties of polylactide modified by thermal treatment, filling with layered silicates and plasticization, Polymer. 45 (2004) 8239–8251.

[21] S. Gumus, G. Ozkoc, A. Aytac, Plasticized and unplasticized PLA/organoclay nanocomposites: Short- and long-term thermal properties, morphology, and nonisothermal crystallization behavior, J. Appl. Polym. Sci. 123 (2012) 2837–2848.

[22] H. Xiao, L. Yang, X. Ren, T. Jiang, J.-T. Yeh, Kinetics and crystal structure of poly (lactic acid) crystallized nonisothermally: effect of plasticizer and nucleating agent, Polym. Compos. 31 (2010) 2057–2068.

[23] G.-X. Zou, Q.-W. Jiao, X. Zhang, C.-X. Zhao, J.-C. Li, Crystallization behavior and morphology of poly (lactic acid) with a novel nucleating agent, J. Appl. Polym. Sci. 132 (2015). http://onlinelibrary.wiley.com/doi/10.1002/app.41367/full (accessed June 9, 2015).

[24] J. You, W. Yu, C. Zhou, Accelerated Crystallization of Poly (lactic acid): Synergistic Effect of Poly (ethylene glycol), Dibenzylidene Sorbitol, and Long-Chain Branching, Ind. Eng. Chem. Res. 53 (2014) 1097–1107.
[25] Y. Li, H. Wu, Y. Wang, L. Liu, L. Han, J. Wu, F. Xiang, Synergistic effects of PEG and MWCNTs on crystallization behavior of PLLA, J. Polym. Sci. Part B Polym. Phys. 48 (2010) 520–528.
[26] M. Murariu, A. Da Silva Ferreira, M. Alexandre, P. Dubois, Polylactide (PLA) designed with desired end-use properties: 1. PLA compositions with low molecular weight ester-like plasticizers and related performances, Polym. Adv. Technol. 19 (2008) 636–646.
[27] Y. Aoyagi, K. Yamashita, Y. Doi, Thermal degradation of poly [(R)-3-hydroxybutyrate], poly [ε-caprolactone], and poly [(S)-lactide], Polym. Degrad. Stab. 76 (2002) 53–59.
[28] F.-D. Kopinke, M. Remmler, K. Mackenzie, M. Möder, O. Wachsen, Thermal decomposition of biodegradable polyesters—II. Poly (lactic acid), Polym. Degrad. Stab. 53 (1996) 329–342.
[29] O. Wachsen, K. Platkowski, K.-H. Reichert, Thermal degradation of poly-L-lactide—studies on kinetics, modelling and melt stabilisation, Polym. Degrad. Stab. 57 (1997) 87–94.
[30] J.D. Badia, E. Strömberg, A. Ribes-Greus, S. Karlsson, Assessing the MALDI-TOF MS sample preparation procedure to analyze the influence of thermo-oxidative ageing and thermo-mechanical degradation on poly (Lactide), Eur. Polym. J. 47 (2011) 1416–1428.
[31] Q. Zhou, M. Xanthos, Nanosize and microsize clay effects on the kinetics of the thermal degradation of polylactides, Polym. Degrad. Stab. 94 (2009) 327–338.
[32] M. Sepe, The Problem of Confounded Mechanisms in Accelerated Testing Protocols, (2015). http://knowledge.ulprospector.com/3262/pe-the-problem-of-confounded-mechanisms-in-accelerated-testing-protocols-presented-by-michael-sepe/.
[33] ISO 2578:1993 - Plastics -- Determination of time-temperature limits after prolonged exposure to heat, ISO. (n.d.). http://www.iso.org/iso/home/store/catalogue_ics/catalogue_detail_ics.htm?csnumber=7547 (accessed June 13, 2016).

Table of Contents

Chapter 1. General introduction

1.1. Motivation

Since the early 20th century fossil resources have been widely used to produce electricity, heat, and transportation fuels, as well as the vast majority of chemicals. Unfortunately, such uses have contributed to the exhaustion of fossil resources and serious environmental problems, as represented by global warming. From this standpoint, the replacement of old-carbon feedstocks like petroleum by renewable sources like biomass to obtain fuels and chemicals has become a key factor to enable the sustainability of the 21st century's society. However, current processes for production of commodity chemicals have evolved through considerable investment during decades to become highly efficient. Thus, in order to be successful, new biological processes must quickly reach similar levels of efficiency and productivity. Supporting policies, evolving technologies and environmental imperatives make the use of biomass and biological methods for industrial chemical production not only feasible but highly attractive from multiple perspectives [1].

Plastic materials are versatile, used worldwide and find applications in all parts of our lives, from agriculture to electronics, medical devices or packaging. From 1.65 million tons in 1950 to 255.5 million tons in 2010 worldwide, plastics usage is still expanding and expected to grow at a steady rate of 3–4% per year [2]. In particular, rapid industrialization in populous countries such as India and China has led to an accelerated rate of plastic materials production. This is because plastics are lightweight (energy saving), low-cost, processable at low temperatures and present unique and versatile properties that can be tailored for specific applications. The current society and the average quality of life would be inconceivable

without the use of plastics for commodity products. However, the elevated carbon footprint levels of the petroleum based plastics has been a matter of debate, specially boosted when the society has become sensitive to their effect on the global warming, besides landfilling and marine contamination problems.

In this context, plastics with lower carbon footprint than the conventional ones have gained a lot of interest from the industry since 1980's decade. The focus has been put on two characteristics: the source and the end of life management of plastics. Thus, plastics that can be obtained from renewable feedstocks and/or with intrinsic biodegradable nature have been extensively studied in order to upgrade them into feasible alternatives to the current petrochemical plastics. Among others, Polylactide (PLA, a.k.a. polylactic acid) was one of the most promising ones from the very beginning. However, even though it was first produced by Carothers in 1932 and further developed by DuPont in after the Second World War, applications for this polymer were limited to resorbable sutures until 1980's. In 1989, the Cargill family believed in the potentiality of PLA and bet for its mass production and commercialization. Its biosourced and compostable nature enabled to close the life cycle loop, thus making PLA a great candidate for short life applications like packaging.

However, two limiting properties have closed the way for semi-durable and durable applications to PLA: its brittleness and low thermal resistance (Fig. 1-1). The improvement of those two properties by different approaches and the lifespan prediction of the resulting compounds have been studied in this PhD thesis.

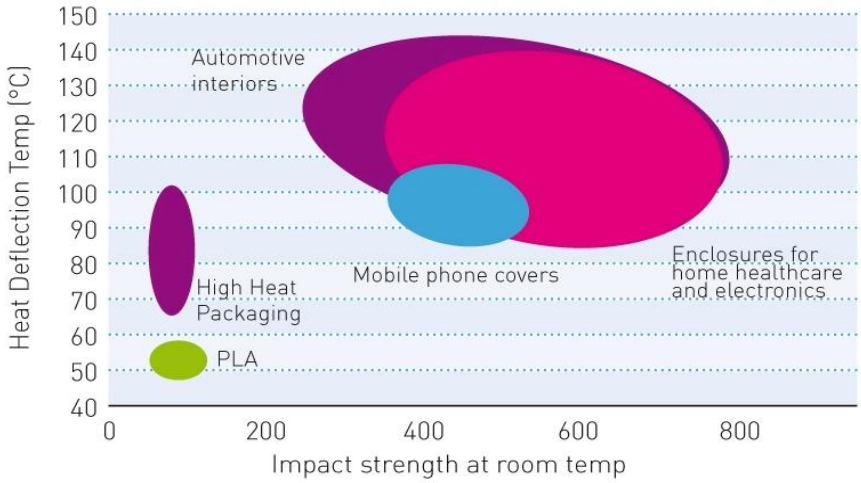

Fig. 1-1. Heat resistance (HDT, ISO 75) and impact strength of amorphous PLA and performance requirements for potential applications [3].

1.2. Aim of the thesis

This thesis aims to expand the current scientific knowledge concerning polylactide and the different approaches which could lead to get over its limiting properties, i.e.: brittleness and thermal resistance; and the measurement of their lifespan in order to evaluate their use in semidurable or durable applications.

1.3. The structure of the thesis

The manuscript of this thesis has been divided into 6 chapters, as follows:

In the first chapter the motivation and the aim of the thesis are defined. On the other hand, the structure of the thesis, the human group behind the work and the entities that have given financial support have been described within this chapter, too.

The second chapter summarizes the state of the art concerning bioplastics, emphasizing on polylactide, its properties, current market, and the different approaches to obtain PLA based compounds with enhanced properties.

The next two chapters focus on the different ways that have been experimentally researched to get over the limiting properties of neat PLA. In the third chapter, blends of PLA with PMMA have been studied at different ratios by twin screw extrusion. Moreover, the properties of the most interesting blend have been subsequently studied by Reactive Extrusion in the presence of a styrenic-glycidyl acrylate copolymer. The fourth chapter encloses a deep study concerning the combinational effect of plasticizer and nucleating agents on the crystallization kinetics of PLAs with different L-lactic acid contents.

The fifth chapter focuses on the lifespan predictions of two of the most interesting compounds developed at the previous chapters. It has been experimentally measured the effect of ageing on the mechanical properties of the compounds, carried out by accelerated ageing at high temperatures.

The sixth chapter contains the general conclusions of the thesis, prospects for future research work and the list of scientific publications and communications arisen from this thesis work.

This thesis work has been carried out in close cooperation of the Materials and Technologies Group of the Basque University (EHU-UPV) and Leartiker S. Coop, both of them entities that are enclosed in the Basque Net of Science, Technology and Innovation (RVCTI). It was first co-conducted by Proff. Iñaki Mondragon and PhD Ane Miren Zaldua. However, after the unexpected and shattering passing of Proff. Mondragon in February 2012, his co-conducting position was assumed by PhD. Aitor Arbelaiz. Besides, a 4 months long stage in the Bioteam group (ICPEES) led by Proff. Luc Avérous of the University of Strasbourg was especially helpful to achieve the goals reported in 0. The Basque Country Government (EJ-GV) in the frame of Consolidated Groups (IT-776-13), SAIOTEK SA-2010/00135, Elkartek 2015 FORPLA3D and Elkartek 2016 PLAPU3D; along with the Regional Government of Bizkaia (BFA-DFB) EXP: 6-13-LA-2013-004 have provided financial support to this PhD thesis.

Chapter 2. Literature review

2.1. Biopolymers

Although the use of fossil fuels such as naphtha and natural gas for producing plastic resins only accounts for about 4 to 5% of the world's oil consumption, there is a growing demand from society to preserve the environment from the effects of excessive use of fossil based fuels and indiscriminate waste disposal, which includes plastics, in order to prevent the devastating predictions of global warming [4]. This concern is in part translated in the form of market demand for eco-friendly products made of renewable raw materials. In this context, considerable efforts have been devoted to develop bio-based substitutes to fossil-based polymers. These bio-based materials have the great advantage of using renewable raw materials and some of them enable composting or anaerobic digestion, hence allowing an end-of-life waste management which would reduce landfilling. Some of these bio-based polymers are already commercialized at large scale.

On the other hand, the issue of the disposal of plastic wastes in the environment stimulated a demand for harmless biodegradable materials. This evolved to the adoption of the recycling concept through mechanical recovery and composting of wastes or energy production by plastic incineration, which directly contribute towards the reduction, in equivalent quantities, of the consumption of fossil raw materials in industry. The focus soon shifted to the production of plastics from renewable sources. However, more recently, proper importance was given to an approach that encompasses the carbon cycle and sustainability, integrating several of these aspects [4].

Thermoplastics can be classified by their origin (raw materials) and end of life behaviour (biodegradability) in a four quadrant scheme (Fig. 2-1). The inferior left quadrant contains the conventional petrochemical plastics, while the superior right presents the bioplastics, those that are bio-based and biodegradable. The word bioplastic has been misleadingly used for marketing reasons during the last two decades, but it is being settled that this word should only be used for plastics which are both bio-based and biodegradable [5]. However, there are another two groups of plastics that, despite not being bioplastics, can fulfil the "green" or "eco-friendly" needs of different industries and market sectors. In the superior left quadrant we can find the bio-based counterparts of the conventional petrochemical plastics, which have identical molecular structure but are produced by renewable feedstocks instead of petrol. These bio-based plastics avoid the influence of petrol price fluctuations and can be interesting for semidurable or durable applications like automotive, household appliances, toys, etc. Finally, in the inferior right quadrant we have biodegradable petrochemical polymers, interesting for applications with short shelf-life like packaging.

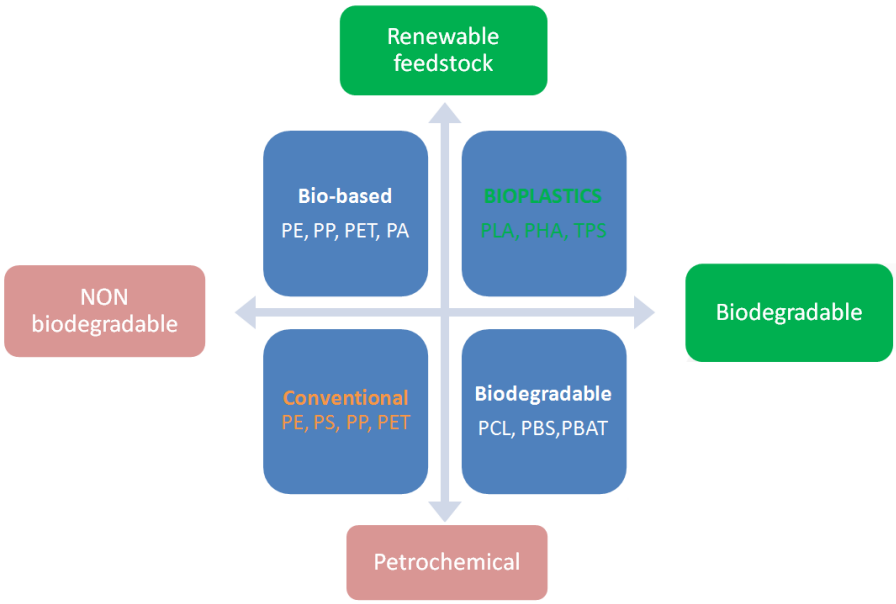

Fig. 2-1. Classification of plastics by raw materials and biodegradability.

Biodegradable polymers can be obtained from biomass products, extraction from living micro-organisms, synthesis of bio-derived monomers or petrochemical products. Fig. 2-2 shows a wide classification of different biodegradable polymers.

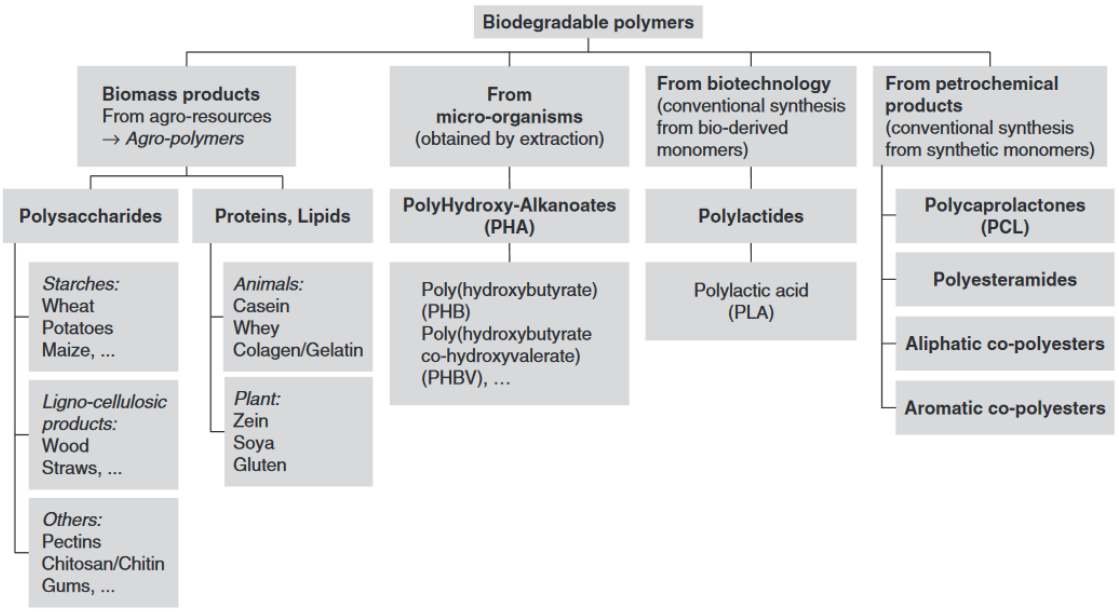

Fig. 2-2. Classification of biodegradable polymers (from *Avérous* [6]).

2.1.1. Renewable feedstocks. Bio-based polymers

From an environmental point of view bio-based polymers have great advantages over fossil-based polymers. Among others, the possibility to avoid the unpredictable oil price fluctuations, which directly affect the price of conventional polymers. This fact has been a strong driving force in their fast evolution during the last two decades, especially to strengthen the interest and investment from industrial companies. Intense research effort has been focused to find technically feasible new routes to obtain bio-based polymers. Fig. 2-3 shows a scheme of these routes, from renewable feedstocks like starch, lignocellulose, plant oils or saccharose to a wide spectrum of polymers, passing through versatile chemical platforms like glucose, adipic acid, glycerol or fatty acids.

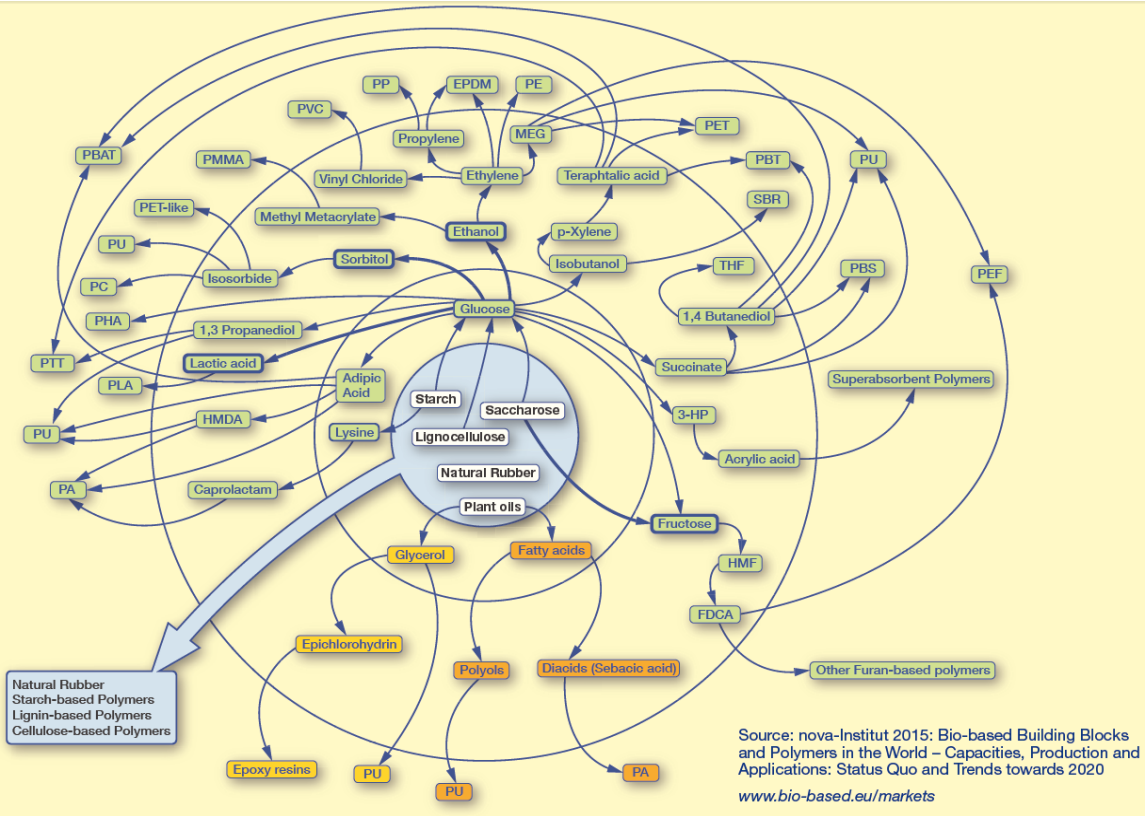

Fig. 2-3. Pathways to bio-based polymers [7].

Among all these bio-based polymers, there are some that correspond to the bio-based analogues of conventional thermoplastics like PE, PP, PS, ABS, PA and PET. Companies like Braskem (Brasil) and Neste Oil (Finland) are able to provide commercial volumes of these plastics, which are produced (at least partly) from renewable feedstocks. The mechanical and physical properties of these so-called "drop-in" bio-based plastics are fully comparable with those of plastics produced from fossil feedstocks [8].

In 2015, the association "European Bioplastics" published a market study carried out by the nova-Institute [9]. The study indicated that bio-based polymers production capacities are projected to grow more than 400% by 2019. Table 2-1 gives an overview on the covered bio-based polymers and the producing companies with their locations and production capacities from 2012 to 2014. In 2013, the production capacities of most of the polymers increased and contributed to the observed 10% compound annual growth rate (CAGR) from 2012 to 2013. Polyamides, polyethylene terephthalate and polytrimethylene terephthalate showed the highest CAGR (around 30%). In 2014, a few polymers contributed to the 11%

CAGR from 2013 to 2014. Only epoxies and poly(butylene adipate-co-terephthalate) showed a strong market growth. Epichlorhydrin, whose production capacity increased, is precursor of epoxies and is produced from bio-based glycerine, a by-product from the biodiesel production.

					2012	2013		2014	
BIO-BASED STRUCTURAL POLYMERS		CURRENT BIO-BASED CARBON CONTENT*	PRODUCING COMPANIES IN 2014 AND UNTIL 2020	LOCATIONS IN 2014 AND UNTIL 2020	PRODUCTION CAPACITIES (TONNES)	PRODUCTION CAPACITIES (TONNES)	CAGR 2012-2013	PRODUCTION CAPACITIES (TONNES)	CAGR 2013-2014
Cellulose acetate	CA	50%	15	16	835,000	845,000	1%	855,000	1%
Epoxies	–	30%	–	–	1,120,000	1,210,000	8%	1,520,000	26%
Ethylene propylene diene monomer rubber	EPDM	50% to 70%	1	1	45,000	45,000	0%	45,000	0%
Polyamides	PA	40% to 100%	9	12	65,000	85,000	31%	95,000	12%
Poly(butylene adipate-co-terephthalate)	PBAT	Up to 50%**	4	5	75,000	75,000	0%	95,000	27%
Polybutylene succinate	PBS	Up to 100%**	10	11	125,000	125,000	0%	125,000	0%
Polyethylene	PE	100%	1	1	200,000	200,000	0%	200,000	0%
Polyethylene terephtalate	PET	20%	5	5	450,000	600,000	33%	600,000	0%
Polyhydroxyalkanoates	PHA	100%	16	19	30,000	32,000	7%	35,000	9%
Polylactic acid	PLA	100%	27	33	180,000	195,000	8%	205,000	5%
Polytrimethylene terephthalate	PTT	27%	2	3	90,000	120,000	33%	120,000	0%
Polyurethanes	PUR	10% to 100%	7	7	1,100,000	1,200,000	9%	1,400,000	17%
Starch blends***	–	25% to 100%	15	16	365,000	400,000	10%	395,000	-1%
Total			112	129	4,680,000	5,132,000	10%	5,690,000	11%

* Bio-based carbon content: fraction of carbon derived from biomass in a product (EN 16575 Bio-based products – Vocabulary)

** Currently still mostly fossil-based with existing drop-in solutions and a steady upward trend

*** Starch in plastic compound

Green: Growth over the previous year

© nova-Institut GmbH 2015

Full study available at www.bio-based.eu/markets

Table 2-1. Bio-based polymers and the producing companies with their locations and production capacities [9].

The production capacity for bio-based polymers boasts very impressive development and annual growth rates, with a CAGR of about 10% whereas petrochemical polymers have a CAGR between 3-4%. The 5.7 million tonnes bio-based polymer production capacity represented approximately a 2% share of the overall polymer production of 256 million tonnes in 2013 and a bio-based polymer turnover of about €11 billion in 2014. With an expected total polymer production of about 400 million tonnes in 2020, the bio-based share should increase to more than 4% in 2020, meaning that bio-based production capacity will grow faster than overall production.

Fig. 2-4 shows the evolution of worldwide production capacities of bio-based polymers. The fastest development is foreseen for drop-in bio-based polymers, but this is closely followed by new bio-based polymers. This group is led by partly bio-based polyethylene terephthalate (PET), largely due to the Plant PET Technology Collaborative initiative launched by The

Coca-Cola Company, which have recently led the company to unveil the first PET plastic bottle made entirely from renewable materials [10]. The second most dynamic development is foreseen for polyhydroxyalkanoates (PHA), which, contrary to bio-based PET, are new polymers, but still have similar growth rates to those of bio-based PET. Polybutylene succinate (PBS) and polylactic acid (PLA) are showing impressive growth as well: their production capacities are expected to almost quadruple between 2014 and 2020.

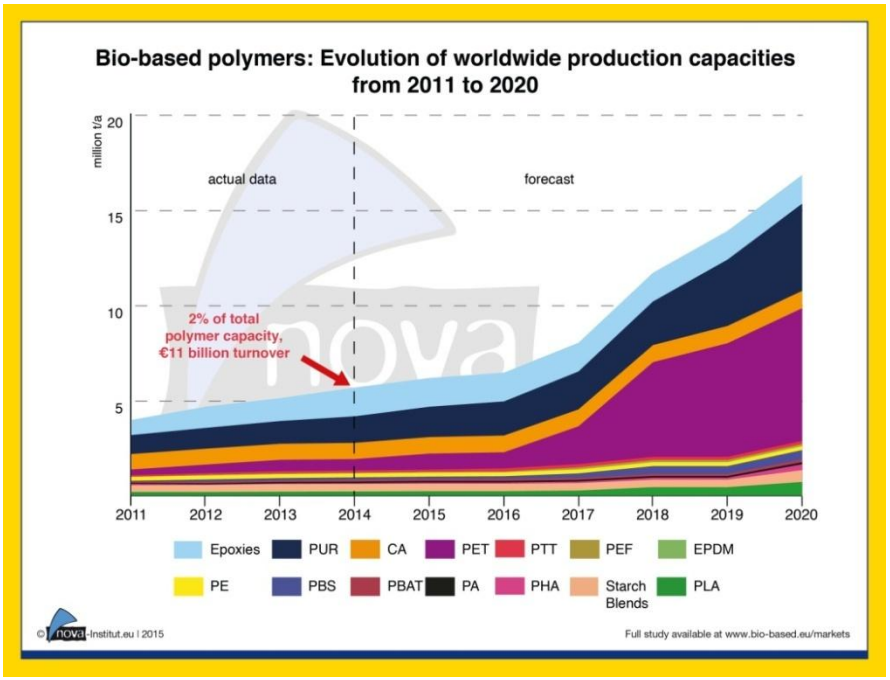

Fig. 2-4. Evolution of worldwide production capacities of bio-based polymers [9].

Concerning geographic market share, most investment in new bio-based polymer capacities will take place in Asia because of better access to feedstocks and favourable political framework. Europe's share is projected to decrease from 15.4% to 4.9%, and North America's share is set to fall from 14% to 4.1%, whereas Asia's is predicted to increase from 58.1% to 80.6%. South America is likely to remain constant with a share between 10% and 12%. In other words, world market shares are expected to shift dramatically. Asia is predicted to experience most of the developments in the field of bio-based building block and polymer production, while Europe and North America are slated to lose more than two thirds of their shares.

Regarding the demand of bio-based plastics in the short and medium term, it may be appreciably enhanced if a positive dialogue among industry and the social movements concerned with the sustainability concept is established, disclosing to the public at large the benefits involved in the adoption of bioplastic products. Governments at local and national levels can also promote the use of bio-based by passing legislation encompassing economic incentives to the adoption of bio-based in the industrial supply chain, and at the same time enforcing restrictions to the trade of environmental-unfriendly products [4]. In this sense, in December 2014, the Norwegian parliament decided to instruct the government to evaluate different options of tax incentives for bio-based polymers – or to introduce a new tax on fossil CO_2 content in polymers, which is not taxed today. The aim is to create a market pull for the bio-based economy. If Norway really were to implement tax incentives for bio-based products, it could be a worldwide forerunner [11].

An important drawback to the future expansion of the bioplastic industry could be posed by the competition with the food industry for the same bio, renewable raw materials, as indicated by the recent price increase of US corn triggered by the unexpectedly strong bio-fuel demand. This reality over the midterm probably will favour tropical countries to host the first large bioplastic plants due to their comparative advantages such as areas with high solar insolation levels, available farm land, and abundant water resources [4]. However, the results of European Bioplastics' annual market data update, presented in November 2015 in the 10th European Bioplastics Conference in Berlin, the land used to grow the renewable feedstock for the production of bioplastics amounted to approximately 0.68 million hectares in 2014, which accounted for only 0.01 percent of the global agricultural area of 5 billion hectares, 97 percent of which were used for pasture, feed, food, other material uses, bioenergy, and biofuels (Fig. 2-5). This clearly shows that there is no competition between the renewable feedstock for food, feed, and the production of bioplastics [12]. Despite this fact, different biopolymer producers have successfully produced and marketed bioplastic resins from second generation feedstocks. These second generation feedstocks are those which are not suitable for human consumption, and include plant-based materials like bagasse, corn stover, wheat straw and wood chips. Among others, Corbion Purac announced the successful production of PLA from this kind of feedstocks in September 2015 [13].

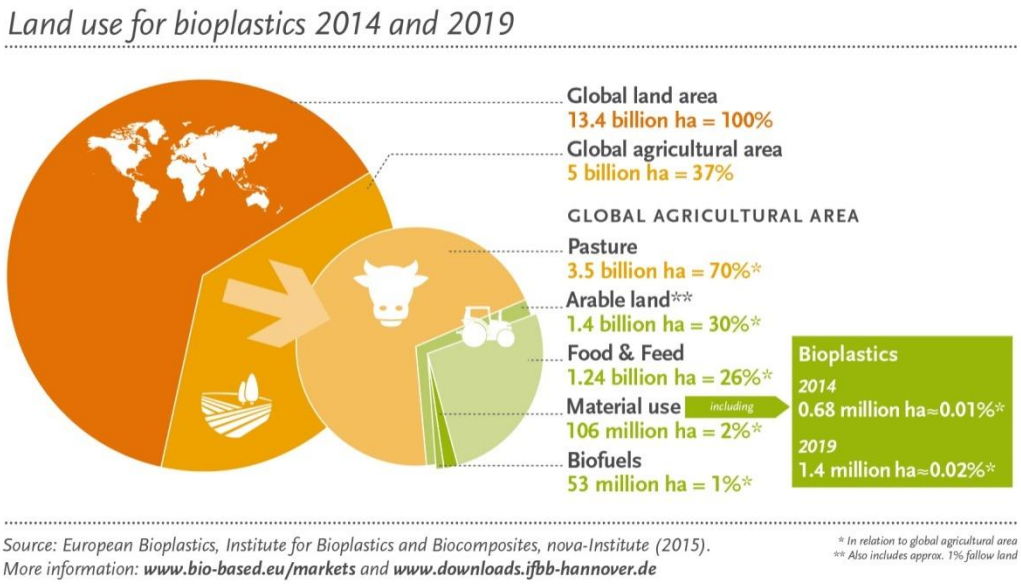

Fig. 2-5. Land use for bioplastics [14].

2.1.2. End-of-life management. Biodegradable plastics

2.1.2.1. Plastic waste. A worldwide problem

Waste plastics contribute to great environmental and social problems due to the environmental pollution and depletion of landfill space. Polymer recycling has received great attention, but only a small fraction of plastic waste is recycled due to contamination and technical limitations. Thus, huge volumes of wastes are still landfilled or incinerated [15]. Moreover, the plastic waste is bulkier than other organic residues and thus occupies massive space in landfills and the proper disposal and incineration have high costs.

The world production and usage of plastics has increased sharply from 1.5 million tons in 1950 to 299 million tons in 2013, and it has been estimated that global plastic production could triple by 2050 [16]. This indicates that the plastic waste issue is in its way to become even more dangerous for the environmental sustainability than it already is. Concerning landfill and oceanic litter, scientific studies have shown that the litter found in oceans and inland waters is dominated by plastics [17]. Enormous efforts are being carried out to try to diminish the plastic waste concentration in the sea, like the recently self-claimed world's first feasible method to rid the oceans "Ocean Cleanup project" [18]. However, besides large items such as plastic bottles and bags, the occurrence of microplastics has also been verified

in water bodies, sediments, sea ice and on the beaches of the world's oceans. Plastic particles with a diameter smaller than 5 mm are referred to as microplastics [19]. These can be secondary fragments created by the breaking up of larger pieces of plastic such as packaging materials, or fibres that are washed out of textiles. They can also be primary plastic particles produced in microscopic sizes; including microplastics used in hand wash, toothpaste, detergents, and cleaners along with microplastics from secondary sources such as tyre abrasion, road paints or granulates on playgrounds. About 8 to 10 million tonnes of plastic waste (Fig. 2-6) are assumed to find their way into the sea worldwide every year [18,20,21].

Fig. 2-6. Plastic waste inputs from land into the ocean in 2010 (from Jambeck *et al.* [21]).

The estimations of annual microplastic emissions to the marine environment in Europe range between 25000 and 60000 tonnes for tyre dust, 25000 and 50000 tonnes for pellet spills, 8000 and 52000 tonnes for textiles, 12000 and 30000 tonnes for building paints, 8000 and 18000 tonnes for road paints, 3 and 9 tonnes for cosmetics and less than 5 tonnes for marine paint according to a study of Eunomia for the European Commission [22]. Furthermore, without waste management infrastructure improvements, the cumulative quantity of plastic waste available to enter the ocean from land is predicted to increase by an order of magnitude by 2025 [21]. It was agreed during the "Microplastics in the Environment" conference (November 2015) [23] that all types of plastic waste should be collected,

materially recycled or used for energy recovery and that landfilling is not an option and neither is the disposal into the environment. Biodegradable plastics should also never be disposed into the sea; in particular because the conditions for degradation in marine environments are quite unfavourable and hard to predict. In this sense, American Society for testing and Materials (ASTM) has recently published an international standard to test and better understand biodegradability of plastics in marine environments [24].

2.1.2.2. The correct management pathway

An increasing concern in the continued use of plastics, especially plastics packaging, is its end-of-life (i.e. what happens to plastic after use when it enters the waste stream). The European Union relies on a five-level waste hierarchy which has been defined in the Waste Framework Directive 2008/98/EG from 19 November 2008. Above all, waste has to be avoided. When this is not possible, it should be reused, and if needed materially recycled. Only at the forth step is waste to be used thermally and as a very last option to be deposited.

Recycling is clearly an important end-of-life strategy for plastics which is in continuous growth. However, the use of recycled plastic depend on the quality and polymer homogeneity of the material. If the polymer is clean and contaminant-free, it can be used to substitute virgin plastic, but if the polymer is mixed with other polymers, the options for marketing materials often involve using the recycled plastics for less expensive and less demanding applications.

On the other hand, biodegradability offers an environmentally responsible end-of-life strategy for plastic products, especially disposable and single use packaging. Fig. 2-7 shows some examples of real applications in which biodegradable plastics can be a suitable solution [23]. This allows closing the loop and ensuing that the compostable plastics are safely and efficaciously removed from the environment via microbial metabolism. The truly biodegradable/compostable plastics are an important sub-set of plastics for end-of-life options and complements (does not substitute) traditional plastics recycling. Conventional plastics are more suitable for long-life applications and for mechanical recycling, while biodegradable plastics make more sense for short-life applications associated with food waste, soil contact, moisture, etc. [25]

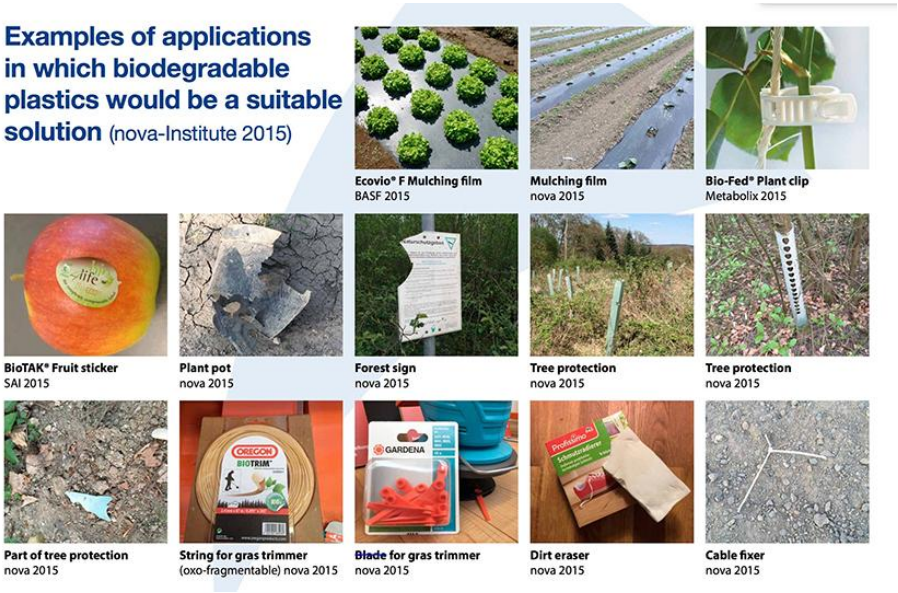

Fig. 2-7. Applications in which biodegradable plastics can be a suitable solution [23].

2.1.3. Carbon footprint of bioplastics

Carbon is the major building block of plastics, fuels and even living organisms. Thus, carbon needs to be managed in a sustainable and environmentally responsible way in order to achieve feedstock sustainability by replacing old carbon (fossil resources) with new carbon (trees, plants, crops...).

Bio-based plastics, in which the fossil carbon is replaced by bio-based/new carbon, offer the intrinsic value proposition of a reduced carbon footprint and are in complete harmony with the rates and time scale of the biological carbon cycle. Identification and quantification of bio-based content is based on the radioactive ^{14}C signature associated with new carbon. Using experimentally determined bio-carbon content values, the achieved intrinsic CO_2 emissions reduction can be calculated by substituting petro-carbon with bio-carbon (this is the "material carbon footprint" value proposition). The "process carbon footprint" arising from the conversion of feedstock to final product is computed using life-cycle assessment methodology (LCA) [26].

Regarding the material carbon footprint, moving from fossil carbon to renewable carbon feedstock offers an intrinsic zero carbon footprint option. This can be seen in the biological carbon cycle scheme shown in Fig. 2-8.

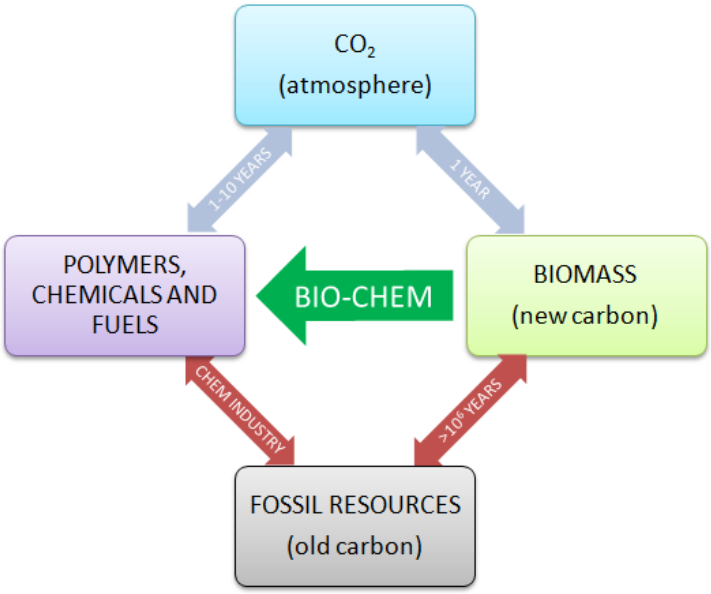

Fig. 2-8. Biological carbon cycle.

Carbon is present in the atmosphere as CO_2. The current level of CO_2 in the atmosphere is around 380 ppm (parts per million) and is increasing. CO_2 and other greenhouse gases in the atmosphere trap the sun's heat from radiating back to space, thereby providing a life-sustaining average planet temperature of 7.2 ºC. Increasing levels of CO_2 and other greenhouse gas emissions to the atmosphere would trap more of the sun's heat, thereby raising the average temperature of the planet. Thus, an uncontrolled, continued increase in levels of CO_2 in the atmosphere will result in a slow rise of the earth's temperature, global warming, and with it an associated severity of effects that will affect life on this planet. It is therefore necessary to try and maintain current CO_2 levels. This can best be done by using renewable biomass crops to manufacture carbon-based products so that the CO_2 released at the end-of life of the product is captured by planting new crops in the next season. Specifically, the rate of CO_2 release to the environment at end-of-life equals the rate of photosynthetic CO_2 fixation by the next generation of crops planted (zero material carbon footprint). In the case of fossil feedstocks, the rate of carbon fixation is measured in millions of years, while the end-of-life release rate into the environment is in 1–10 years. Therefore, using fossil feedstocks is not sustainable. It causes more CO_2 release than fixation, resulting in a high carbon footprint, and with it the global warming and climate change problems.

Using basic stoichiometry, for every 100 kg of Polyolefin (PE, PP) manufactured, a net 314 kg CO_2 is released into the environment at its end-of-life (100 kg of PE contains 85.7% kg carbon and upon combustion will yield 314 kg of CO_2 (44/12) × 85.7). Similarly, PET contains 62.5% carbon and would result in 229 kg of CO_2 released into the environment at end-of life [2]. However, if the carbon in the polyester or polyolefin comes from a biological feedstock, the net release of CO_2 into the environment is zero, because the CO_2 released is fixed in a short time period by the next crop or biomass plantation. This is the intrinsic zero material carbon footprint value proposition for using a bio/renewable feedstocks. Thus, the fundamental driver or switch to bio-based products is the material carbon footprint reduction arising from the "short-term" biogenic carbon cycle (the rate and time scales of CO_2 sequestration is in balance with the use and release, resulting in a carbon neutral footprint).

In 2015 NatureWorks LLC published some peer-reviewed Life cycle assessment data [27] regarding their Ingeo PLA , which indicated that greenhouse gas emissions and energy usage during PLA manufacture is lower than that of all commonly used plastics. The chart shown in Fig. 2-9 compares the greenhouse gas emissions (including bio-based carbon uptake in the case of PLA) for Ingeo manufacture with the emissions resulting from the manufacture of a number of different polymers produced in the US and Europe using the latest available industry assessments for each. The numbers represent the totals for the first part of the life cycle of the polymers, starting with fossil or renewable feedstock production up to and including the final polymerization step.

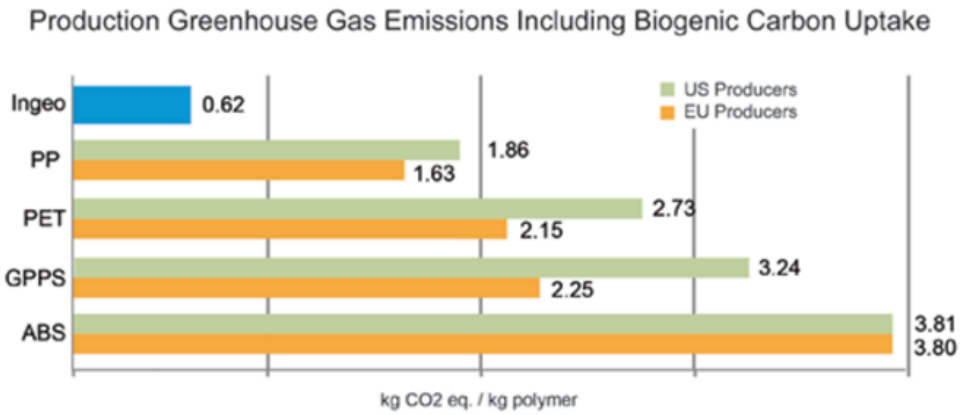

Fig. 2-9. Global warming potential chart [28].

As an example NatureWorks calculated that if 500.000 mobile phones were moulded from Ingeo PLA instead of from ABS the non-renewable energy saved would be equivalent to 2893 litres of gasoline. The reduction in green house gas emissions would lead to savings equivalent to a car driven for 30.000 km with no emissions [29].

Despite its interesting potential as a bioplastic alternative for other conventional petrochemical plastics like PS, PBT, PET or even ABS, the intrinsic properties of this polymer show some drawbacks which complicate the direct replacement. However, PLA is one of the most interesting bioplastic to move on from packaging to semidurable applications due to its high mechanical properties and glass transition temperature. On the contrary, its brittleness and low thermal resistance (amorphous structure) are the main handicaps to get over.

2.2. Poly(lactic acid)

Traditionally, lactic acid-based polymers have been named poly(lactic acid), whereas polylactide refers to the polymer derived from the lactide monomer. Both polymers have the same constitutional repeating unit H-[$OCH(CH_3)CO]_n$-OH, therefore a distinction between the two terms is not essential. However, most of the commercial PLA is produced by lactide ring opening polymerization nowadays, hence, from a technical point of view, the term polylactide should be preferred for commercial PLA. In order to better understand the nature of PLA, a review of its synthesis, properties and market situation are described in the next sections.

2.2.1. Synthesis of PLA

2.2.1.1. Production of lactic acid (LA)

Lactic acid (2-hydroxypropanoic acid), $CH_3CHOHCOOH$ [CAS: 50-21-5], is the most abundant hydroxycarboxylic acid in nature. It was first discovered in 1780 by the Swedish chemist Scheele [30] and first commercially produced by Charles E. Avery at Littleton in 1881 [31]. Lactic acid is a naturally occurring organic acid that can be produced by fermentation or chemical synthesis. It is present in many foods both naturally or as a product

of in situ microbial fermentation, as in sauerkraut, yogurt, buttermilk, sourdough breads and many other fermented foods. Lactic acid is also a principal metabolic intermediate in most living organisms, from anaerobic prokaryotes to humans [32].

The lactic acid molecule has one asymmetric carbon atom and is therefore optically active. Depending on the synthesis conditions and selected microorganisms, two optical isomers of lactic acid can be formed: L-lactic acid and D-lactic acid, as shown in Fig. 2-10. The L form differs from the D form in its effect on polarized light. For L-lactic acid, the plane is rotated in a clockwise (dextro) direction, whereas the D form rotates the plane in a counter-clockwise (levo) direction [33].

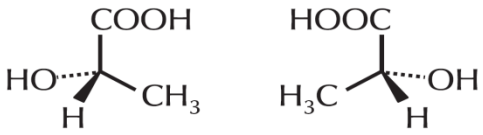

Fig. 2-10. Molecular structure of L- (left) and D- (right) lactic acid.

The interest in the fermentative production of lactic acid has increased due to the prospects of environmental friendliness and of using renewable resources instead of petrochemicals. Besides high product specificity, as it produces an optically pure L- or D-lactic acid, the biotechnological production of lactic acid offers several advantages compared to chemical synthesis like low cost of substrates, low production temperature, and low energy consumption [34]. Lactic acid bacteria (LAB) and some filamentous fungi are the chief microbial sources of lactic acid [35]. Okano et al. published a review regarding optimization of LA production using several kinds of genetically modified microorganisms such as LAB, *Exchericcia coli*, *Corynebacterium glutamicum* and yeast. Using gene manipulation and metabolic engineering, the yield and optical purity of LA produced from biomass were significantly improved [36].

The carbon source for microbial production of lactic acid can be either sugar in pure form such as glucose, sucrose, lactose etc. or sugar-containing materials such as molasses, whey, sugar cane bagasse and cassava bagasse, starchy materials from potato, tapioca, wheat, barley etc. Different food/agro industrial products or residues form are a cheaper alternative to refined sugars for lactic acid production [37]. Some agricultural byproducts, which are

potential substrates for lactic acid production, are corn starch, cassava, lignocellulose/hemicellulose hydrolyzates, corn stalks, beet molasses, wheat bran, rye flour, sugarcane press mud, barley starch, cellulose, etc. [35] Recently, Idler et al. published a review which summarizes the fermentation systems used for the biotechnological production, the various raw materials and applications of lactic acid [38].

By 2003, two manufacturers from the USA, Archer Daniels Midland (ADM) and Cargill Dow (a joint venture between Dow Chemical Company and Cargill Corporation), entered the lactic acid production business, both using carbohydrate fermentation technology. Fig. 2-11 shows the scheme of this process. In 2005, Cargill bought out Dow's participation in the joint venture and established Natureworks LLC as a wholly owned subsidiary. ADM's focus has been on lactic acid and its derivatives for conventional and other uses whereas Natureworks LLC has been the primary leader in the lactic-based polymer business. In Europe, the major manufacturers of fermentative lactic acid include Purac in the Netherlands and Galactic in Belgium. In the Far East, Musashino has been reportedly manufacturing lactic acid by carbohydrate fermentation technology with Chinese partners [32].

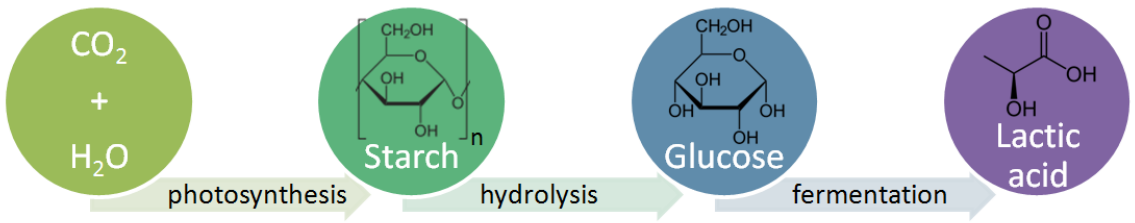

Fig. 2-11 Lactic acid production scheme.

2.2.1.2. Polymerization of PLA

Lactic acid has attracted considerable attention for polymerization to poly(lactic acid). The dimerization of polycondensated lactic acid into lactide and the ring-opening polymerization thereof was first reported by Carothers *et al*. in 1932 [39]. The polymer was, however, found to be unstable at humid conditions and its use was not relevant until 1960s, when PLA was used for medical applications [40]. One of the main drivers for the expanded use of PLA during the last two decades is attributable to the economical production of high molecular

weight PLA polymers (>100000 g/mol). These polymers can be produced using several techniques, including azeotropic dehydrative condensation [41,42], direct condensation polymerization [43–45] and polymerization through lactide formation [6,45–54] (Fig. 2-12). However, commercially available high molecular weight PLA resins are mostly produced via the lactide ring-opening polymerization route [3,4,29]. Indeed, this was the route of the process first presented by Cargill (nowadays NatureWorks LLC) in the late nineties, which made this company to be the current leading producer of commercial PLA worldwide. The essential novelty of the process lied in the ability to go from lactic acid to a low molecular weight poly(lactic acid), followed by controlled depolymerisation to produce the cyclic dimer (lactide). This lactide was then maintained in the liquid form and purified by distillation. Catalytic ring opening of the lactide intermediate results in the production of PLAs with controlled molecular weights [33].

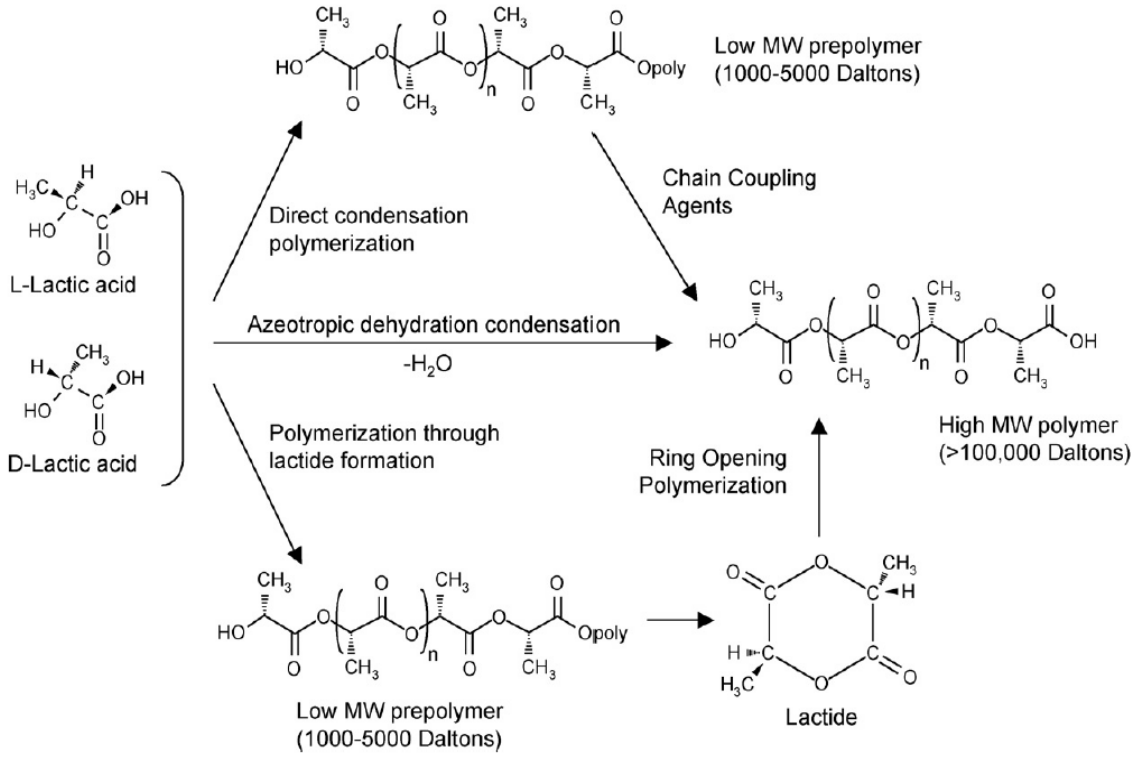

Fig. 2-12. Synthesis of PLA from L- and D- lactic acids [55].

Commercial PLA are copolymers of poly(L-lactic acid-co-D-lactic acid) (PDLLA), which are produced from L-lactides and D,L-lactides [3] (Fig. 2-13). The L-isomer constitutes the

main fraction of PLA derived from renewable sources since the majority of lactic acid from biological sources exists in this form.

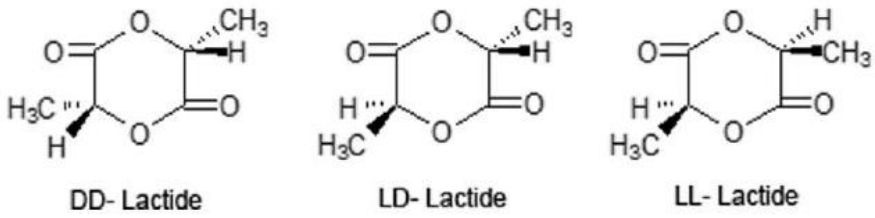

Fig. 2-13. Chemical structure of different lactides.

2.2.2. Types and properties of PLA

Poly(lactic acid) represents a family of copolymers with the same chemical structure but different stereochemistry (Fig. 2-14). PLAs with low L/D lactate ratio behave as an amorphous thermoplastic (A-PLA) while PLAs with high L/D lactate ratio can achieve high crystallinity degree. It is generally considered that for PLA mainly based on L-lactic acid, the incorporation of D-lactic acid in proportions above around 7% induces some imperfections, which prevent polymer crystallization [56]. Thus, different amorphous or semi-crystalline PLA materials can be elaborated according to the L/D ratio and, consequently, formulations with strong variations on thermal, mechanical and barrier properties can be obtained [57,58].

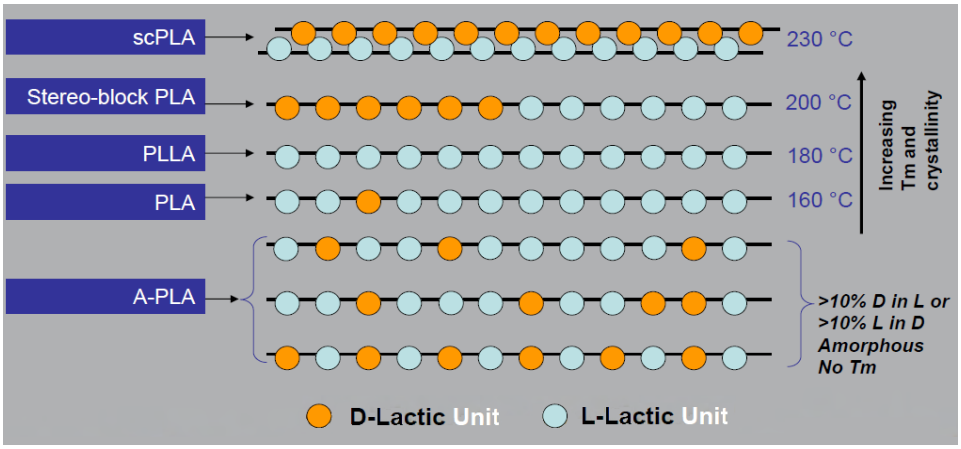

Fig. 2-14. PLA with different L/D ratio and tacticity [59].

Thus, careful selection of the appropriate PLA resin grade is important. Usually, PLA articles which require heat-resistant properties can be injection moulded using PLA resins with a D-isomer content below 1%. Additionally, nucleating agents may be added to promote the development of crystallinity under short moulding cycles. In contrast, PLA resins of higher D-isomer contents (4–8%) are more suitable for thermoformed, extruded, and blow moulded products, since they are more easily processed when the crystallinity is low [60,61]. In addition, stereocomplex PLA (scPLA), which is a blend of PLLA and PDLA macromolecules, is known to have high thermal stability. ScPLA have stereocomplex crystals, which show a high melting point (≈230 ºC). The melting temperature of these crystals is approximately 50 ºC higher than the respective homochiral PLA crystals.

As mentioned previously, lactic acid has two optical isomers (D- and L-) and its optical purity is crucial to the physical properties of PLA (Fig. 2-15). Therefore, the production of enantiomeric pure D- or L-lactic acid is an important goal when some properties are desired.

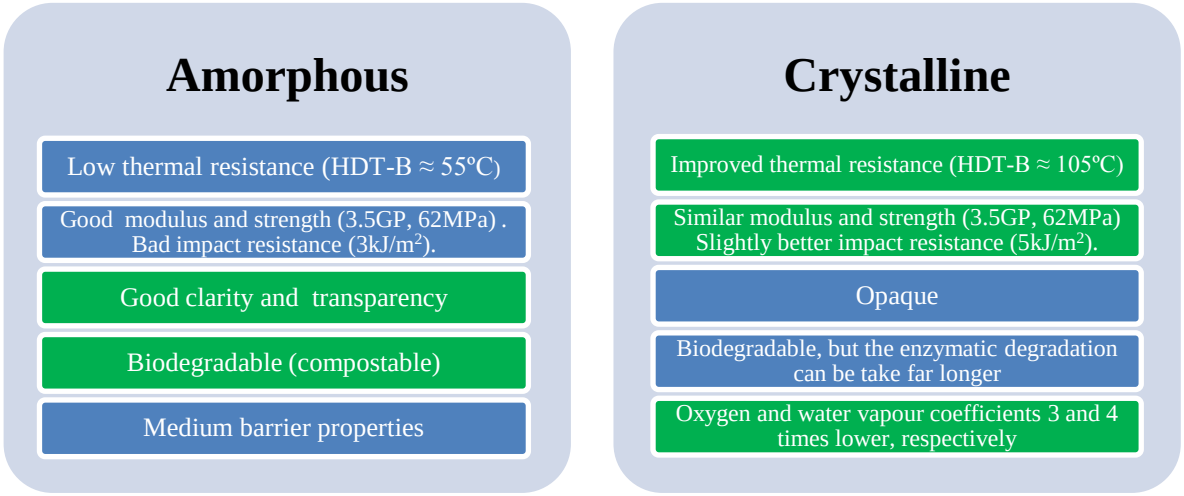

Fig. 2-15. A comparison of some generic properties of amorphous and crystalline PLA.

In the next sections the thermophysical, solubility, rheological, mechanical and degradation properties of PLA are summarized.

2.2.2.1. Thermophysical properties

Like many thermoplastic polymers, semicrystalline PLA exhibits T_g and T_m. At temperatures above T_g (~58 ºC) PLA is in the rubbery state, below T_g it becomes a glass which is still capable to creep until it is cooled to its β transition temperature at

approximately −45 ºC, below which it behaves as a brittle polymer [62]. As shown in Fig. 2-16, PLA has relatively high T_g and low T_m as compared to other thermoplastics. The T_g of PLA is dependent on both the molecular weight and the optical purity of the polymer. The T_g increases with molecular weight to maximum values at infinite molecular weight of 60.2, 56.4 and 54.6 ºC for PLA consisting of 100, 80, and 50% L-lactide contents, respectively [63].

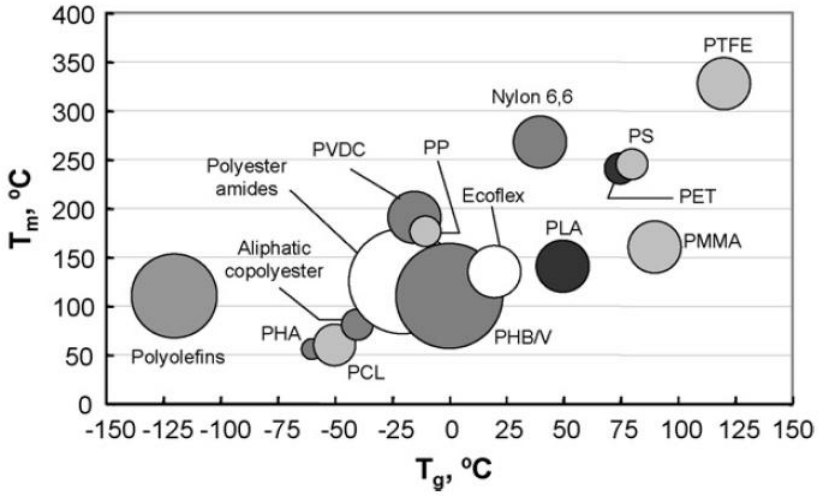

Fig. 2-16. Comparison of $T_g$and T_m of PLA with other thermoplastics [61].

The glass transition behaviour of PLA is also dependent on the thermal history of the polymer. Quenching the polymer from the melt at a high cooling rate (such as during injection moulding) will result in an amorphous polymer. PLA polymers with low crystallinity have a tendency to undergo rapid aging in a matter of days under ambient conditions [64,65]. The T_m of PLA is also a function of its optical purity. The melt enthalpy estimated for an enantiomerically pure PLLA of 100% crystallinity (ΔH_m^0) by Fischer et al. [66], 93 J/g, is the value most often referred to in the literature. The maximum practical obtainable T_m for enantiomerically pure PLA (either L- or D-) is around 180 ºC with an enthalpy of 40–50 J/g. The presence of D-lactate in the PLLA structure can depress the T_m by as much as 50 ºC, depending on the amount of D-lactide incorporated to the polymer. Typical T_m values for PLA are in the range of 130–160 ºC. The T_m depression effect of D-lactide has several important implications as it helps expand the process windows, reduce thermal and hydrolytic degradation, and decrease lactide formation [61]. Pyda et al.

determined the heat capacity of PLA in solid and liquid states ranging from 5 to 600K [67]. The heat capacity ($C_{p\text{-liquid}}$, J/(K mol) can be represented in a simple form: $C_{p\text{-liquid}} = 120.17 + 0.076\ T$, where T is in Kelvin (K).

2.2.2.2. Solubility

The solubility of lactic acid based polymers is highly dependent on the molar mass, degree of crystallinity and L/D lactic acid ratio. Good solvents for PLLA (L/D ratio > 99%) are for example chlorinated or fluorinated organic solvents, dioxane, dioxolane and furane. PLA with lower L/D ratio are, in addition to the previously mentioned ones, also soluble in many other organic solvents like acetone, pyridine, ethyl lactate, tetrahydrofuran, xylene, ethyl acetate, dimethylsulfoxide, N,N-dimethylformamide and methylethyl ketone. On the contrary, typical non-solvents for lactic acid based polymers are water, alcohols (e.g. methanol, ethanol, propylene glycol) and unsubstituted hydrocarbons (e.g. hexane, heptane) [68]. Two of the most used solvents for PLA in the literature, especially for GPC technique, are tetrahydrofurane and chloroform. Table 2-2 shows the solubility of two specific PLA grades by NatureWorks in different solvents. Both are high molecular weight extrusion grades ($M_n \approx 120000$), but Ingeo 4060D has around 10% of D-lactic acid content (amorphous) whereas 4032D has around 1.6% of D-lactic acid content (semicrystalline).

Solvent	**Amorphous PLA** % Soluble	**Semicrystalline PLA** % Soluble
1,2 Dichloroethane	99.8 ±0	99.9 ±0
DMF	99.8 ±0.1	67.5 ±5.2
Heptane	8.6 ±3.9	27.5 ±12.3
Isopropyl alcohol	0 ±0.2	0 ±1.8
Methyl isobutyl ketone	20.6 ±1.7	0 ±0.4
Octanol	1.3 ±3.8	5.2 ±0.5
THF	99.8 ±0	99.9 ±0
Toluene	99.8 ±0.1	0.4 ±1.6

Table 2-2. Solubility of amorphous and semicrystalline PLA in different solvents [69]

2.2.2.3. Rheological properties

The rheological properties of PLA are highly dependent on temperature, molecular weight and shear rate, they must be taken into consideration during tooling design, process optimization, and process modelling/simulation. Melt viscosities of high-molecular-weight PLA are in the order of 500–1000 Pa s at shear rates of 10–50 s^{-1}.

The melts of high molecular weight PLA (~100000 g/mol for injection moulding to ~300000 g/mol for film cast extrusion applications) behave like a pseudoplastic, non-Newtonian fluid. Moreover, as shear rates increase, the viscosities of the melt decrease considerably, i.e. the polymer melt exhibits shear-thinning behaviour [61,70]. In contrast, low molecular weight PLA (~40000 g/mol) shows Newtonian-like behaviour at shear rates typical of film extrusion [45,71].

PLA produced either via the lactide process or by direct condensation is normally a linear polymer. In comparison with polyolefins, the polymer has poor melt elasticity as evidenced by low die swell. This poor elasticity results from the low degree of molecular chain entanglement. The most promising method of increasing the level of entanglement is to introduce branching into the polymer. Cargill utilises low levels of an epoxidised natural oil to introduce branching into the polymer chain during polymerisation [72]. For certain applications where higher melt elasticity is required beyond that presently achieved by the in-situ polymerisation approach, additional techniques can be utilised. Practical modifications involve the use of cross-linking agents such as peroxides, which, when used at very low levels, can lead to significant further increases in melt elasticity, but at the cost of a slight increase in melt viscosity. Essentially, as the polydispersity of the polymer increases, the melt elasticity increases [33].

2.2.2.4. Mechanical properties

Semicrystalline PLA is preferred to the amorphous polymer when higher mechanical properties are desired. Semicrystalline PLA has an approximate tensile modulus of 3.5 GPa, tensile strength of 50-70 MPa, flexural modulus of 5 GPa, flexural strength of 100 MPa, and elongation at break of about 4% [73–76]. The molecular weight of the polymer [58,77–79], as well as the degree of crystallinity [80,81] have a significant influence on the mechanical

properties. It has been shown that the tensile strength and modulus of PLLA increases by a factor of 2 when the weight average molecular weight is raised from 50000 to 100000 g/mol [78]. A further increase in molecular weight to 300000 g/mol seemed not to influence the properties of the polymers in any significant way [68]. On the other hand, the mechanical properties of similar molecular weight PLA prepared by different polymerization processes have been shown not to differ. This has been noticed for polylactides prepared by polycondensation and ring-opening polymerization [82].

PLLA of high molecular weight has sufficient strength to be used as load bearing material in medical applications, but the material degrades slowly because of the reinforcing crystalline domains [83]. The crystallinity can be reduced by copolymerizing with D-lactide, leading to an amorphous PLA with a faster degradation profile [84]. However, this will also reduce the toughness of the polymer and the impact strength of PLA has been shown to decrease threefold when copolymerizing with 5% D-lactide [73].

2.2.2.5. Degradation

Polymer degradation occurs mainly through scission of the main chains or side chains of macromolecules. A variety of chemical, physical and biological processes and thus different degradation mechanisms can be involved in the degradation of a polymer. Regarding PLA, its degradation has been found to be dependent on different factors such as molecular weight, crystallinity, L/D ratio, temperature, pH, presence of terminal carboxyl or hydroxyl groups, water permeability, and additives acting catalytically that may include enzymes, bacteria or inorganic fillers [85]. In the next subsections the thermal, hydrolytic and biological degradation of PLA are summarised.

2.2.2.5.1. Thermal degradation

Polyesters in general present a limited thermal stability. In the case of PLA the degradation can start at temperatures as low as 215 ºC. The carbon to oxygen bond of the carbonyl group is the first to split during heating [68]. Thus, one of the drawbacks of processing PLA by melt blending is its tendency to undergo thermal degradation at the processing temperature range, which is related both to the melt temperature and the residence time in the extruder. Thermal degradation of PLA can be attributed to hydrolysis by trace amounts of water,

zipper-like depolymerisation, oxidative random main-chain scission, intermolecular transesterification to monomer and oligomeric esters, and intramolecular transesterification resulting in formation of monomer and oligomer lactide of low molecular weight [68]. Depending where in the backbone the reaction occurs, the product can be a lactide molecule, an oligomeric ring, or acetaldehyde plus carbon monoxide. Although acetaldehyde is considered to be non-toxic and it is naturally present in many foods, the acetaldehyde generated during melt processing of PLA must be minimized if the processed product is meant to be used in food packaging, because it can impact the organoleptic properties [61]. Moreover, the thermal degradation can be catalyzed by the reactive carboxyl and hydroxyl end groups and the presence of residual catalyser or monomers.

2.2.2.5.2. Hydrolysis

The hydrolytic degradation is the most common way of degradation of PLA. It is an undesired phenomenon during processing or material storage, but might be interesting in biomedical applications or compostable packages, among other applications. It starts with a water uptake phase followed by hydrolytic splitting of the ester bonds, which leads to molecular weight loss. Carboxylic end groups concentration is increased due to chain excision, which autocatalyses the degradation. When the resulting oligomers are short enough sample weight loss becomes noticeable [86].

The amorphous parts of polyesters have been noticed to undergo hydrolysis before the crystalline regions due to a higher rate of water uptake [68]. Thus, the initial degree of crystallinity affects the rate of hydrolytic degradation. The first stage is accordingly located to the amorphous regions. Subsequently, the remaining undegraded chain segments gain more space and mobility, which lead to reorganizations of the polymer chains, an increased crystallinity and a simultaneous loss in mechanical properties and molecular weight [66,87]. The temperature during the hydrolysis is of major importance for the degradation rate due to an increased degradation rate and mobility of macromolecules above the T_g, temperatures at which the activation energy suffers a drastic change [88].

2.2.2.5.3. Biodegradation

Dr. Ramani Narayan proposed the following definition for biodegradability in a plastic context: “biodegradability is an end-of-life option that allows one to use the power of

microorganisms present in the selected disposal environment to completely remove biodegradable plastic products from the environmental compartment in a timely, safe, and efficacious way" [2]. Concerning PLA, a two stage degradation mechanism has been determined as the main biodegradation process [33]. First, the cleavage of the ester linkages by absorbed water produces a successive reduction in molecular weight. As the average molecular weight reaches approximately 10000 g/mol (as determined by GPC in reference to polystyrene standards), micro-organisms present in the soil begin to digest the lower molecular weight lactic acid oligomers [35], producing carbon dioxide and water Fig. 2-17.

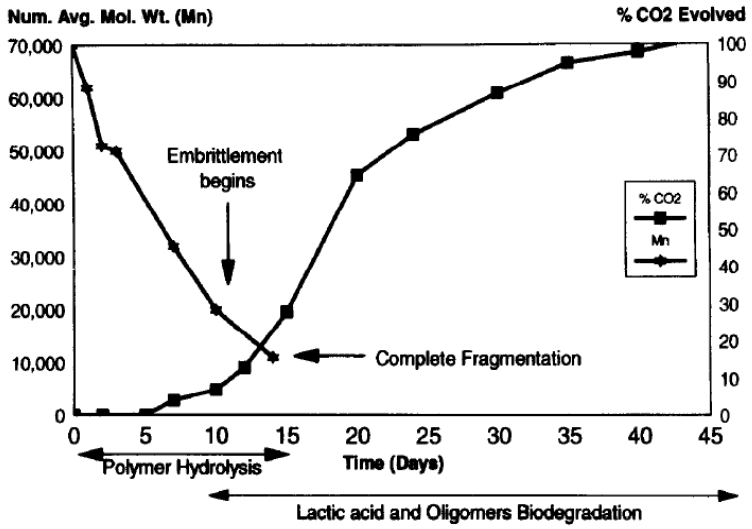

Fig. 2-17. Biodegradation of PLA at 60 ºC compost [33].

This two-stage mechanism is different to many other biodegradable products presently on the market. Typically, biodegradable polymers degrade by a single step process, involving bacterial attack on the polymer itself. Thus, it has to be noted that PLA is biodegradable in compost at temperatures above its T_g. In this environment of high moisture and temperature (55-70 ºC), PLA polymers will degrade rapidly. However, at lower temperatures and/or lower moisture, the storage stability of PLA products is considered to be acceptable [33].

2.2.3. Production and market of PLA

The predominant lactic acid/lactide and polylactide producers up to date (June 2016) have been summarized in Table 2-3. NatureWorks (USA) and Corbion (Europe) are the main

global producers of lactide worldwide. Contrary to NatureWorks, Corbion's production is based on non-GMO crops. Concerning PLA, NatureWorks is the leading worldwide producer, subsequently offering the best price (around 1.80 €/kg) and a broad portfolio, which comprises high and low L-lactate purity grades and different molecular weights. On the other hand, Corbion (formerly PURAC) had first tried to limit their business model to the production and sale of lactide to anyone interested in its polymerization. However, after being formally informed of the strong interest to have access to a reliable major 2nd source for PLA resins, Corbion informed in May 2015 that they decided to widen the business model by having access to a 75kt/year polymerization plant [89]. Currently, Corbion offers a narrower PLA grade portfolio, but includes PDLA grades of different molecular weights, which are in the core of their business model based on high heat resistant PLA, partly focused on stereocomplex PLLA/PDLA blends. A similar focus on high heat resistant PLA is also shared by other smaller Asian producers like Teijin. The current state of Futerro, which is one of the few companies producing PLA by reactive extrusion, is not clear. Even though the investment of Galactic and Total Petrochemical on the business seems to have been strongly attenuated in the last years, it has not been officially closed. Shenzen is one of the biggest PLA producers in China, but the seriousness of the company is uncertain because the offered PLA grades suggest they are trading with NatureWorks grades. Besides the companies shown in Table 2-3, huge companies like Toray, Samsung or Unitika, among others, produce PLA for internal consumption, but their business model does not include the commercialization of PLA. Finally, the harshness of the bioplastic market has given different indicators including big company fails, like Cereplast in 2014, which was bought by Trellis Earth when it was liquidated in bankruptcy court. In November 2016 Total and Corbion announced they were joining forces to develop bioplastics by creating a 50/50 joint venture to produce and market PLA. The two partners planned to build a PLA polymerization plant with a capacity of 75000 tons per year at Corbion's site in Thailand that already had a lactide production unit. Corbion would supply the lactic acid necessary for the production of the PLA and the lactide [90].

Lactic acid / lactide

Producer	Country	Observations
NatureWorks LLC	USA	Owned by Cargill. Formerly JV of Cargill/Dow (until 2005) and Cargill/Teijin (until 2009). Lactide from GMO corn (USA) and sugarcane/cassava (Asia).
Corbion	Netherlands	Owned by CSM. JV: Purac/Caravan Ingredients. Lactide from GMO-free sugarcane.
Galactic	Belgium	
Henan Jindan Lactic Acid tech.	China	

PLA

Producer	Country	Grade	Capacity (t/year)	Observations
NatureWorks	USA	Ingeo	150000	Production in Nebraska and South-east Asia (2018). Price≈ 1.8 €/kg
Corbion	Netherlands	-	75000	Production in Thailand. Price≈ 2-2.5 €/kg
Shenzhen Bright China	China	-	10000	
Supla	Taiwan	Plantura	10000	Lactide from Corbion.
Zhejiang Hisun	China	Revode	5000	Lactide from Corbion. leading PLA supplier in China
Futerro	Belgium	-	1500	JV: Galactic/Total Petrochemical. Lactide from Galactic
Teijin	Japan		1200	
WinGram Industrial	Hong Kong			
Biomer	Germany			
Natureplast	France			
Hycail	Netherlands			
Synbra	Netherlands	Synterra		Lactide from Corbion. Producer of Expanded PLA

Table 2-3. Lactide and polylactide producers by country and production capacity.

Because of the intrinsic degradation mechanism, PLA is ideally suited for many applications in the environment where recovery of the product is not practical, such as agricultural mulch films and bags. Composting of post consumer PLA items is also a viable solution for many PLA products. Recently, Expanded PLA (EPLA) has reached packaging market segments which were dominated by petrochemical foams as Expanded Polystyrene (EPS). Products like fish boxes, packaging for electrical components, protective packaging for white and brown goods, packaging for technical products, protective packaging for the pharmaceutical and medical industries and horticultural trays, among others, have now the potential to be applications for PLA foams. However, due to the low T_g of PLA, these products show poor dimensional stability (leading to squashing, deformation and collapse) when exposed to temperatures above 60 ºC. Since 2011, companies like Synbra Technology b.v. (Netherlands) and Biopolymer Network Ltd (New Zealand) have made big efforts to find a market place to PLA foams [91,92]. Besides, PLA is bioabsorbable in the body, and thus it has extensive applications in biomedical fields, including suture, bone fixation material, drug delivery microsphere, and tissue engineering [93,94]. Spun into fibres, PLA is silk-like and the fabrics produced are smooth, skin flattering and with a pleasing drape. Elongation at break can be adjusted between 20% and 200% depending on the degree of stretching. As a textile, PLA has many attractive properties, which are similar or even superior to PET. Such properties include higher tenacity than natural fibres, excellent moisture transport away from the skin (wicking), natural UV resistance, low flammability and low smoke formation [95]. Up to now, PLA has played a limited role in the textile market due to relatively high prices and some processing handicaps of PLA in the textile production chain. However, solutions already exist to overcome these deficiencies and various efforts are ongoing to meet these challenges [96].

The use of modified PLA in the durables and semidurables market has attracted great interest during the last few years. Big efforts have been made in order to use PLA instead of ABS or HIPS in different products. For instance, Kuender & Co. (Taiwan) presented an all-in-one Pc whose housings were made of SUPLA Material and Technology's modified PLA in 2013. This was claimed to be the first time that PLA was used for mass production of consumer electronics in replacement of ABS [97]. NEC, Fujitsu, and Canon are using PLA blends (mostly with PC) in electronic consumer good housings. NEC even has a proprietary branding for its PLA based application called NuCycle, a flame-resistant compound

developed with Sumitomo Dow. Toyota has been an early adopter of PLA for car parts, including a floor mat for the third-generation Toyota Prius that uses PLA based fibre. On the other hand, Röchling Automotive (German-based Tier II) developed their own modified PLA compounds which are claimed to be capable of competing with most polyesters available on the market (PC, PET, PBT), styrenics (ABS), polyolefins (PP) and even polyamides (PA6). They have shown different automotive prototype parts produced in different grades, all based on PLA and having biobased carbon contents as high as 95%. One problem of automotive applications is humidity and thermal requirements in standard accelerated aging tests. These materials show improved hydrolysis and thermal resistance up to 140 °C with fibre reinforcement. Impressive results were also obtained for scratch and UV resistance, which is of key importance for vehicle interior applications. Air-filter housings, deflectors and interior trim parts are an example of what can be produced on PLA based compounds for the automotive industry [98].

2.3. Processing of PLA based formulations

PLA is a highly versatile polymer which can be tailor-made into different resin grades for processing into a wide spectrum of products. The main conversion methods for PLA are based on melt processing. This approach involves heating the polymer above its melting point, shaping it to the desired forms, and cooling to stabilize its dimensions. Thus, understanding of thermal, crystallization, and melt rheological behaviours of the polymer is critical in order to optimize the process and part quality. Some of the examples of melt processed PLA are injection moulded disposable cutlery, thermoformed containers and cups, injection stretch blown bottles, extruded cast and oriented films, and melt spun fibres for nonwovens, textiles and carpets [99–101].

PLA can be processed using conventional production equipment with minimal modification. However, its unique properties must be taken into consideration in order to optimize the conversion of PLA into processed parts, films, foams, and fibres.

2.3.1. Drying

A major problem in the manufacturing of PLA based compounds is the limited thermal stability during melt processing. Polymers containing ester linkages tend to suffer chain scission when exposed to heat even for short times (thermal degradation of PLA is discussed more in detail in section *2.2.2.1. Thermophysical properties*). Hence, before melt processing, PLA must be carefully dried in order to prevent excessive hydrolysis, which can compromise the physicomechanical properties of the polymer. Typically the polymer is dried to less than 100ppm moisture content (0.01%, w/w). Natureworks LLC, the main worldwide supplier for PLA, recommends that resins should be dried below 250 ppm moisture content before processing [102]. For processes that have long residence times or require temperatures close to 240 ºC the resin should be dried below 50 ppm to achieve maximum retention of molecular weight [103,104].

Drying of PLA takes place in the temperature range of 80–100 ºC. Commercial grade PLA pellets are usually crystallized, which permits drying at higher temperatures to reduce the required drying time. In contrast, amorphous pellets must be dried below the T_g (<60 ºC) to prevent the resin pellets from sticking together, which can bridge and block the drying hopper. PLA degrades at elevated temperatures and high relative humidity; hence it is noteworthy that the resins should be protected from hot and humid environments. Henton et al. reported that amorphous PLA can dramatically reduce its M_w in less than a month when exposed to 60 ºC and 80% RH [62]. Concerning the equipment, the dew point of the dryer should be −40 ºC or lower to achieve an effective drying [61].

2.3.2. Twin screw extrusion

A twin screw extruder is a machine with two single screws. The most obvious classification in a twin screw machine is whether the two screws rotate in the same (co-rotating) or opposite (counter-rotating) directions. The basic principle of twin screw extruders was conceived in Italy in the late 1930s by Roberto Colombo of Lavorazione Materie Plastiche (LMP) to address the problem of mixing cellulose acetate without solvent. Colombo developed a system of intermeshing co-rotating screws, which proved effective to the purpose [105,106]. Since then, intermeshing co-rotating twin screw extruders have been used for mixing different ingredients into polymer matrices. This may involve particulates (compounding) and/or a second polymer (blending). The goal of mixing is to reduce the

non-uniformity of the mixture, and can be accomplished by inducing physical motion of the ingredients. The convective flow is the predominant mechanism of mixing in polymer melts, and the mixing action generally occurs by shear flow or elongational flow [107]. If the components to be mixed are fluids or cohesionless clusters which do not exhibit a yield point, then the mixing is distributive. On the contrary, if the mixture contains a component that exhibits a yield stress (i.e.: fluids or cohesive clusters), then the mixing is dispersive. In dispersive mixing a solid component needs to be broken down, but the breakdown occurs only after a certain minimum stress has been exceeded. Therefore, mixing mechanisms may be generally classified according to whether they are concerned with the dispersion of small particles in a polymer melt matrix or with the mixing of two viscous melts. They may be further classified into distributive mixing and or dispersive mixing (Fig. 2-18). Distributive mixing means the repeated arrangement of the two components to reduce non-uniformity. Permanent strain must be imposed on the system to achieve it. Dispersive mixing usually refers to the breakup of agglomerates of solid particles in a fluid matrix, though it has also been applied to homogenisation of liquid-liquid systems. The local strain rate and stress play important roles here. Note that distributive and dispersive mixing often come together. In dispersive mixing there is always distributive mixing. However, the reverse is not always true. In twin screw extrusion, the dispersive sections of the screw are usually followed by a distributive section.

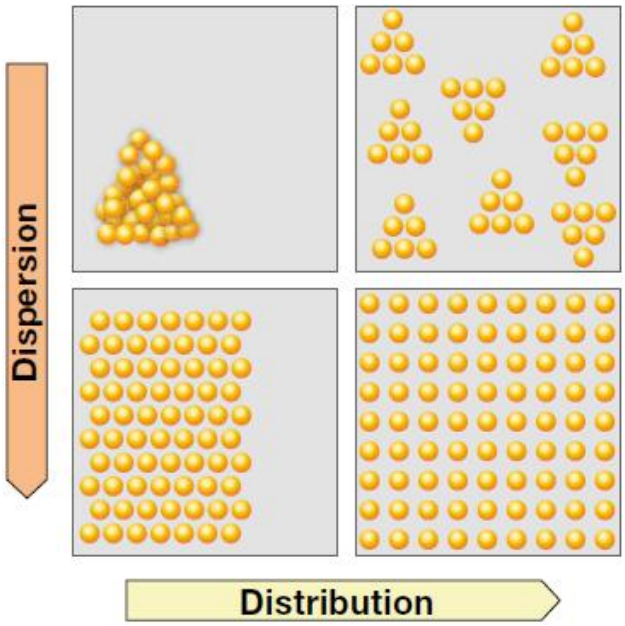

Fig. 2-18. Scheme of the effect of distributive and dispersive mixing.

Twin screw extrusion of PLA based compounds is in general linked to a subsequent processing step (e.g. injection moulding, thermoforming, fibre drawing...). Thus, the properties of the compound will depend on the specific conditions during the second processing step (e.g. shear rate, temperature...). However, the main parameters for compounding will potentially have a great influence on the properties, i.e. the processing temperature, residence time, moisture content of the polymer and shear rate (screw design and speed) [108].

2.3.3. Injection moulding

Injection moulding is the most widely used converting process for thermoplastic articles, especially for those that are complex in shape and require high dimensional precision. All injection moulding machines have an extruder for plasticizing the polymer melt. Unlike a standard extruder, the extruder unit for injection moulding machine is designed such the screw can reciprocate within the barrel to provide enough injection pressure to deliver the polymer melt into the mould cavities.

In general, injection moulded PLA articles are relatively brittle. The brittleness of PLA has been attributed to the rapid physical ageing of the polymer since room temperature is only about 25 ºC below the T_g [63,64]. Injection moulded articles tested immediately after quenching to very cold temperatures exhibited a much larger extension to break. However, when the moulded specimens were aged at room temperature for 3–8 h, they became very brittle [61]. This phenomenon was attributed to the reduction of free volume of the polymer due to rapid relaxation towards the equilibrium amorphous state. Ageing below T_g is exclusively related to the amorphous phase of the polymer; accordingly, increasing the crystallinity of the polymer (e.g. by adjusting D-isomer content or the use of nucleating agents) will reduce the ageing effect. Furthermore, the crystallites formed also act like physical crosslinks to retard the polymer chain mobility. On the other hand, the tendency of lactide to condensate on the cold tooling surfaces, which can affect the surface finish and weight of the moulded articles, limits the minimal mould temperature that can be used during injection moulding of PLA to 25–30 ºC. Moreover, process parameters such as packing pressure, cooling rate, and post-mould cooling treatment are expected to influence the PLA aging behaviour as well [109].

The reason behind the limited available information regarding injection moulding of PLA is that the main application for this material has been packaging, sector in which other technologies like thermoforming or blow moulding are more interesting. Hence, there is a lack of knowledge concerning the behaviour of PLA injected at different mould temperatures and crystallinity levels that can be achieved in situ. This issue has been studied during this thesis.

2.3.4. Other processing methods

Due to the increasing environmental awareness of the consumers, there is a sustained interest from the food industry to replace the existing non-biodegradable thermoplastics with PLA for certain beverage products. The production of PLA bottles is based on injection stretch blow moulding (ISBM) technique. This process produces biaxial orientated PLA bottles with much improved physical and barrier properties compared to injection moulded amorphous PLA. In the blow moulding machine, the previously injected preform (also known as parison) is heated by IR to a suitable temperature (85–110 ºC) for blow moulding. PLA preforms have a tendency to shrink after reheating, especially the regions near the neck and the end cap where the residual injection moulding stresses are concentrated. This may be moderated through proper preform design with gradual transition regions. Similarly to PET, PLA exhibits strain-hardening when stretched to high strain. This phenomenon is desirable for blow moulding of preforms to achieve optimal bottle side wall orientation and minimize wall thickness variation. Since strain-hardening occurs only when the PLA is stretched beyond its natural stretch ratio, the preform must be designed to match the target bottle size and shape, such that optimal stretch ratios are achieved during blow moulding. Preforms that are under-stretched will result in bottles with excessive wall thickness variation, weak mechanical properties and poor aesthetic appeal. In contrast, overstretched bottles can also result in stress whitening due to the formation of micro-cracks on the bottle surfaces that diffract light. Typical commercial grade PLA resins for bottle applications require preform axial stretch ratios of 2.8–3.2 and hoop stretch ratios of 2–3, with the desirable planar stretch ratio of 8–11 [110,111].

Thermoforming is commonly used for forming packaging containers that do not have complicated features. PLA polymers have been successfully thermoformed into disposable

cups, single-use food trays, lids, and blister packaging. In this process, PLA sheet is heated to soften the polymer, forced either pneumatic and/or mechanically against the mould, allowed to cool, removed from the mould, and then trimmed. In general, the thermoforming temperatures for PLA are much lower than other conventional thermoformed plastics (e.g., PET, PS, and PP) in the range of 80–110 ºC when the sheet enters the mould [112,113]. Moulds, trim tools and ovens designed for thermoforming of PET, high impact polystyrene (HIPS) and PS can be used for forming PLA containers. However, moulds for thermoforming of PP may not be used interchangeably for PLA, since PP shrinks more considerably than PLA during cooling. For a given part thickness, cooling times required for PLA containers in the mould tend to be higher than PET and PS containers due to the lower thermal conductivity and T_g for PLA polymers [61].

Due to their biocompatibility and large surface area, PLA foams have a niche in tissue engineering and medical implant applications [114–116]. On the other hand, loose-fill packaging materials provide cushioning, protection, and stabilization of packaged goods during shipping. Over the past decade, the use of expanded PS foams for loose-fill packaging has declined due to the replacement with the more environmentally benign starch based expanded foams. To overcome the hydrophilic nature of starch, these biobased foams are often blended with PLA or petroleum polymers [117]. Neat foamed PLA is also being commercialized for these and other applications [118]. Foaming of PLA is generally carried out by dissolving a blowing agent in the PLA matrix. The solubility of the blowing agent is then reduced rapidly by producing thermodynamic instability in the structure (e.g., temperature increase or pressure decrease) to induce nucleation of the bubbles. To stabilize the bubbles, the foam cells are vitrified when the temperature is reduced below the T_g [119,120].

2.4. Different approaches to modify the properties of PLA

Some of the intrinsic properties of neat PLA need to be improved for applications where PLA is intended to be used as a substitute for other thermoplastics. For instance, the brittleness of PLA may prevent its use in applications where toughness and impact resistance are critical. The fact that PLA being biodegradable (compostable) may in some cases lead to unpredicted performance if the polymer is exposed to excessive temperature

and humidity conditions. Some of these challenges are expected to be achieved through blending PLA with other polymers, improving its crystallization capabilities, reinforcing it to obtain micro- or nanocomposites, or by the modification of the polymer itself. Research and development in these areas are opening new potential opportunities for PLA in order to be used as a high performance biodegradable polymer. Fig. 2-19 shows the evolution of different Ingeo PLA grades by NatureWorks LLC, which are expected to invade part of the PS or SAN based semidurable market first and the ABS or PC/ABS based durable market afterwards. These optimised PLA polymers are usually modified to enhance and adjust their properties to specific applications by compounders or other polymer processors in the value chain.

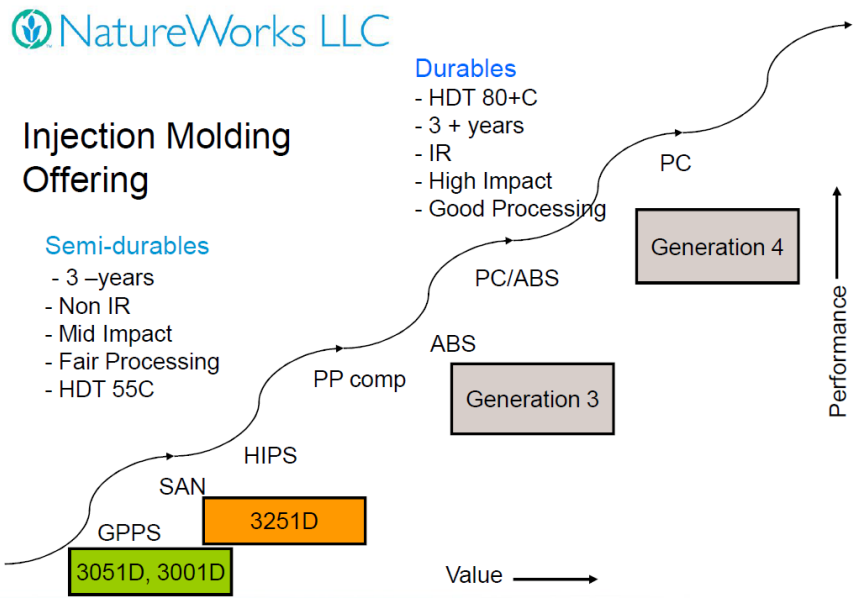

Fig. 2-19. Evolution of PLA in terms of value and performance in comparison to other conventional thermoplastics (by NatureWorks LLC [121]).

The next sections summarize the insights of some of the main approaches to modify PLA.

2.4.1. Melt blending of PLA with other thermoplastics

Blending different polymers is as one of the most versatile and economical methods to produce new multiphase polymeric materials that are able to satisfy the market demands. Polymer blends with enhanced thermal, mechanical, physical, chemical, optical and other properties represent over 30% of the total consumption of polymers, and the world market for the blends is expected to increase at a rate of about 9% per year [122].

In a perspective of production scale-up, melt blending of PLA with other polymers is a sustainable and effective approach to improve the thermo-mechanical behaviour of PLA based materials. Blends can exhibit advantageous physical and chemical properties that each individual polymer does not possess. However, the properties of the obtained blends depend on the chemical composition and the compatibility or miscibility of the components. Thus, many attempts have been made to modify poly(lactic acid) by blending with other polymers, including poly(acrylonitrile-butadiene-styrene) [123], poly(vinyl acetate) [124], poly(vinyl chloride) [125], polystyrene [126,127], polycarbonate [128,129], polyethylene [130–132], thermoplastic starch [133], poly(ethylene oxide) [134–136], poly(ethylene glycol) [137–139], poly(ethylene-co-vinyl acetate) [140,141], poly(butylene succinate) [142], poly(butylenes-adipate-co-terephthalate) [143], polyhydroxyalkanoates [144,145] and polyacrylates [146,147]. However, the most reported studies on blends have been on PLA of different enantiomer concentrations [148]. Especially, the stereocomplexation of the enantiomerically pure PLLA and PDLA has been extensively studied because of the increased melting temperature and improved mechanical properties [77,149–152]. None of these attempts have led to the obtention of a big enough simultaneous thermal and impact resistance improvement. Therefore, the study of PLA based compounds with enhanced properties is still being studied.

2.4.2. Reactive extrusion (REx) of PLA based blends

Due to the inherent low entropy of polymers, the melt-mixing among them usually results in an immiscible blend system, characterized by a coarse and unstable phase morphology, and poor adhesion between the phases. To overcome these limitations, compatibilization is required, which should reduce the interfacial tension, stabilize the blend phase morphology against coalescence, and enhance the adhesion between the phases [153,154].

When a chemical reaction is carried out during extrusion, the process is called reactive extrusion (REx). The reaction can be of varied nature, including polymerization, branching, chain extension or reactive compatibilization. For example, the technology used by Futerro to polymerize lactide to polylactide is based on REx, different reactive agents are commonly used to tune melt viscosity of thermoplastics inducing branching, recent efforts to increase the molecular weight of recycled PET by chain extension are based on REx, etc. Hence, REx is a very promising technique to obtain enhanced properties in blends, especially for the polymer couples that do not lead to interesting properties by simple physical blending due to immiscibility. For example, concerning PLA, REx has been shown to be an interesting technique to obtain improved properties on PLA/ABS blends using SAN-GMA as reactive agent [155], PLA/PCL by using coupling agents and catalysts [156–158], PLA/TPS by maleic anhydride or isocianates [159–165], or PLA/PBAT blends by inducing transesterification using $Ti(OBu)_4$ as catalyst [166]. Besides, melt modification of PLA by peroxides has been found to cause drastic changes in its properties. Branching has been suggested to be the dominating structural change in PLLA at peroxide amounts in the range of 0.1-0.25 wt% and also crosslinking at peroxide additions above 0.25 wt% [68]. The peroxide reactions increased the melt strength. Morphological changes occurred in the peroxide modified PLLA as a result of a reduced crystallization rate, which resulted in a faster hydrolytic degradation. The tensile modulus was reduced and a more flexible material was obtained [167].

2.4.3. Crystalline PLA

Owing to the chiral nature of lactic acid (L and D) and the corresponding lactides, different PLA architectures are obtained by ring opening polymerization. The crystallization rates, maximum degree of crystallization and melting temperature of PLA are strongly dependent on the L/D ratio [168–170]. It is generally considered that for PLA mainly based on L-lactic acid, the incorporation of D-lactic acid in proportions above around 7% prevents or strongly limits polymer crystallization [56]. According to the L/D ratio, amorphous or semi-crystalline PLA can be synthesized and, consequently, strong variations on thermal, mechanical and barrier properties can be obtained [57,58]. Semicrystalline PLA shows some improved properties when compared to amorphous PLA, especially regarding thermal

resistance, which is one of the limiting properties of PLA to enter the semidurable applications segment. However, to achieve high crystallization rates, it is necessary to improve both nucleation and growth steps. The nucleation density could be increased by the addition of nucleation agents, and the growth step could be accelerated by adding plasticizers that could improve polymer chain mobility [171,172]. In the literature different types of nucleating agents such as talc, clay, calcium carbonate, nanotubes, fullerenes, polymers like PDLA and low molar mass organic compounds like ethylene bis(stearamide) (EBS) have been reported to be very effective for seeding the crystallization of PLLA [57,168,173–180]. The main interest of PDLA as nucleating agent for PLLA is linked to the creation of stereocomplex crystals during cooling, which would act as nucleating sites for the subsequent homochiral crystallization [77,181–184]. The construction of stereocomplex crystals require long enough L-lactic acid segments to meet D-lactic acid segments of PDLA polymer chains [77]. The effect of the molecular weight and fraction of PDLA on the nucleation and homo-crystallization rate of PLLA has also been reported in the literature [183,184]. EBS is an organic compound with a low molar mass and a melting temperature at around 140 ºC, which crystallizes very quickly while cooling from the melt. These EBS crystals act as nucleating agents during the subsequent crystallization of PLA [180]. Besides, plenty of other nucleating agents have been studied for PLA, as summarized by Zhao et al. [185].

2.4.4. Fibre reinforced PLA

Different type of fibres can be used as reinforcement of PLA in order to overcome its low thermal resistance besides increasing stiffness. Even though synthetic fibres have been studied with PLA [186,187], natural fibres such as the lignocellulosic ones have attracted a lot of interest during the last decade because they are a more environmentally conscious alternative [188–191]. Natural fibres are abundant around the word and they exhibit many advantages as the biodegradability, fair specific mechanical properties due to their low density and its ease for processing [188–190]. In this context, PLA has been extensively used for preparing fully biobased and biodegradable composites based on natural fibres [188,192]. The performance of fibre reinforced polymeric composites depends not only on the strength of the fibre and the polymeric matrix, but also on the fibre/matrix interface

adhesion because interfacial debonding is one of the most usual failure modes [193–195]. This type of failure is due to a poor interface adhesion between the fibre and the matrix, which leads to an inefficient stress transfer under load, hence resulting in low mechanical strength. Indeed, the main disadvantage of lignocellulosic fibres is the poor interfacial adhesion with PLA [188,192]. Therefore, there is a need to modify the surface of the fibre before mixing them with PLA and several methods to do so can be found in the literature [188,192].

On the other hand, the addition of nanofillers represents another interesting way to extend and improve the properties of PLA in order to prepare high-performance polymer nanocomposites. Due to the nanometric size of nanofillers, nanocomposites could present unique outstanding properties when compared to their microcomposite counterparts [196]. A fine dispersion and uniform distribution of nanoparticles within the PLA matrix is essential in order to maximize the matrix-reinforcement interfacial area and thus improve the properties of PLA. The most investigated nanofillers have been carbon nanotubes (CNTs), montmorillonite (MMT) and cellulose nanocrystals (CNC). Concerning PLA-based nanocomposites, Raquez et al. published a comprehensive review which highlights the main researches and developments [197].

Chapter 3. Modification of PLA with PMMA by melt blending and reactive extrusion (REx)

3.1. Introduction

Poly(methyl methacrylate) (PMMA) is a synthetic polymer with good chemical and physical properties. There is little scientific literature regarding PLA/PMMA blends and most of papers are for blends prepared by solution methods [147,198–201]. However, two studies of PLA/PMMA blends prepared by melt processing can be found in the literature [202,203] but reported results seemed to be contradictory. Samuel et al. [202] observed that all PLA/PMMA blends prepared by melt compounding were miscible. PLA/PMMA blends prepared via melt processing were also studied by Le et al. [203]. They concluded that the obtained blends were immiscible and regions of co-continuous structures were identified using SEM images.

In this chapter, melt blending of PLA with PMMA was carried out using a semi-industrial twin screw extruder and the characterization of different blends is presented and compared with the scarce results reported in the literature. Phase structure, morphology, thermal properties and mechanical properties of obtained blends were studied. Flory–Huggins interaction parameter of PLA/PMMA blends was estimated using the solubility parameters calculated by group contribution method according to Small and Van Krevelen. An attempt was made to relate miscibility, morphology and properties in the studied blends.

On the other hand, the effect of the addition of poly(styrene-co-glycidyl methacrylate) (P(S-co-GMA)) copolymer on the rheology, phase morphology, thermal stability, mechanical properties and impact resistance of melt compounded PLA/PMMA 80/20 (%wt) blend was studied, too.

3.2. Experimental

3.2.1. Materials

PLA was purchased from NatureWorks LLC (Ingeo™ 3051D, M_n= 106.000 g/mol; PDI: 1.7; ≈4.6% D-lactate) and PMMA was purchased from Evonic ROM GmbH (PLEXIGLAS® zk5BR, M_n= 70000 g/mol; PDI: 2.3). Molecular weights and molecular weight distribution were determined by GPC. Poly(styrene-co-glycidyl methacrylate) copolymer (CAS: 25167-42-4; M_n= 29.000 g/mol; Đ: 1.9) was kindly supplied by Macro-M (Kuo Group). NMR ^{13}C analysis indicated that copolymer composition consisted of 80% styrene and 20% methacrylate, and glycidyl substitution was present at 50% of the methacrylate groups. Fig. 3-1 shows the molecular structure of the copolymer.

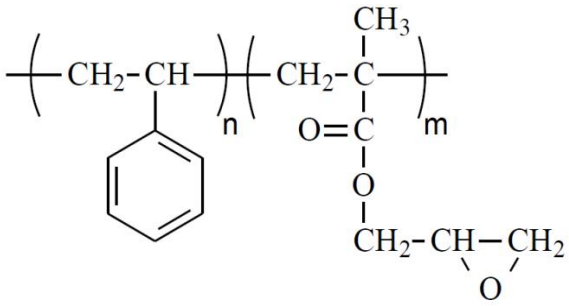

Fig. 3-1. The chemical structure of poly(styrene-co-glycidyl methacrylate).

3.2.2. Sample preparation

PLA/PMMA blends with weight ratio of: 100/0, 80/20, 60/40, 50/50, 40/60, 20/80 and 0/100 were prepared by means of a Brabender DSE 20/40 corrotating twin screw extruder (Ø=20mm, L/D=40). Manually premixed pellets were fed to the extruder using a gravimetric feeder at a constant 2 kg/h rate. Screws were configured with three separated high shear mixing stages based on kneading blocks, a vacuum aided venting zone after the third mixing stage and distributive mixing screw elements at the final stage (Fig. 3-2).

Fig. 3-2. Screw configuration used for melt compounding.

Prior to extrusion, all systems were dried for 4h at 80 ºC by a dehumidifying dryer. Neat PLA was extruded at 200 ºC and neat PMMA at 240 ºC, the lowest recommended processing temperature for this grade. Due to the difference on the recommended processing temperatures of both polymers, all blends were extruded at 215 ºC and 180 rpm. Obtained blends were dried for 12h at 50 ºC and moulded in a full electric DEMAG IntElect injection machine at 60 mm/s injection rate (600-700 bar injection pressure) to obtain 90x90x2 mm^3 platelets. Samples for FTIR, DSC, DMA and impact tests were cut from the platelets. On the other hand, V type specimens (ASTM D638) for tensile tests were injected at 300 bar injection pressure by means of a Haake MiniJet II injection machine. Neat PLA, all blends and neat PMMA were injection moulded at 200 ºC, 215 ºC and 240 ºC, respectively.

In addition, PLA/PMMA 80/20 (%wt) based systems containing 1, 2, 3 and 5 grams of P(S-co-GMA) copolymer per hundred grams of PLA/PMMA blend were prepared by reactive extrusion (REx); subsequently designated as 1, 2, 3 and 5 pph. Produced pellets were dried for 12h at 50 ºC and then injection moulded in a Haake MiniJet II (8s of injection plus 25s holding time at 300 bar) to obtain V type specimens (ASTM D638) for tensile and impact tests. Mould temperature was set at 25-30 ºC.

3.2.3. Characterization techniques

The molecular weight and molecular weight distribution were determined by Gel Permeation Cromatography (GPC) with a PerkinElmer chromatograph equipped with a binary pump and a refractive-index detector. The mobile phase was THF and elution rate of 1 mL/min at 30 °C was used. The separation was carried out with four Phenomenex columns, 10^5 Å, 10^3 Å, 100 Å and 50 Å, with 5 μm particle size. The columns were calibrated with polystyrene standards before the measurements according to standard

procedures, Mark-Houwink constants taken from literature were used, K_{PLA}=0.0153 mL/g, α_{PLA}=0.759 and K_{PMMA}=0.00944 mL/g, α_{PMMA}=0.719 [204,205]. Fourier Transform Infrared transmission (FTIR) measurements were performed by a Nicolet Protégé 460 spectrometer from 400 to 4000 cm^{-1}. FTIR spectra were collected by performing 32 scans with a resolution of 4 cm^{-1} on hot pressed films. Differential Scanning Calorimeter (DSC) was used to determine thermal properties of all systems. Samples of 6 to 8 mg were analysed. Two heating scans were performed from -10 to 250 ºC at a heating rate of 10 ºC/min using a TA Instruments Q100 model, previously calibrated by indium and sapphire standards following the indications of the supplier [206]. Dynamic Mechanical Analysis (DMA) was carried out in a Rheometrics Solid Analyzer RSA II applying a 2% deformation at a 1Hz frequency by dual cantilever bending method. Specimens with 50x5x2 mm^3 dimensions cut from injection moulded platelets were heated from 35 to 140 ºC at a rate of 2 ºC/min. Tensile tests were carried out according to ASTM D638 standard (1 mm/min) by means of a MTS Insight electromechanical tensile test machine equipped with a 2.5 kN load cell and a contact mechanical extensometer. Unnotched Charpy impact tests were carried out by means of an ATS faar IMPats-15 impact pendulum with a 2J hammer using a support span of 40 mm. Impact fractured surfaces coated with Au were analyzed by a Hitachi S-4800 Field Emission Scanning Electron Microscope (FE-SEM). Even though sample geometry used for impact test did not follow any standards, for comparison purposes injection moulded V type specimens were cut to have the length of 63.5 mm and the constant section of 3.18 x 3.29 mm^2. Thermogravimetric measurements were carried out using samples of about 10 mg on a TA Q50 thermobalance. Mass loss was recorded at 10 ºC/min during a heating scan from 30 ºC to 600 ºC in N_2 atmosphere.

Regarding the systems prepared by REx, rotational rheometry analysis was carried out using a HAAKE MARS III device, equipped by parallel plates. Hot pressed samples of PLA/PMMA 80/20 wt% were die-cut to obtain specimens (Ø=20 mm, 400-500 mg) and 1, 2, 3 and 5 pph of P(S-co-GMA) copolymer was added to monitor the reaction. The temperature of 215 ºC was set, the same as for extrusion process. The radius of the plates (r) and the gap between the plates (h) were 10 mm and 0.5 mm, respectively.

The apparent viscosity was calculated from the shear stress and shear strain values by Eq. 3-1, Eq. 3-2 and Eq. 3-3.

$$\eta_{ap} = \frac{\sigma}{\dot{\gamma}_{ap}} \quad \text{Eq. 3-1}$$

$$\sigma = \frac{2}{\pi r^3} M_d \quad \text{Eq. 3-2}$$

$$\dot{\gamma}_{ap} = \frac{r}{h} x \frac{2\pi n}{60} \quad \text{Eq. 3-3}$$

Where r and h are the radius of the plates and the gap between the plates, respectively; M_d is the torque (Nm); and n is the rotating speed (min^{-1}).

3.3. Results and discussion

3.3.1. PLA/PMMA blends.

3.3.1.1. FT-IR Analysis

FTIR spectroscopy is a powerful tool for investigating polymer blends. Differences in band positions and shapes in the spectra suggest interactions between two polymer components. Fig. 3-3 shows FTIR spectra of neat polymers and PLA/PMMA blends.

The differences between PLA and PMMA spectra were in the ranges 2000-1500 and 1050-750 cm^{-1}. The stretching mode of the carbonyl groups showed an absorption band at 1749 cm^{-1} and 1724 cm^{-1} for PLA and PMMA, respectively. A clear evolution of this band was noticeable in the spectra of the blends, increasing PMMA content in the blend the intensity of the band at 1724 cm^{-1} was higher. PMMA showed a band at 987 cm^{-1} due to C-C stretching influenced by CH_2 bending and a band at 841 cm^{-1} related to CH_2 rocking band [207,208] which were not present in PLA spectra. The band at 866 cm^{-1} was related to skeletal stretching and CH_3 rocking of amorphous PLA [209] and it was not present in PMMA spectra. There were no obvious changes in PLA and PMMA band positions in

blends, which suggested that interactions between the two components are weak or negligible [210].

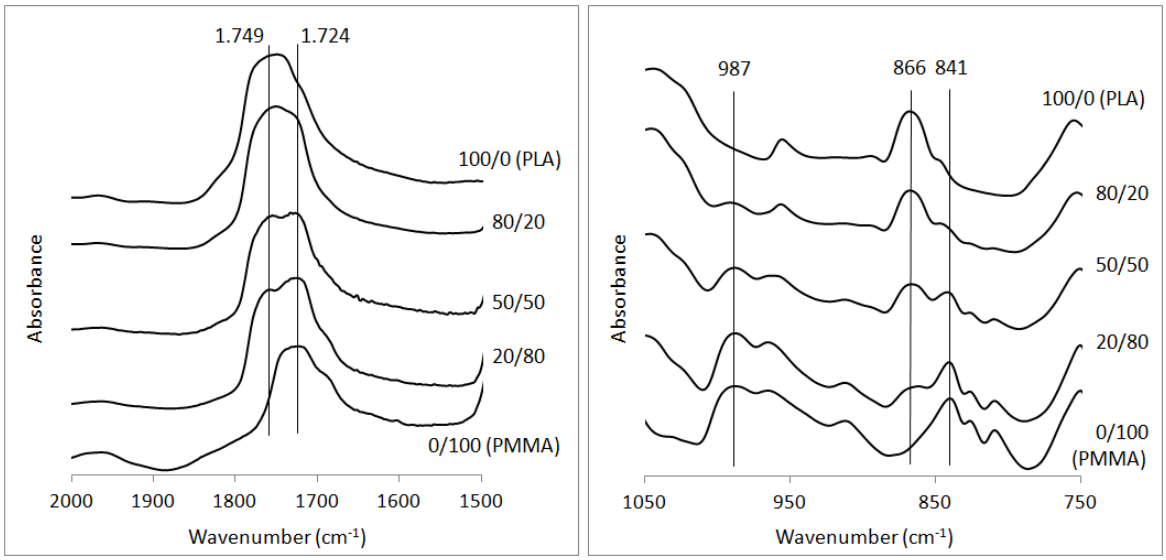

Fig. 3-3. FTIR spectra of all systems.

3.3.1.2. Miscibility of PLA/PMMA blends

Injection moulded platelets are shown in Fig. 3-4. Neat PMMA platelet was transparent due to the unique amorphous phase. Neat PLA platelet was almost transparent which indicated a very low crystallization degree. All blends were translucent suggesting the coexistence of more than one phase in all PLA/PMMA blends.

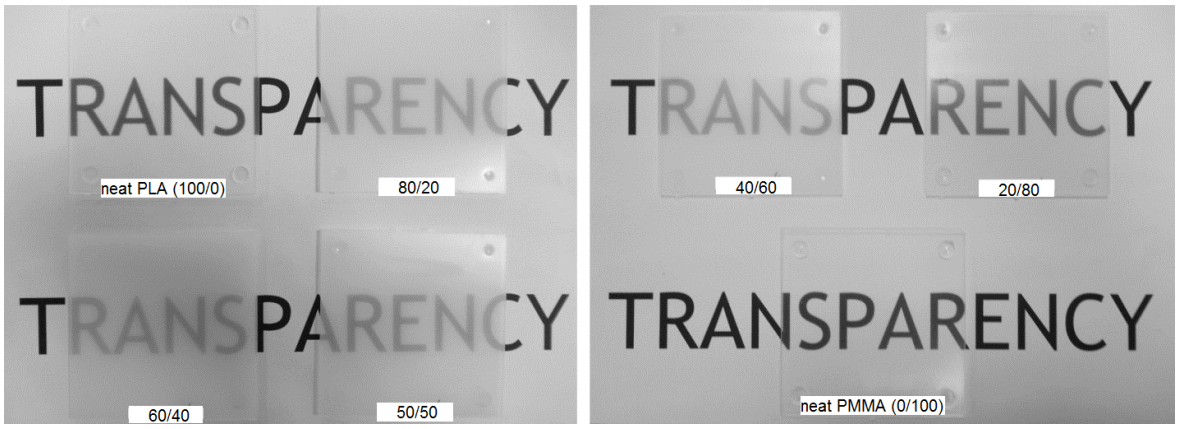

Fig. 3-4. Injection moulded platelets for all systems.

The miscibility of PMMA and PLA was studied by Differential Scanning Calorimeter and Dynamic Mechanical Analysis. Glass transition temperature (T_g) of a polymer blend is one of the most important criteria to study the miscibility of its components. Miscibility between two polymers in the amorphous state is characterized by the presence of a single T_g intermediate between those of the two components. On the contrary, immiscibility of two polymers is demonstrated by retention of the T_g values of both individual components [198,211]. Fig. 3-5 and Fig. 3-6 show the first and second DSC heating scan thermograms for all systems, respectively.

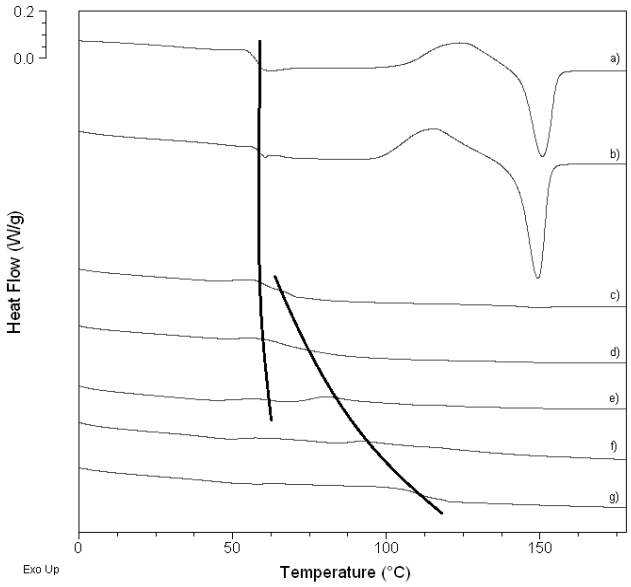

Fig. 3-5. DSC first heating scan thermograms: a) 100/0 (neat PLA), b) 80/20, c) 60/40, d) 50/50, e) 40/60, f) 20/80 and g) 0/100 (neat PMMA).

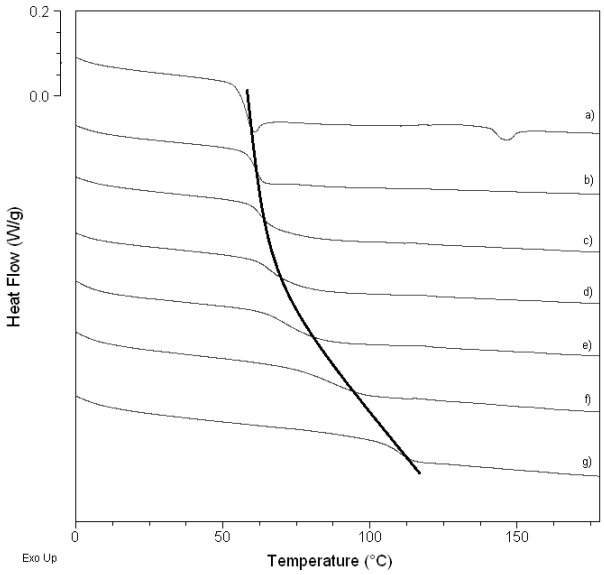

Fig. 3-6. DSC second heating scan thermograms: a) 100/0 (neat PLA), b) 80/20, c) 60/40, d) 50/50, e) 40/60, f) 20/80 and g) 0/100 (neat PMMA).

First and second scan thermograms were completely different. In Fig. 3-5 two T_g were observed whereas in Fig. 3-6 only one T_g was observed. In the first scans, the T_g of PLA remained almost constant at around 58-65 ºC until weight ratio reached 50/50, while the T_g of PMMA decreased from 107 to 65 ºC more rapidly. Hence, T_g variations of PMMA-rich and PLA-rich phases were very different. This peculiar behaviour seemed to indicate that interactions and the miscibility in PLA rich phases and PMMA rich phases were different and depend on blend composition. T_g variations observed in the first scans could indicate that PMMA-rich phases showed better miscibility than PLA-rich phases ones.

Fig. 3-7 shows the evolution of tanδ as a function of blend composition. A clear peak related to the blend major component T_g was observed and in some compositions a shoulder was noticed related to the blend minor component T_g.

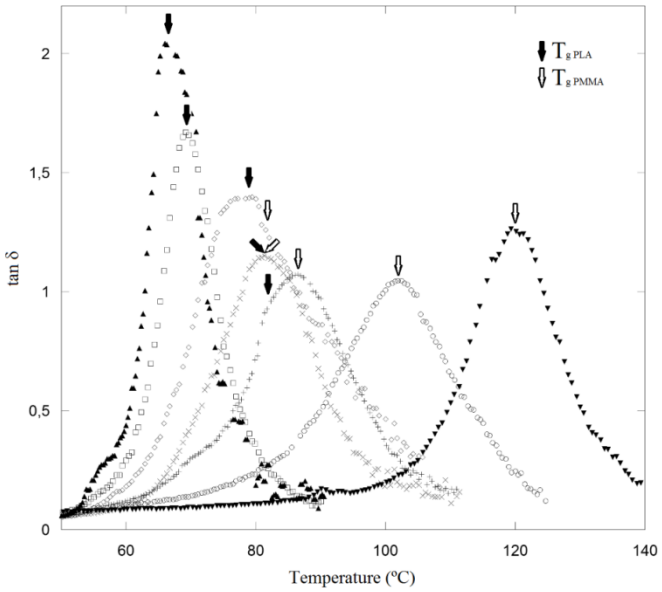

Fig. 3-7. The influence of PMMA content in the evolution of blends tanδ: ▲100/0(neat PLA), □80/20, ◊60/40, ×50/50, +40/60, ○20/80 and ▼0/100 (neat PMMA)

Partial miscibility of PLA and PMMA was demonstrated by a clear displacement of the glass transition temperatures of components in the blends. The peak and shoulder locations varied with the blend composition and the glass transition temperature of PLA increased as the proportion of PMMA in the blend was increased, indicating that after melt blending PLA and PMMA certain miscibility was achieved. From the analysis of the tanδ peaks it was observed that neat PLA and 80/20 blend had relatively similar full widths at half maximum (FWHM) (Table 3-1), which has been related to the temperature range which is needed to gain mobility during glass transition [147]. The FWHM of 50/50, 40/60 and 20/80 blends resembled to that of neat PMMA.

PLA/PMMA	FWHM (ºC)
100/0	9
80/20	10
60/40	20
50/50	18
40/60	19
20/80	19
0/100	16

Table 3-1. Full widths at half maximum of tanδ peaks.

In the first DSC scan thermograms, neat PLA and some blends showed some degree of crystallinity (X_c) which was calculated by Eq 3-4:

$$X_c = \frac{\Delta H_m - \Delta H_c}{\omega_f \Delta H_0} \quad \text{Eq. 3-4}$$

Where ΔH_m, ΔH_c and ω_f are the melting enthalpy, crystallization enthalpy, and weight fraction of PLA in the blend, respectively. Theoretical melting enthalpy value for a 100% crystalline PLA (ΔH_o) was estimated to be 93 J/g [66]. Thermal transition temperatures, crystallization enthalpies, melting enthalpies and the degree of crystallinity of different samples are reported in Table 3-2.

Neat PLA was almost amorphous and the addition of PMMA prevented the crystallization of PLA. Only when the content of PLA in blends was higher than 50% some crystallization took place during the heating scan (due to the low enthalpy, the melting peak of the 60/40 blend is hardly noticeable in Fig. 3-5). Zhang et al. mentioned that crystallization kinetics of PLA was highly restricted by amorphous PMMA [198]. The DSC thermograms of the second heating scans were completely different. In the blends PLA was amorphous and only one T_g was observed, located between the T_g of individual components. The T_g position changed with the composition of the blend indicating the miscibility between PLA and PMMA. The fact that no crystallization process was observed in the second DSC scan could be due to a better degree of miscibility between the components of the blend [198]. Besides, PLA grade used in this work has low optical purity (≈4.6% D- enantiomer in L-) resulting in a low rate of crystallization kinetics of PLA. Nam et al observed that crystallization rate of a PLA with D content of 0.8% was very slow [180].

Eguiburu et al. obtained similar results for PLLA/PMMA blends prepared by solution/precipitation method. They reported a clear difference on the miscibility degree of polymers from the first to second DSC heating scans. In the first scan two T_g were noticeable slightly different from the T_g of the homopolymers in the pure state. Only one T_g was observed during the second heating scan and T_g value increased as the PMMA content increased in the blend [147].

PLA/PMMA	Scan	T_g (ºC)	T_{cc} (ºC)	T_m (ºC)	ΔH_{cc} (J/g)	ΔH_m (J/g)	X_c (%)
100/0	1st	58 (65)	124	151	14.4	17.5	3.3
	2nd	58	-	146	-	1.0	1.1
80/20	1st	58 (68)	116	149	18.7	20.6	2.5
	2nd	62	-	-	-	-	0
60/40	1st	61-69 (77-80)	-	150	-	0.8	1.5
	2nd	63	-	-	-	-	0
50/50	1st	65 (81)	-	-	-	-	0
	2nd	65	-	-	-	-	0
40/60	1st	64-86 (82-85)	-	-	-	-	0
	2nd	71	-	-	-	-	0
20/80	1st	76-97 (103)	-	-	-	-	0
	2nd	87	-	-	-	-	0
0/100	1st	107 (121)	-	-	-	-	0
	2nd	110	-	-	-	-	0

Table 3-2. Thermal transition temperatures, crystallization and melting enthalpies and the degree of crystallinity of different samples. Values in brackets correspond to DMA data.

Only two works were found in the literature where PLA/PMMA blends were obtained by melt compounding. In contrast to the results reported in this work, Samuel et al. observed that all PLA/PMMA blends processed at 210 ºC were miscible since they observed a unique α-relaxation transition and a unique glass transition at intermediate temperature between pure PLA and pure PMMA. They blended PLA (M_w=218.000 g/mol) with two different PMMA grades with different average molecular weights M_n=52000 and M_n=37000, respectively. The molecular weight of PMMA used in our work was higher and even though the processing temperature was slightly higher (215 ºC) immiscible blends were obtained. DSC results confirmed that after heating the blends until the temperature of 250 ºC, miscible samples were obtained. The obtained results suggested that PLA/PMMA blends were miscible but the mixing process seemed to be controlled by the diffusion of PMMA chains. Increasing the temperature the diffusion of PMMA in the blends could be accelerated and this could be the reason for the miscibility after the first DSC scan. Le et al. [203] prepared PLA/PMMA blends using a single screw extruder at 200 ºC and 100 rpm. In agreement with the results reported in this work, they observed by SEM that the obtained blends were immiscible. Unfortunately Le et al did not report the molecular weight of PMMA.

For ideal systems that are miscible and amorphous over the whole composition range, the relationship between the T_g and the composition of the blend can be predicted by the Gordon–Taylor equation (Eq. 3-5) [198].

$$T_g = T_{g1} + \frac{k w_2 (T_{g2} - T_{g1})}{(w_1 + k w_2)} \qquad \text{Eq. 3-5}$$

Where ω_1 and ω_2 are the weight fractions, T_{g1} and T_{g2} are the glass transition temperatures of pure components and k is the adjustment parameter. In this work PLA and PMMA were components 1 and 2, respectively. *k* is an adjustable parameter which was related to the interaction strength between the components in the blend. The theoretical curve and experimental data obtained from the second heating of DSC best fitted when *k* was 0.24. Experimental T_g values obtained were below weight average (Fig. 3-8).

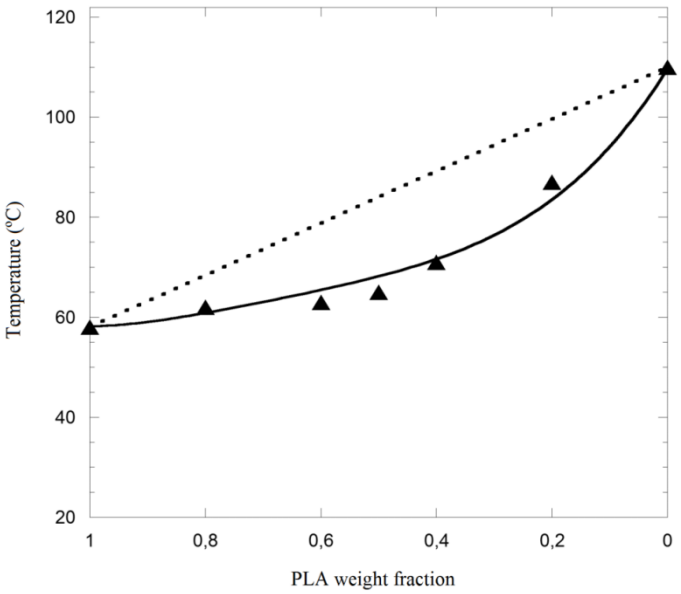

Fig. 3-8. Glass transition temperature vs. weight fraction of PLA: experimental DSC T_g values (▲);Gordon-Taylor adjustment curve for k=0.24 (line) and weight average T_g values (dots).

Although both polymers were miscible, this low value suggested that there was no strong interaction between PLA and PMMA macromolecules which agreed with FTIR results

obtained. Similar results were found in the literature for the same blend system prepared by solution method [198,199].

In polymer-polymer mixtures, the entropy of mixing is very small, regarding the enthalpy of mixing, miscibility generally requires some favourable interactions such as hydrogen bonding, donor-acceptor interaction, charge transfer, and so forth, resulting in a negative exchange interaction contribution to the free energy of mixing. However, for the PLA/PMMA blends, no such strong specific interaction existed and only some kind of weak dipolar interaction could take place owing to the chemical structure of two polymers [198]. Miscibility can also be studied by the differential solubility parameter (Δδ) of blend components. The solubility parameter of a given material can be calculated either from the cohesive energy (Eq. 3-6) or from the molar attraction constant (Eq. 3-7).

$$\delta = \sqrt{\frac{E_{coh}}{V}} \qquad \text{Eq. 3-6}$$

$$\delta = \frac{F}{V} \qquad \text{Eq. 3-7}$$

Where δ is the solubility parameter, E_{coh} the cohesive energy, F is the molar attraction constant and V is the molar volume of the repeating unit. The solubility parameters of PLA and PMMA were estimated (Table 3-3) according to the group contribution approaches described by Small and Van Krevelen [212].

Component	M_o (g/mol)	Density (g/cm^3)	δ_{Small} (J/cm^3)$^{1/2}$	δ_{VKrev} (J/cm^3)$^{1/2}$
PLA	72	1.25	19.6	18.61
PMMA	100.1	1.17	18.61	19.08

Table 3-3. Estimation of the solubility parameters of PLA and PMMA according to the group contribution approaches described by Small and Van Krevelen.

The differential solubility parameter values calculated for PLA/PMMA were Δδ=0.99 (J/cm^3)$^{1/2}$ and Δδ=0.46 (J/cm^3)$^{1/2}$ for Small and Van Krevelen, respectively. Two polymers are thermodynamically miscible when the difference is Δδ<5. As Δδ values obtained are

below, PLA and PMMA are thermodynamically miscible. However, taking into account Δδ values obtained it could not explain why partially miscible PLA/PMMA blends were observed during the DSC first heating scan, while miscible blends were observed at the second heating scan. Even though the approach has several limitations, the Flory-Huggins interaction parameter (χ_{12}) can be derived from the solubility parameter of the components using Eq. 3-8:

$$\chi_{12} = \frac{V_r}{RT}(\delta_1 - \delta_2)^2 + 0.34 \qquad \text{Eq. 3-8}$$

Where the δ_1 and δ_2 are the solubility parameters of the components, V_r is a reference volume, which corresponds to the molar volume of PLA repeating unit, R is the universal gas constant and T is the absolute temperature during blending process (473K). Using the solubility parameters estimated according to Small and Van Krevelen, Flory-Huggins interaction parameters calculated were 0.35 and 0.34, respectively. These similar values were below the critical value for miscible polymer blends, established at χ_{crit}=0.5 [212] suggesting that from a thermodynamically point of view PLA/PMMA blends should be miscible. However, the used grades of PLA and PMMA have high molecular weights and PMMA has very high viscosity [213] at the applied processing temperatures, which slows down the kinetics of mixing. Therefore, depending on the processing conditions, partially or completely miscible PLA/PMMA blends might be obtained, which is in agreement with previously reported results [202]. Hence, the obtained experimental results suggested that the mixing process of PLA/PMMA blends seems to be diffusion controlled.

3.3.1.3. Mechanical properties of PLA/PMMA blends

Fig. 3-9 and Fig. 3-10 show the influence of PMMA content in the tensile and impact properties of blends. Increasing the PMMA content in the blend resulted in a lower strength and modulus values. Regarding impact resistance, the blends with high PLA presence (80/20, 60/40) behaved like neat PLA, whereas the blends with high PMMA presence (40/60, 20/80) behaved like neat PMMA (Fig. 3-10).

Thus, the blends exhibited similar impact resistance to the neat polymers. Impact performance is mainly influenced by the phase structure of the blends. Therefore, these results suggested a phase inversion at 50/50 composition.

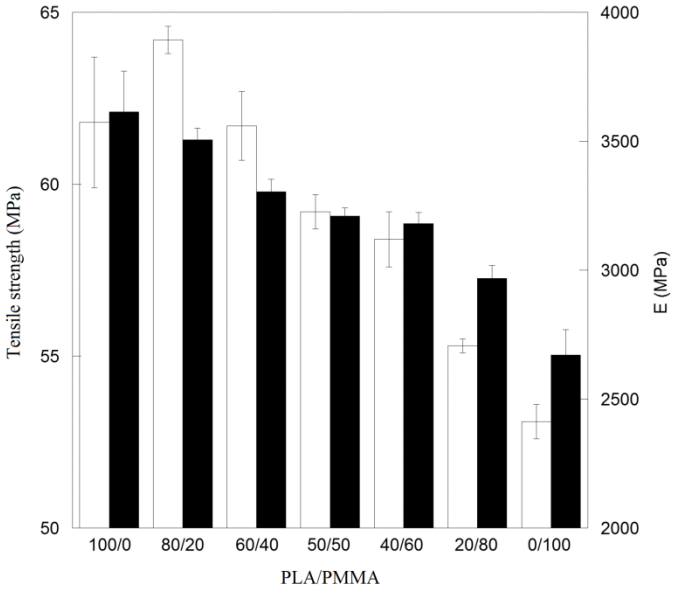

Fig. 3-9. The influence of PMMA content in the tensile properties: tensile strength (white columns) and modulus (black columns).

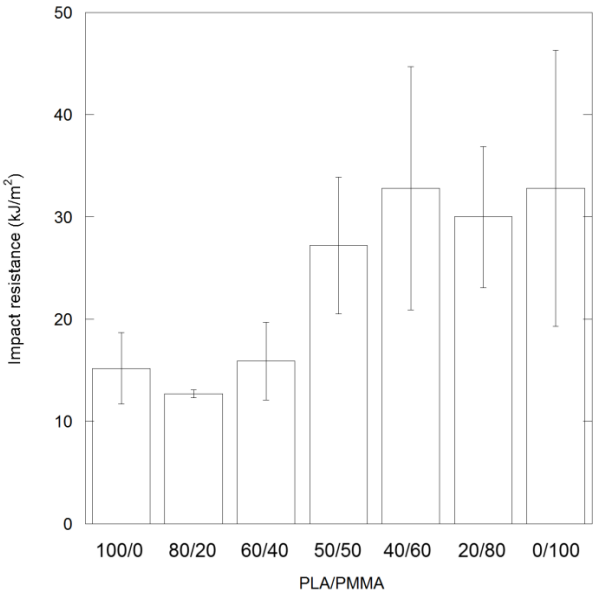

Fig. 3-10. The influence of PMMA content in the impact resistance.

3.3.1.4. Phase morphology of PLA/PMMA blends

Fig. 3-11a-g show SEM micrographs of fractured surfaces.

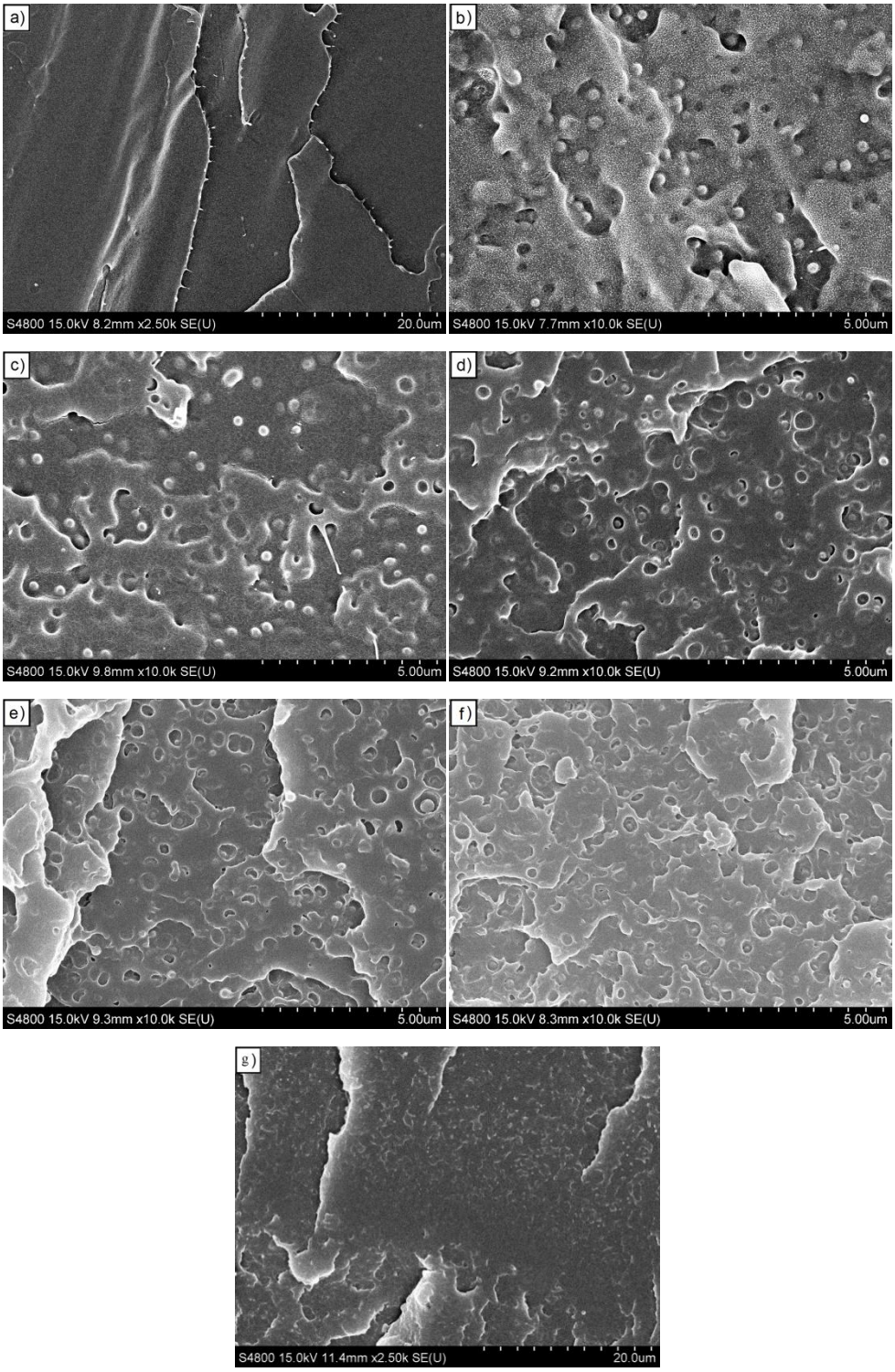

Fig. 3-11. SEM micrographs of fractured surfaces: a) 100/0 (neat PLA), b) 80/20, c) 60/40, d) 50/50, e) 40/60, f) 20/80 and g) 0/100 (neat PMMA)

Neat PLA (Fig. 3-11a) showed smooth fracture surface indicating a brittle failure mechanism. On the contrary, neat PMMA (Fig. 3-11g) showed a rougher fracture surface, indicating a more ductile behaviour. All blends showed roughened fracture surfaces, due to the ductility gained by the addition of PMMA. In all blends a sphere shaped dispersed phase of around 200-350 nm in diameter was observed evenly distributed in the continuous phase. These dispersed spheres were supposed to be PMMA-rich phases in blends with high PLA contents and PLA-rich phases in blends based with high PMMA contents. In contrast to the morphology observed in this work, Li et al. observed a co-continuous morphology probably because processing conditions and polymers molecular weights were different. Besides, they reported an average phase size of 25 μm while we obtained nanometre sized phase separation, which indicates more contact surface among the two phases and therefore higher compatibility.

Voids due to the removal of the dispersed phase and spheres with limited surface contact with the matrix were seen in the micrographs, indicating a poor interphase between the matrix and the dispersed spheres. Hence, limited interfacial adhesion can be expected. This is in agreement with the impact resistance of the blends, which showed similar impact resistance to the neat polymers, indicating that the dispersed phase was not able to enhance the impact resistance of the matrix in the blends. On the other hand, needle-like and wave-like were observed in high PLA content blend micrographs (Fig. 3-11a-c). These effects are very common in SEM micrograph of amorphous PLA [214–216], which can be easily overheated by the electron beam at high resolutions due to its low T_g. The two thermoplastic grades used in this work seem not to be completely miscible by melt blending at the mixing conditions used, which was in agreement with the results obtained by DSC (first heating scans) and DMA.

3.3.1.5. Thermal stability

TGA results (Fig. 3-12) show that degradation of neat PLA takes place in a temperature range from 310 ºC to 378 ºC giving a narrow peak of decomposition rate with its maximum at around 360 ºC. Similarly, thermal degradation of PMMA takes place between 310 ºC and 418 ºC, showing a maximum decomposition rate at around 375 ºC. When PLA is blended with PMMA, as the proportion of PMMA increases, a shoulder owing to its decomposition

becomes noticeable overlapped to the main PLA degradation peak. However, the maximum decomposition rate temperature remains unaltered at around 360 ºC.

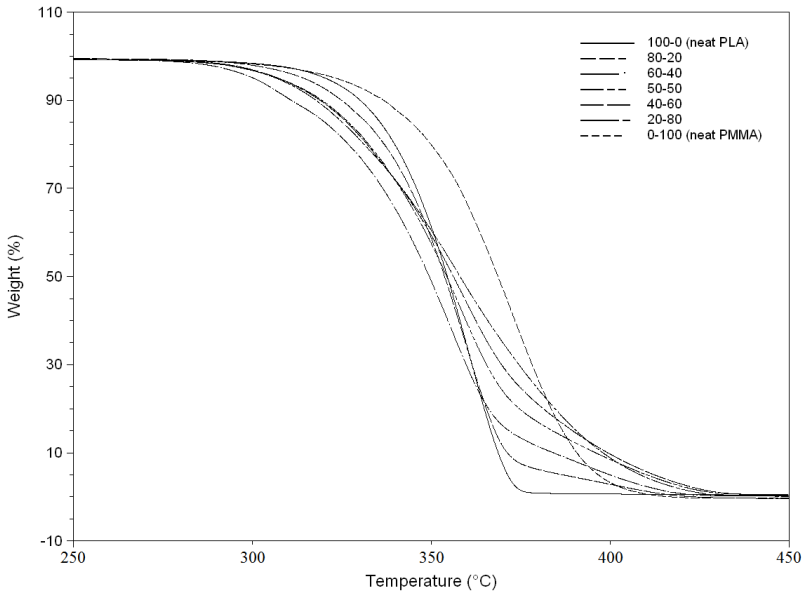

Fig. 3-12. Thermogravimetric analysis of blends.

3.3.2. Modification of PLA/PMMA blends by Reactive extrusion (REx).

Reactive processing with epoxy groups has been reported to improve the compatibility of PLA containing systems [217,218]. The reaction of the epoxy groups with PLA's carboxyl and hydroxyl end-groups can lead to branching and consequently enhances melt strength and some mechanical properties [219,220]. On the other hand, styrenic-glycidyl acrylate copolymers has been previously studied to cause chain extension of PLA in order to melt strengthen the neat polymer with the objective to enlarge its processing window [221] or enhance the extrusion and injection foamability of PLA [219,222]. Besides, glycidyl methacrylate based copolymers have been studied as reactive compatibilizer to improve interfacial adhesion between immiscible blends like PLA/PCL [223], PLA/ABS [123], PLA/SEBS [129], PLA/PBSA [224] or to improve the dispersion of nanoclays in a PLA matrix [225]. Core-shell structured GMA functionalised MMA-BA or MB-g-GMA copolymers have also been used to toughen PLA [226,227].

A clear displacement of T_g of the neat components in the PLA/PMMA blends was observed by DMA, indicating partial miscibility. The impact resistance exhibited by the blends was similar to that of the neat polymer they were rich in. SEM micrographs of PLA/PMMA blends showed a dispersed phase of around 200-350 nm in diameter evenly distributed in the continuous phase. However, the dispersed phase was not able to enhance the impact resistance of the matrix due to the observed limited interfacial adhesion. Therefore, to make PLA/PMMA blends suitable for engineering applications, toughness and impact resistance should be improved.

In this section, the effect of the addition of poly(styrene-co-glycidyl methacrylate) copolymer on the rheology, phase morphology, thermal stability, mechanical properties and impact resistance of melt compounded PLA/PMMA 80/20 (%wt) blend has been studied. As observed in the previous section of this chapter, this blend composition showed the highest tensile strength and elastic modulus among all compositions studied. However, it also showed low impact resistance due to the poor interfacial adhesion between the PLA-rich matrix and the dispersed PMMA-rich phase.

3.3.2.1. FT-IR Analysis

Fig. 3-13 shows FTIR spectra of the P(S-co-GMA) copolymer and PLA/PMMA (80/20) blends with different copolymer content.

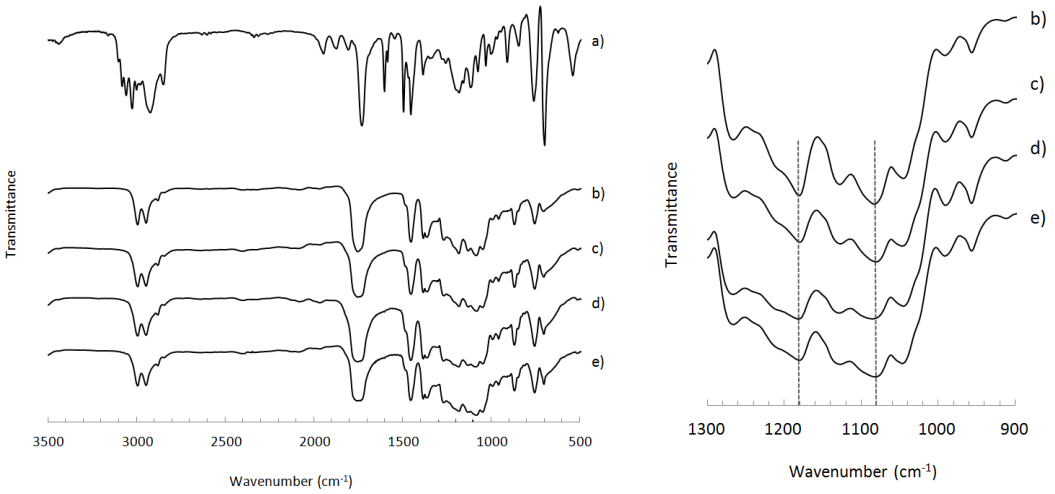

Fig. 3-13. FTIR spectra of a) P(S-co-GMA) copolymer, and PLA/PMMA (80/20) blend with different copolymer contents: b) without copolymer, c) 1 pph, d) 2 pph and e) 3 pph.

Styrenic groups in the P(S-co-GMA) copolymer showed absorption bands of aromatic C-H stretches at 3059 and 3025 cm^{-1}, aromatic ring breathing modes at 1600, 1493 and 1452 cm^{-1}, and out of plane C-H bending of monosubstituted aromatic ring at 757 and 698 cm^{-1}. On the other hand, the copolymer spectrum showed bands at 1728 and 1180-1113 cm^{-1} corresponded to C=O and C-O stretching of the methacrylate groups, respectively. The bands at 908 cm^{-1}, 1255 cm^{-1} and 849 cm^{-1} were related to glycidyl characteristic group [227–229]. The bands at 1083 and 1181 cm^{-1} were assigned to the C-O stretching of the -CH(CH_3)-OH end group of PLA [227]. These bands showed slightly lower intensity when the copolymer was added to the blend, regardless the amount of copolymer (Fig. 3-13). This loss in intensity suggested that some of the end groups of PLA seemed to react, leading to ester and ether linkages together with another hydroxyl group (Fig. 3-14). In addition a slight sharpening of the band at 700 cm^{-1} due to the presence of styrenic groups of the copolymer, no other important changes were noticeable in the spectra of PLA/PMMA blend modified with copolymer. Epoxy groups of copolymer could react with carboxyl and hydroxyl end-groups of the PLA chains [217,219] creating new ester groups. However, as unmodified PLA/PMMA blend contained ester linkages of PLA and PMMA, the presence of those new ester groups was not easily detectable by FTIR. In the literature it was reported that the reactivity of the epoxy ring was greater with carboxyl groups (Fig. 3-14a) than with hydroxyl groups (Fig. 3-14b) of polyesters [230–234].

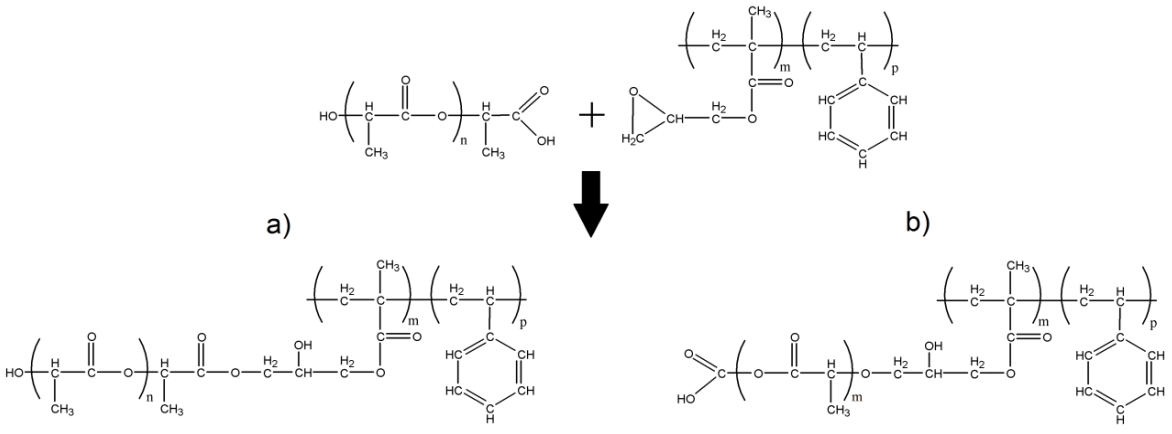

Fig. 3-14. Possible primary reactions between PLA and the P(S-co-GMA) copolymer.

These possible primary reactions would lead to chain extension, but grafting/crosslinking could happen by subsequent secondary reactions between the epoxy rings and the new side hydroxyl groups, inducing a branched or even crosslinked architecture, especially at high copolymer concentrations. Similar reaction mechanism was recently proposed by Ojijo et al. for PLA/PBSA blends in presence of styrene-acrylic oligomer with epoxy functionalities [224].

3.3.2.2. The effect of the addition of P(S-co-GMA) on the melt rheology

During the extrusion process of PLA/PMMA blends with copolymer a rise in melt viscosity was noticed indicating reactive extrusion. The higher was the amount of added copolymer, the higher was the torque needed to process the blend by the twin screw extruder. When processing PLA/PMMA blend with 3 pph of copolymer the needed torque was at the limit of the extrusion machine capacity. Hence, blends containing more than 3 pph of copolymer cannot be processed by extrusion.

The effect of the addition of copolymer on the melt viscosity of PLA/PMMA blend was analyzed by rotational rheometry. Although it was not possible to process by extrusion, a blend containing 5pph of copolymer was also studied by rotational rheometry.

The blend without copolymer showed a decrease in viscosity during the test, suggesting thermo-oxidative degradation. On the contrary, as the presence of the P(S-co-GMA) copolymer was increased, the viscosity of the blend showed an exponential rise. The reaction times observed by rotational rheometry were not equivalent of those needed when processing by twin screw extrusion, however, rheometric characterization evidenced that the viscosity of PLA/PMMA blends increased in presence of the copolymer (Fig. 3-15). Such increase in viscosity during reactive processing of polyesters have been attributed to chain extension/branching [235]. The blend containing 5 pph of copolymer showed a huge increase in viscosity, beyond the double of that showed by the compound containing 3 pph, being this viscosity value excessive for extrusion process.

Rheological results suggested that the molecular architecture of the blends was changed when the P(S-co-GMA) copolymer was added, leading to a more viscous melt probably due to chain extension and a partially branched architecture which restricted the polymer flow.

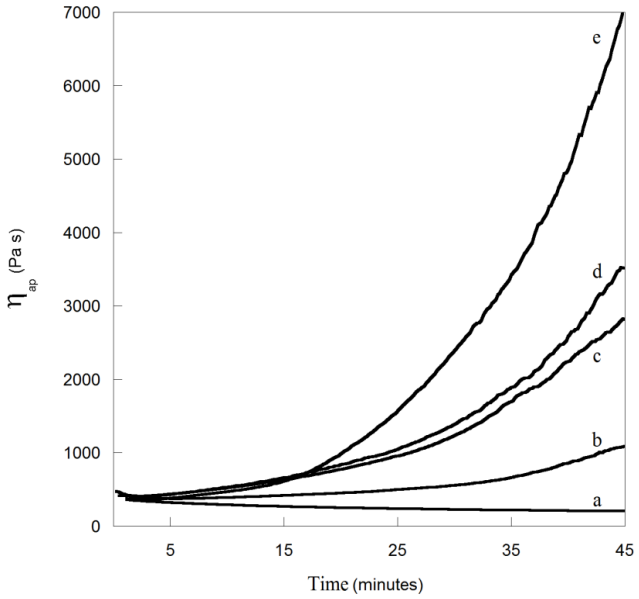

Fig. 3-15. Viscosity vs reaction time of PLA/PMMA blends with different copolymer content: a) without copolymer, b) 1 pph, c) 2 pph, d) 3 pph and e) 5 pph.

3.3.2.3. The effect of the addition of P(S-co-GMA) on the molecular weight distribution

The effect of the addition of P(S-co-GMA) copolymer on the molecular weight distribution of the blends is shown in Fig. 3-16.

The PLA/PMMA blend without copolymer showed a monomodal distribution. On the contrary, after the addition of the copolymer a bimodal distribution was detected, where the second peak corresponded to an important group of molecules with higher hydrodynamic volume. The evolution of the peaks indicated that the greater was the amount of copolymer added, the bigger was the population corresponding to higher molecular weights and smaller the population corresponding to lower molecular weights. The main peak, which corresponded to lower molecular weights, was attributed to the initial unreacted molecules and the second peak to the extended/branched population of polymers [236]. The weight average molecular weight and the polydispersity index increased as the presence of the reactive copolymer in the blend was increased (Table 3-4), which was in agreement with the results obtained by rheometry.

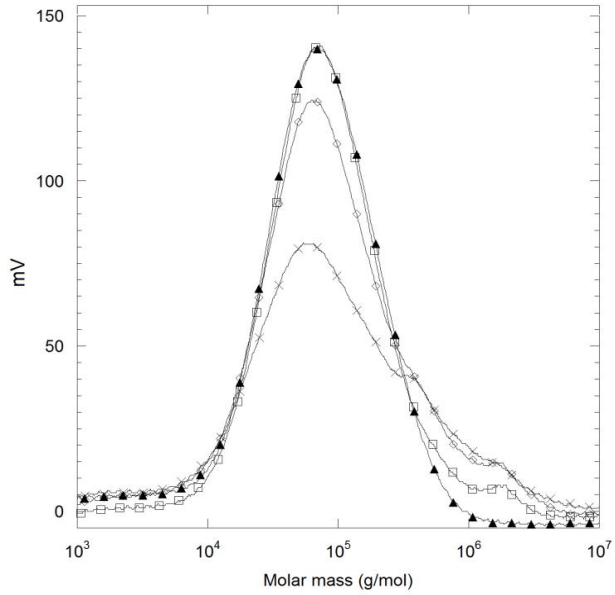

Fig. 3-16. Molecular weight distribution of PLA/PMMA (80/20) blend with different copolymer content: ▲without copolymer, □ 1 pph, ◊ 2 pph and × 3 pph.

Blend	M_n (g/mol)	M_w (g/mol)	PDI
without copolymer	51100	109500	2.1
1 pph	51000	113500	2.2
2 pph	49150	123700	2.5
3 pph	47600	137200	2.9

Table 3-4. Number average molecular weight (M_n), weight average molecular weight (M_w) and polydispersity index (PDI) for PLA/PMMA blends with different P(S-co-GMA) copolymer contents.

3.3.2.4. The effect of the addition of P(S-co-GMA) on thermal properties

Fig. 3-17 shows the first and second heating DSC scans for the P(S-co-GMA) copolymer. Two overlapped glass transitions were detected during the first heating scan. The first, related to the methacrylate segments, at 63 ºC and the second, related to the styrene segments, at 89 ºC. Besides, some reaction enthalpy was detected above 150 ºC, probably due to the reaction of the epoxy rings. On the other hand, only one T_g was detected at 81 ºC during the second heating scan. The reaction which took place during first heating scan seemed to create a different macromolecular structure. Results suggested that the miscibility

between methacrylate and styrene segments was improved because only one T_g was detected during the second heating scan.

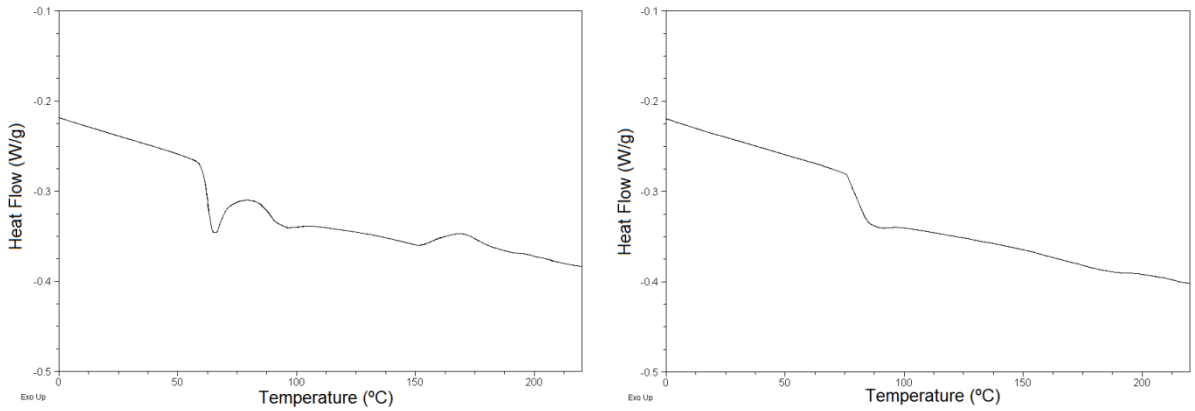

(a) (b)

Fig. 3-17. DSC. First (a) and second (b) heating scans of P(S-co-GMA) copolymer.

Unmodified PLA/PMMA blend showed one T_g at 58 ºC in the first heating run (Fig. 3-18). After the addition of the copolymer the glass transition temperatures of the blends raised to 63 ºC, regardless the amount of added copolymer. The glass transition temperature of a particular polymer increases together with the molecular weight until a maximum value. The higher molecular weight of the reacted blends, as observed by GPC, caused a reduction of chain-end concentration and therefore decreased the free volume. Bouzouita et al. studied different rubber-toughened PLA/PMMA formulations for injection-moulding processes upon the addition of a commercially available ethylene-acrylate impact modifier (BS) [237]. In all blends 17 wt% of ethylene-acrylate impact modifier was added and the ratio of PLA/PMMA was varied. By DSC technique they determined the glass transition temperatures of studied ternary blends (PLA/PMMA/BS) heating samples at 10 ºC/min. They obtained a T_g value similar or higher to 63 ºC only when the PLA content in the blend was 58 wt% or lower, which means that the PLA content of the studied blends was considerably lower than the PLA content in our work. On the other hand, all the blends showed very low crystallinity (3.5-7.3%), and the blends containing copolymer showed slower crystallization kinetics during cold crystallization than the blend without copolymer.

The slight decrease in the melting point of the PLA crystals shown by the blend with 3 pph copolymer compared with the unmodified PLA/PMMA blend could be a result of the imperfect crystal formation. The restricted chain mobility in the branched structure could lead to difficulties in the thickening of the lamella, hence, thinner and imperfect crystals with lower melting point could be formed [224]. The reaction happened due to the presence of copolymer seemed to reduce the chain mobility of PLA, leading to a higher glass transition and slower crystallization kinetics.

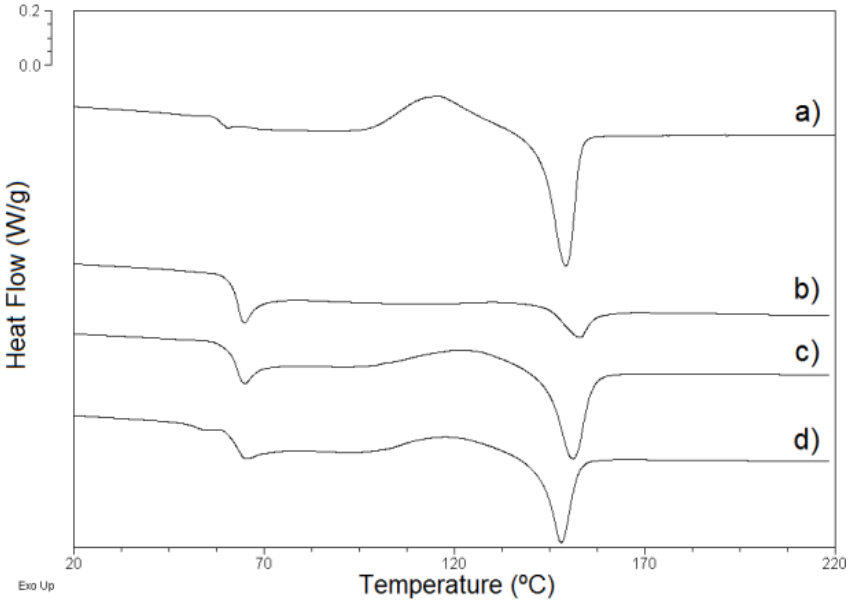

Fig. 3-18. DSC first heating scans of PLA/PMMA blend with different copolymer content: a) without copolymer, b) 1 pph, c) 2 pph and d) 3 pph.

3.3.2.5. The effect of the addition of P(S-co-GMA) on the phase morphology

SEM micrographs of impact-fractured surfaces of the neat PLA and neat PMMA and the blends are shown in Fig. 3-19. Neat PLA (Fig. 3-19a) showed a smooth fracture surface indicating a brittle failure mechanism, while neat PMMA (Fig. 3-19b) showed a rougher fracture surface, indicating a more ductile behaviour. The SEM micrograph of the unmodified PLA/PMMA blend showed the coexistence of two separated phases (Fig. 3-19c). The dispersed phase, which was supposed to be a PMMA-rich phase, was evenly distributed in the continuous phase, which was supposed to be a PLA-rich phase. The dispersed phase showed a limited surface contact with the continuous phase in the SEM micrographs, suggesting a poor interfacial adhesion between them [238]. Blends with P(S-

co-GMA) copolymer (Fig. 3-19d-f) also showed a dispersed PMMA rich phase of around 300-350 nm in diameter in the continuous matrix, confirming that phase separation was also observed after the addition of the copolymer. However, micrograph of PLA/PMMA with 3 pph copolymer (Fig. 3-19f) showed a more strained morphology, which indicated a better interfacial adhesion between both phases. Besides, a lower volume fraction of the dispersed PMMA-rich phase could be observed in this blend indicating that the addition of 3 pph of the copolymer improved the miscibility between both phases.

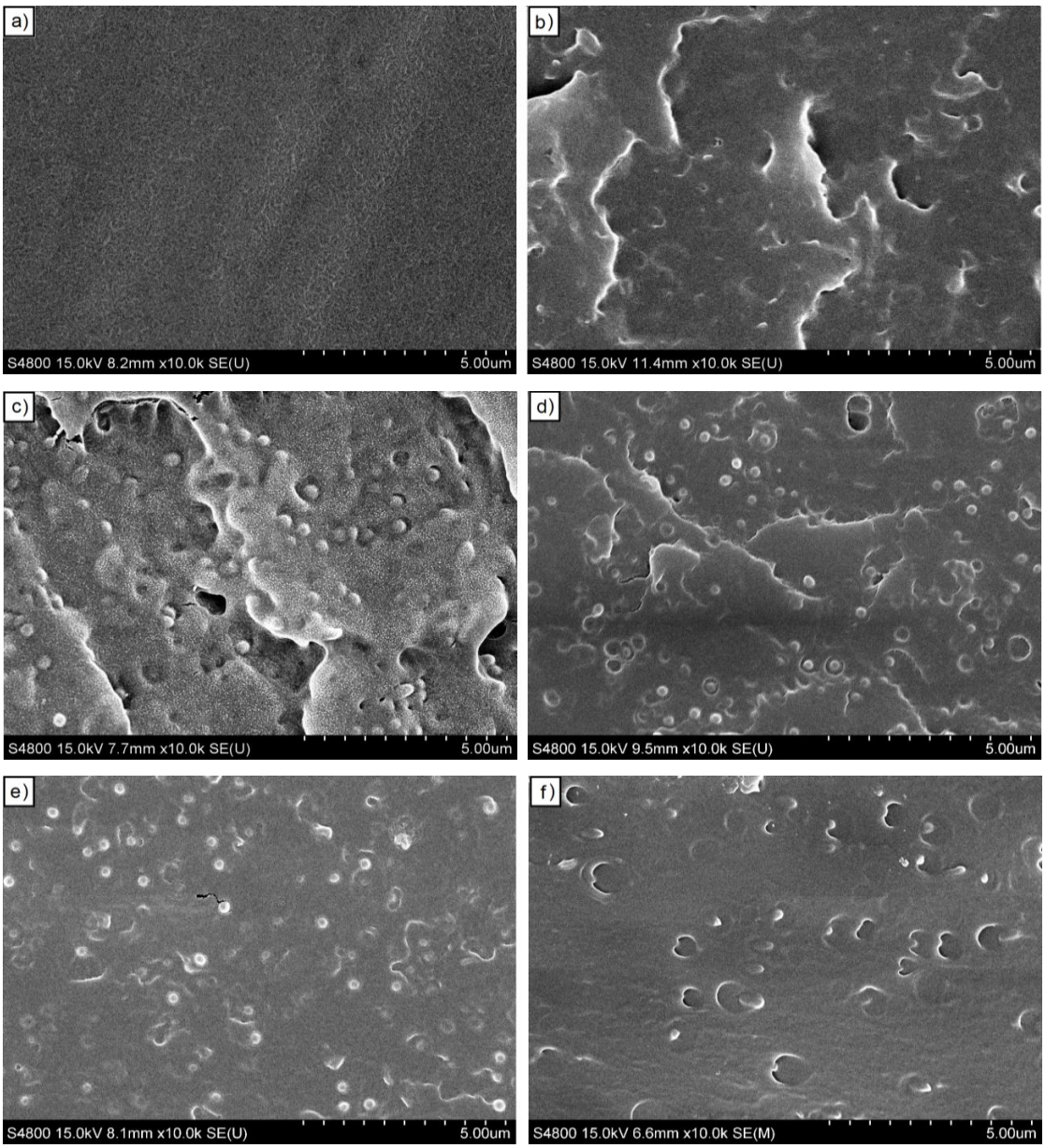

Fig. 3-19. SEM micrographs of: a) neat PLA, b) neat PMMA, c) PLA/PMMA (80/20) blend, d) blend + 1 pph copolymer, e) blend + 2 pph copolymer and f) blend + 3 pph copolymer.

3.3.2.6. The effect of the addition of P(S-co-GMA) on mechanical properties

Fig. 3-20 shows tensile stress vs. strain curves of neat PLA and PLA/PMMA blends with different copolymer content. PLA showed a brittle behaviour since samples broke before yield. Unmodified PLA/PMMA blend showed a slightly higher deformation at break than neat PLA and the failure happened after yield point. After the addition of P(S-co-GMA) copolymer the strain at break of this blend was hugely improved. Very low quantities, even 1 pph, were enough to improve the strain at break above >44%, which corresponded to the maximum measurable elongation of the mechanical extensometer that was used. All blends modified with copolymer showed a more ductile breakage, with a significant necking effect. After the addition of 3 pph of copolymer the modulus decreased 6.5%, while tensile strength remained constant and deformation at break increased more than 1300% with respect to neat PLA. The achieved values, 62 MPa and 3.4 GPa for tensile strength and modulus (Fig. 3-21), respectively, were higher than the values reported in the literature for PLA based blends [237,239].

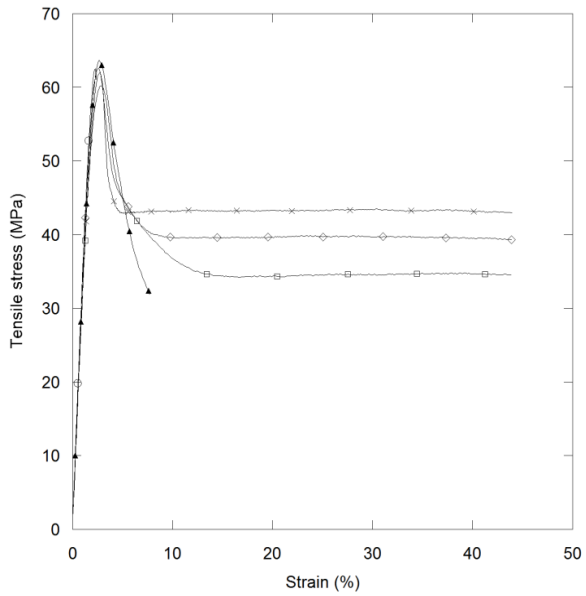

Fig. 3-20. Tensile properties of PLA/PMMA blend: ○ neat PLA, ▲80/20, □80/20+1pph, ◊80/20+2pph, ×80/20+3pph.

Notta-Cuvier et al. [239] studied different PLA based formulations with the aim of their potential use in automotive applications. They observed an increment of ductility of PLA

after the addition of tributyl citrate plasticizer when samples were tested at low testing rates of 1 and 2 mm/min. However, the material remained brittle when 5 and 10 mm/min testing rates were used. The high levels of ductility obtained were counterbalanced by drastic drops in apparent rigidity and the maximum nominal axial stress values with respect to neat PLA, 42% and 46% respectively. The obtained tensile strength and modulus values were around 31 MPa and 1.7 GPa, respectively. They also studied mechanical properties of ternary blends based on PLA, tributyl citrate plasticizer and a commercial impact modifier but the obtained results were not satisfactory. Finally they studied quaternary blends based on PLA, tributyl citrate, impact modifier and organomodified layered silicate. They obtained interesting levels of ductility but the apparent rigidity and the maximum nominal axial stress values decreased about 41% and 60%, respectively, with respect to neat PLA. The tensile strength and modulus values obtained were around 23 MPa and 1.7 GPa, respectively.

Bouzouita et al. [237] studied ternary blends based on PLA, PMMA and a commercial ethylene-acrylate impact modifier bearing epoxy moieties specifically designed for PLA. After the addition of 17 wt% of impact modifier to PLA/PMMA blends, a brittle to ductile transition was highlighted. However, the apparent rigidity and yield stress decreased about 30% and 35%, respectively, with respect to neat PLA. The tensile strength and modulus values obtained for 58 wt% PLA, 25 wt% PMMA and 17 wt% of impact modifier were 49 MPa and 2.5 GPa, respectively. Thus, the compound prepared in our work, which contained more than 75 wt% of polylactide, showed considerably higher tensile and modulus values than those reported in the literature for similar PLA based systems.

On the other hand, the addition of the copolymer improved the behaviour of the blends above yield point. The stress drop at yield point was decreased as the amount of copolymer in the system was increased. The blend with 3 pph of copolymer maintained 69% of its tensile strength above yield point (dropped from 62 to 43 MPa), while pure 80/20 blend failed at 50% after yield point (dropped from 64 to 32 MPa). This was important as the strain at yield remained constant around 2.7% when copolymer was added. Addition of copolymer slightly decreased tensile strength and modulus, even though the loss was not significant as the values were still similar to neat PLA.

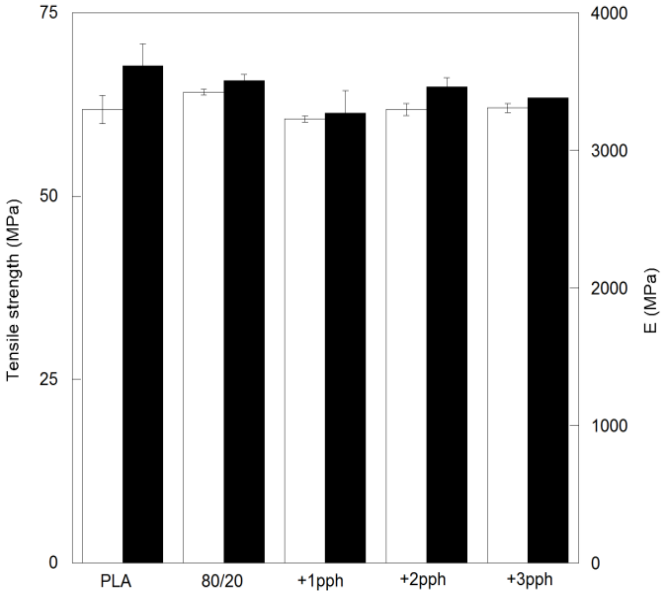

Fig. 3-21. Tensile strength (white columns) and moduli (black columns) (left) of neat PLA and PLA/PMMA (80/20) blend with different P(S-co-GMA) copolymer contents.

Although unmodified PLA/PMMA blend showed a rougher breakage surface than neat PLA ones, it showed slightly lower impact resistance (Fig. 3-22) due to the poor interfacial adhesion between the matrix and the dispersed phase [240]. After adding the P(S-co-GMA) copolymer to the blends, the impact resistance was improved. The blend modified with 1 pph copolymer showed a slightly higher impact resistance than unmodified PLA/PMMA blend, and the impact strength increased together with the copolymer content in the blend. The addition of 3 pph copolymer increased the impact resistance of PLA/PMMA blend from 12.7 to 24.5 kJ/m^2, which was an improvement of 93%. This improvement seemed to be related with the improved interfacial adhesion between PLA-rich and PMMA-rich phases achieved when 3 pph of copolymer was added, as observed in the SEM micrograph (Fig. 3-19f). Jaszkiewicz et al. [220] studied the effect of similar epoxidized styrene-acrylic copolymers (i.e.: CESA and Joncryl) on the impact resistance of PLA 3051D from NatureWorks LLC. They concluded that the addition of Joncryl led to no detectable improvement and more than 5% of CESA was needed to achieve detectable results. These results suggest that the addition of P(S-co-GMA) copolymer, although led to branching/chain extension of PLA, the obtained branching/chain extension was not enough to improve considerably the impact resistance. Therefore, the main reason for impact resistance improvement in PLA/PMMA blends modified with poly(styrene-co-glycidyl

methacrylate) copolymer seemed to be due to the interfacial adhesion improvement between the two phases present in blends, as observed in SEM micrographs.

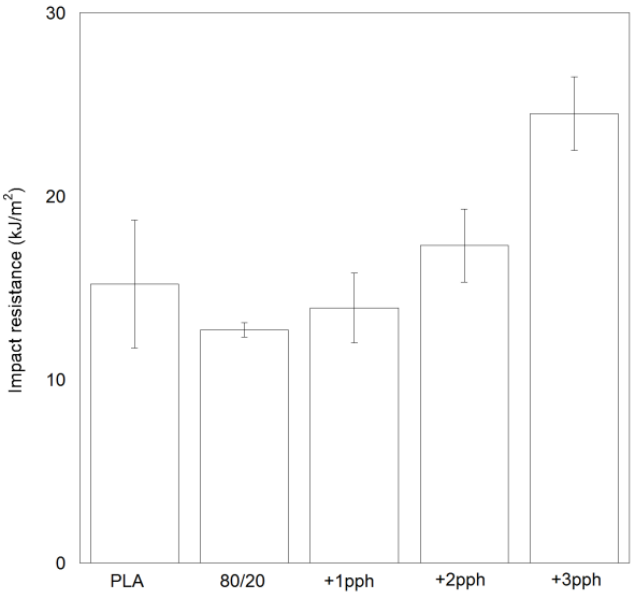

Fig. 3-22. Impact resistance (right) of neat PLA and PLA/PMMA (80/20) blend with different P(S-co-GMA) copolymer contents.

On the other hand, Notta-Cuvier et al. [239] increased the impact strength from 2.7 kJ/m^2 for unfilled PLA to 42.8 kJ/m^2 for a quaternary blend based on PLA, an impact modifier, tributyl citrate plasticizer and organomodified clay. However, for long term applications such as automotive parts, low molecular weight plasticizers have the undesirable tendency to migrate, thus material properties could change.

Bouzouita et al. [237] increased the impact strength of neat PLA from 3.4 kJ/m^2 to 24 kJ/m^2 after adding 17 wt% of impact modifier. Furthermore, they observed an optimum impact resistance of 44 kJ/m^2 when PLA was modified with PMMA and impact modifier for the composition of 58 wt% PLA, 25 wt% and 17 wt%. However, as mentioned previously, the impact strength improvement was linked to a significant drop in tensile strength and modulus values.

3.3.2.7. The effect of the addition of P(S-co-GMA) on thermal stability

TGA results showed that thermal stability of the PLA/PMMA blends was improved when copolymer was added (Fig. 3-23). Thermal degradation onset and offset temperatures were shifted to higher temperatures as the amount of added copolymer was increased (Table 3-5).

Compared with neat PLA, unmodified PLA/PMMA blend showed lower T_{onset} but higher T_{offset}, due to the higher thermal stability of PMMA. With the addition of P(S-co-GMA) copolymer the PLA/PMMA blend showed similar T_{onset} to PLA along with improved T_{offset} and temperature at maximum degradation rate (T_p). This enhancement might be related to the fact that PLA degraded and lost molecular weight during melt processing at 215 ºC, but the loss in molecular weight was counterbalanced by chain extension reactions when the blend was in presence of the copolymer. This is in agreement with what proposed by Ojijo et al. [224] who studied PLA/PBSA blends modified by a similar reactive styrene-acrylic oligomer (Joncryl® ADR 4368 CS) [123] However, they observed that T_{onset} values did not vary within the range of the tested oligomer concentrations, i.e. 0.3-1wt%. On the contrary, as it can be observed in Fig. 3-23, the concentration of P(S-co-GMA) had a clear influence on the thermal stability of the obtained blends, obtaining higher stability at higher copolymer concentrations. A possible explanation of the different performance of analyzed systems can be the different reactive group concentration in those systems.

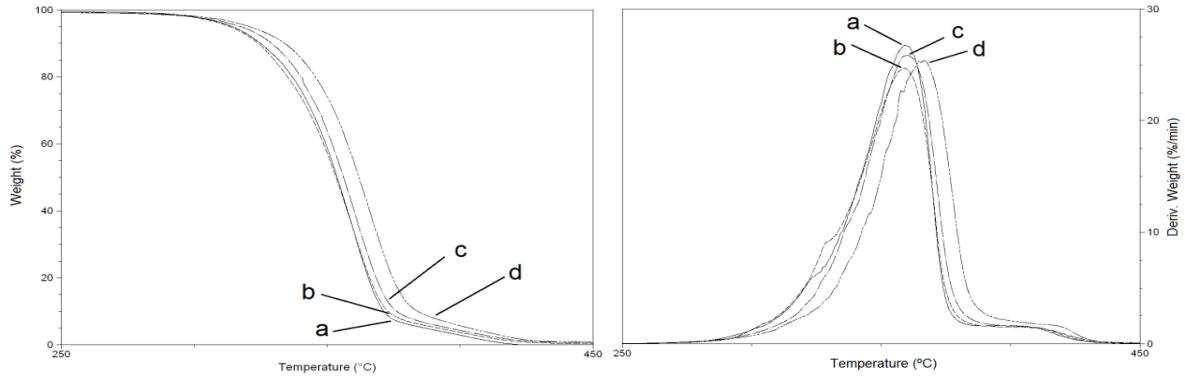

Fig. 3-23. Weight loss and derivative weight loss of PLA/PMMA (80/20) with different copolymer content: a) without copolymer, b) 1 pph copolymer, c) 2 pph copolymer and d) 3 pph copolymer.

Blend	T_{onset} (ºC)	T_{offset} (ºC)	T_p (ºC)
without copolymer	314	387	359
1 pph	314	391	359
2 pph	319	398	360
3 pph	321	403	367

Table 3-5. Thermal degradation of PLA/PMMA (80/20) blend with different P(S-co-GMA) copolymer contents.

3.4. Conclusions

The miscibility of PLA/PMMA blends prepared via melt processing seemed to be dependent to the mixing processing conditions (temperature and rpm) and polymers molecular weights. Injection moulded platelets showed that PLA/PMMA blends were translucent suggesting the coexistence of more than one phase. In the first DSC run and DMA results, even though two T_g were noticed, a clear displacement of T_g of neat components in the blends was observed, T_g increasing together with the presence of PMMA in the blend. This mutual influence on the mobility of molecules of each component indicated partial miscibility. SEM images showed the coexistence of two separated phases in all blends, spheres below 400 nm in diameter were evenly dispersed in a continuous phase. Thus, both thermoplastic grades used were not completely miscible at the mixing conditions used. Finally, the blends exhibited similar impact resistance to that of the neat polymer they were rich in. The impact resistance increased at least 78 % when the presence of PMMA in the blend was 50 wt% or higher, probably due to a phase inversion in the blend.

However, in the second DSC run blends showed only one glass transition temperature, located between the T_g of individual components, indicating miscibility of the same PLA/PMMA systems. Besides, no crystallization of PLA was detected in the second heating scan of the blends, probably due to a better blending degree of the components. Gordon-Taylor equation fitted well with the evolution of the T_g values of the blends when k was 0.24, suggesting that there was no strong interaction between PLA and PMMA, which is in agreement with the FTIR spectra. Flory-Huggins interaction parameters for PLA/PMMA were estimated using the solubility parameters. Interaction parameter values estimated were below the critical value for miscible polymer blends, which meant that from a thermodynamically point of view PLA/PMMA blends were miscible. However, the mixing process of PLA/PMMA blends seemed to be diffusion controlled process. Therefore, depending on the mixing conditions as well as polymers molecular weights used, partially or completely miscible PLA/PMMA blends can be obtained.

On the other hand, reactive extrusion of PLA/PMMA blends with poly(styrene-co-glycidyl methacrylate) was shown to be a good approach to overcome the intrinsic brittleness of PLA maintaining tensile strength and modulus values similar to neat PLA. PLA/PMMA blend, with polylactide content higher than 75 wt%, with improved mechanical and thermal

properties were obtained by this approach. All blends showed a dispersed PMMA-rich phase in a continuous PLA-rich phase. The addition of poly(styrene-co-glycidyl methacrylate) copolymer improved the interfacial adhesion between both phases improving the elongation capability and impact resistance of blends. After the addition of 3 pph of copolymer to the blend the deformation at break increased more than 1300% and the impact resistance increased around 60 % compared with neat PLA, and keeping the modulus and tensile strength values almost constant. This overall improvement of PLA's mechanical properties has not been achieved by other reported approaches like plasticization or addition of impact modifiers. Besides, the thermal stability of the blend was also improved since the onset temperature increased from 314 ºC for neat PLA to 321 ºC for the PLA/PMMA blend with 3 pph of copolymer. Regarding processability, viscosity was considerably increased by the addition of the copolymer; therefore, the amount of added reactive copolymer is a key factor in order to achieve melt-processable modified PLA/PMMA blends.

Chapter 4. Modification of the crystallization kinetics of PLA. Combined effect of plasticiser and nucleating agent

4.1. Introduction

Injection moulding is one of the most common polymer processing methods for durable and semidurable plastic products, which requires low cycle times in order to be economically feasible. Even though annealing of previously injected amorphous PLA can lead to crystallized products, the part can freely shrink and warp due to the evolution of the crystallized phase content. Thus, the formulation of fast crystallizing PLA compounds is still being intensely studied, supported by the aim of obtaining a dimensionally-controlled crystalline PLA product in one step.

Some works analyzed the combined effect of nucleating agents and plasticizers and proved that the crystallization process of PLA was accelerated by this approach [241–248]. However, the reported results are difficult to compare because PLA with different L/D ratio and/or molecular weight were used in each study. PLA grades with D-lactic acid content below 1% are commercially available nowadays, which have not been studied on plasticized and nucleated PLA polymer systems yet.

In this work, the isothermal crystallization behaviour at different temperatures after cooling from the melt of two plasticized PLA with different D-lactic acid content (i.e.: 0.5 and 4%) was studied in presence of different nucleating agents. PLA matrices were plasticized with dioctyl adipate (DOA), which had been previously identified as an efficient plasticizer for PLA at low loading ratios [249]. Plasticized PLA matrices were nucleated by talc, ethylene bis(stearamide) (EBS), or PDLA and studied by differential scanning calorimetry (DSC), wide-angle X-ray diffraction (WAXD) and polarized optical microscopy (POM). The

obtained results were compared with data in the literature. On the other hand, the effect of pressure on the crystallization rate of each PLA was studied by pressure volume temperature (PVT) measurements. The systems that showed the fastest crystallization process by DSC were selected for these measurements. Finally, the processing parameters for in situ crystallization during injection moulding were determined.

4.2. Experimental

4.2.1. Materials

Two PLA have been used as matrices, Ingeo 3052D by Natureworks LLC and a non-commercial low D-lactic acid content PLA by Futerro kindly provided by Total Research and Technology Feluy, Belgium. Table 4-1 shows the designation, commercial brand name, number average molar mass, dispersity and L-lactic acid content of the PLA matrices.

Designation	Brand name	M_n (g/mol)	Đ	% L-
PLA_{96}	Ingeo 3052	103000	1.7	≈ 96
$PLA_{99.5}$	Futerro	87000	1.9	> 99.5

Table 4-1. PLA matrices: designation, commercial brand name, number average molar mass, dispersity and L-lactic acid content.

Dioctyl adipate (DOA) (ester content > 99.5%) was obtained from Vinkaplast (Brazil). Luzenac HAR T84 high aspect ratio talc (B.E.T.=19.5m^2/g (ISO9277) with particle size distribution D50=2.0 μm and D95=11.3 μm (ISO13317-3)) was kindly provided by Imerys Talc. Ethylene bis(stearamide) (EBS) (593.02 g/mol) was purchased from Sigma-Aldrich. The molecular structure of EBS was confirmed by ^{1}H-NMR. PDLA with high D-lactic acid content (≈ 98.5%) and M_n=70000 g/mol was obtained from Corbion Purac. All chemicals were used as received without any purification.

4.2.2. Sample preparation

All compounds were prepared in a Brabender DSE 20/40 co-rotating twin screw extruder (Ø=20mm, L/D ratio=28). A progressively increasing temperature ramp from 175 ºC

(hopper) to 195 ºC (die) was set for extrusion using a screw rotation speed of 300 rpm. Prior to compounding PLA pellets were dried for 4h at 80 ºC whereas EBS and talc were dried in an oven at 100 ºC overnight. The compositions of the PLA_{96} and $PLA_{99.5}$ based systems are summarized in Table 4-2.

PLA matrix (wt%)	DOA Plasticizer (wt%)	Nucleating Agent (wt%)
94.7	5.3	0.0
90.0	5.0	5.0 (Talc)
90.0	5.0	5.0 (EBS)
90.0	5.0	5.0 (PDLA)

Table 4-2. Composition of the different systems.

4.2.3. Characterization methods

The average molar masses and the dispersity were measured by SEC using a Waters Gel Permeation Chromatography apparatus equipped with a Waters 410 differential refractive index detector. The analyses were carried out at 30 ºC and 1 mL/min in THF on two PLgel columns (Polymer Laboratories Ltd, 10 μm particle size, 10^5 Å and 10^3 Å). The calibration was performed with PS standards from 2500 to $1.8x10^6$ g/mol. ^{1}H NMR and ^{13}C NMR spectra were recorded at 100ºC by a Bruker 400 MHz. Deuterated tetrachloroethane $(CDCl_2)_2$ was used as solvent. The following solvent based calibrations were used: δ=6.0 ppm and δ=73.78 ppm for ^{1}H NMR and ^{13}C NMR, respectively.

DSC analyses were performed with TA Instruments Q100 model. Samples of approximately 7 mg were encapsulated in aluminium pans, heated up to 200 ºC and maintained at this temperature for one minute to erase thermal history. Then they were cooled at the rate of 50 ºC/min to the selected crystallization temperature followed by an isothermal period of 20 minutes. Four different crystallization temperatures (Tc) were applied: 90, 100, 110 and 120ºC. These temperatures were chosen on the basis of indications reported in the literature [62,249]. After the isothermal period, samples were cooled down to 0 ºC at 30 ºC/min and then a heating scan from 0 to 200 ºC at 10 ºC/min was carried out. Concerning the samples containing PDLA, samples were heated up to 250 ºC to melt down stereocomplex crystals in order to erase the previous thermal history of all systems and ensure that variables linked to previous material processing had no effect on this study. Yamane et al. [250] observed that the nucleation efficiency of PLA improved when the stereocomplex crystals were not melted

before cooling. In this regard, Narita et al. [183] observed that stereocomplex crystallites that melted and re-crystallized at processing temperatures just above stereocomplex crystallites end-set melting temperature, have a high nucleating effect during cooling process, similar to that of non-melted stereocomplex crystallites.

Crystallinity degree was calculated by Eq. 4-1.

$$X_c(\%) = \frac{\Delta H_m - \Delta H_{cc}}{\omega_{PLA} \Delta H_0} \quad \text{Eq. 4-1}$$

Where ΔH_m is the melting enthalpy of homocrystals (J/g); ΔH_{cc} is the cold crystallization enthalpy (J/g); ω_{PLA} is the weight fraction of PLA in the compound; ΔH_o the theoretical melting enthalpy value for a 100% crystalline PLA, estimated in 93 J/g [251].

Due to the interactions between PLLA and PDLA, the crystallinity degree of the systems nucleated by PDLA must be calculated by modified equations. Homochiral crystals are composed by either PLLA or PDLA chains, while in stereocomplex crystals an equimolar ratio of PLLA and PDLA chains are packed side by side [252]. Hence, weight fraction of potentially stereocomplexable PLA (ω'_{sc}) was used for the calculations of stereocomplex crystallinity degree, calculated as the summation of the weight fraction of PDLA and the equivalent amount of PLLA (Eq. 4-2). Then, the weight fraction of both PLLA and PDLA that did not crystallize in the stereocomplex form continued in the amorphous state and therefore had the potential to crystallize homochiraly. Thus, homochiral crystallinity degree was calculated from the weight fraction which did not crystallize as stereocomplex crystal (Eq. 4-3). The amount of PLLA that had crystallized in the stereocomplex form must be subtracted to the initial PLLA weight fraction in the system and the amount of PDLA that remained amorphous must be added. Finally, $X_{c\text{-}sc}$ and X_c were calculated by Eq. 4-4 and Eq. 4-5, respectively.

$$\omega'_{sc} = 2x\omega_{PDLA} \quad \text{Eq. 4-2}$$

$$\omega'_{\alpha} = \omega_{PLLA} - \chi_{c-sc}\omega_{PDLA} + (1-\chi_{c-sc})\omega_{PDLA} = 1 - 2\chi_{c-sc}\omega_{PDLA} \quad \text{Eq. 4-3}$$

$$\chi_{c-sc}(\%) = \frac{\Delta H_{m-sc}}{\omega'_{sc}\,\Delta H_{0-sc}} \qquad \text{Eq. 4-4}$$

$$\chi_{c}(\%) = \frac{\Delta H_{m} - \Delta H_{cc}}{\omega'_{\alpha}\,\Delta H_{0}} \qquad \text{Eq. 4-5}$$

Where $\Delta H_{m\text{-}sc}$ is the melting enthalpy of stereocomplex crystals (J/g); ω'_{sc} is the weight fraction with the potential to crystallize in the stereocomplex form; $\Delta H_{0\text{-}sc}$ is the theoretical melting enthalpy value for a 100% stereocomplex crystalline PLA, estimated in 142 J/g [252]; and ω'_{α} is the weight fraction with the potential to crystallize in the homochiral forms.

Wide-angle X-ray scattering (WAXS) spectra were recorded on a Bruker AXS D8 Advance system with Cu Kα radiation of wavelength λ=1.5406Å. A range of 2θ from 10º to 24º was recorded, by a step size of 0.01º per 0.2s. A temperature controlled sample holder was used to replicate the same thermal program as for DSC at crystallization temperatures of 90 and 120 ºC. Due to technical limitations of the temperature controller the cooling rate used was around 15 ºC/min.

The evolution of the crystalline structure of the samples was analyzed by a Nikon eclipse 80i optical microscope. Thin films were prepared by melting samples between cover slips in a Linkam hot-stage. Samples were placed between crossed polarisers and the same thermal program as for DSC was applied. Time-lapses were carried out at 1/20s frame capturing rate.

In order to study the effect of pressure on the crystallization rate, a pressure-volume-temperature analyzer was used to measure the volumetric shrinkage during an isothermal crystallization process after cooling from the melt. The systems that showed the fastest crystallization process, previously determined by DSC technique, were selected for this purpose. Isotherms at 120 ºC and 200 bar pressure were carried out to measure specific volume variations along the time. Around 1g of dried pellets were heated to 200 ºC to erase the thermal history of the polymer. Then, 400 bar pressure was applied to release bubbles and samples were cooled at 30 ºC/min cooling rate under 200 bar pressure to 120 ºC and the crystallization process was studied at these conditions during 20 minutes.

4.3. Results and discussion

4.3.1. Crystallization behaviour

DSC thermograms of neat PLA_{96} and $PLA_{99.5}$ (Fig. 4-1) showed that the former could hardly crystallize whereas the latter partially crystallized during the isothermal step at the selected temperatures (Table 4-3 and Table 4-4). During the subsequent heating scan, both PLA showed the glass transition temperature at around 62ºC and only $PLA_{99.5}$ showed cold crystallization. The melting temperature of PLA is strongly dependent on the L/D ratio [168–170], hence $PLA_{99.5}$ showed considerably higher melting temperature than PLA_{96}, 174 ºC and 154 ºC, respectively.

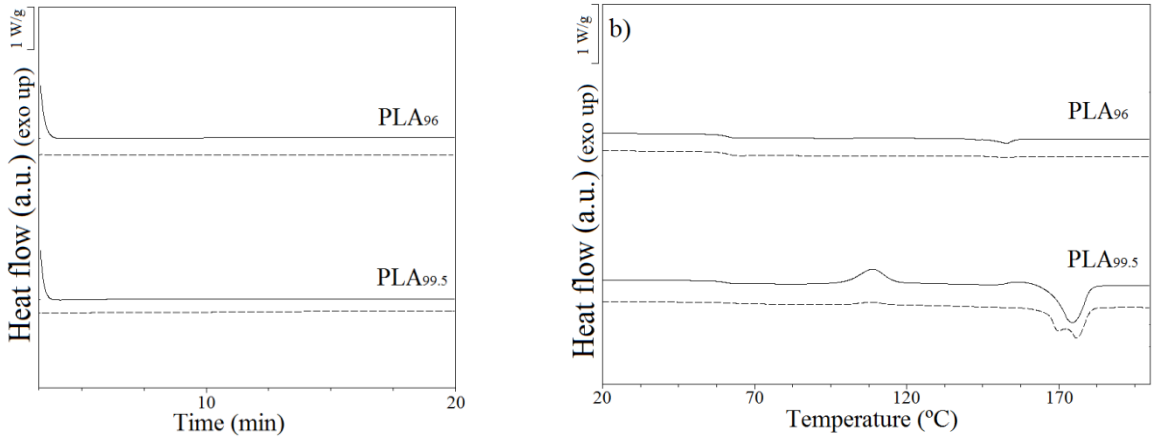

(a) (b)

Fig. 4-1. DSC thermograms of the isothermal crystallization step (a) and the subsequent heating thermograms (b) of neat polymers crystallized at 90 (solid line) and 120 ºC (dash).

Fig. 4-2a and Fig. 4-3a show the isothermal step of the crystallization after the cooling step of plasticized PLA_{96} and $PLA_{99.5}$ based systems, respectively. The time in the abscissa indicates the total time elapsed from the melt. Concerning plasticized PLA without nucleating agent, only $PLA_{99.5}$ was able to crystallize completely during the isothermal period at the selected conditions.

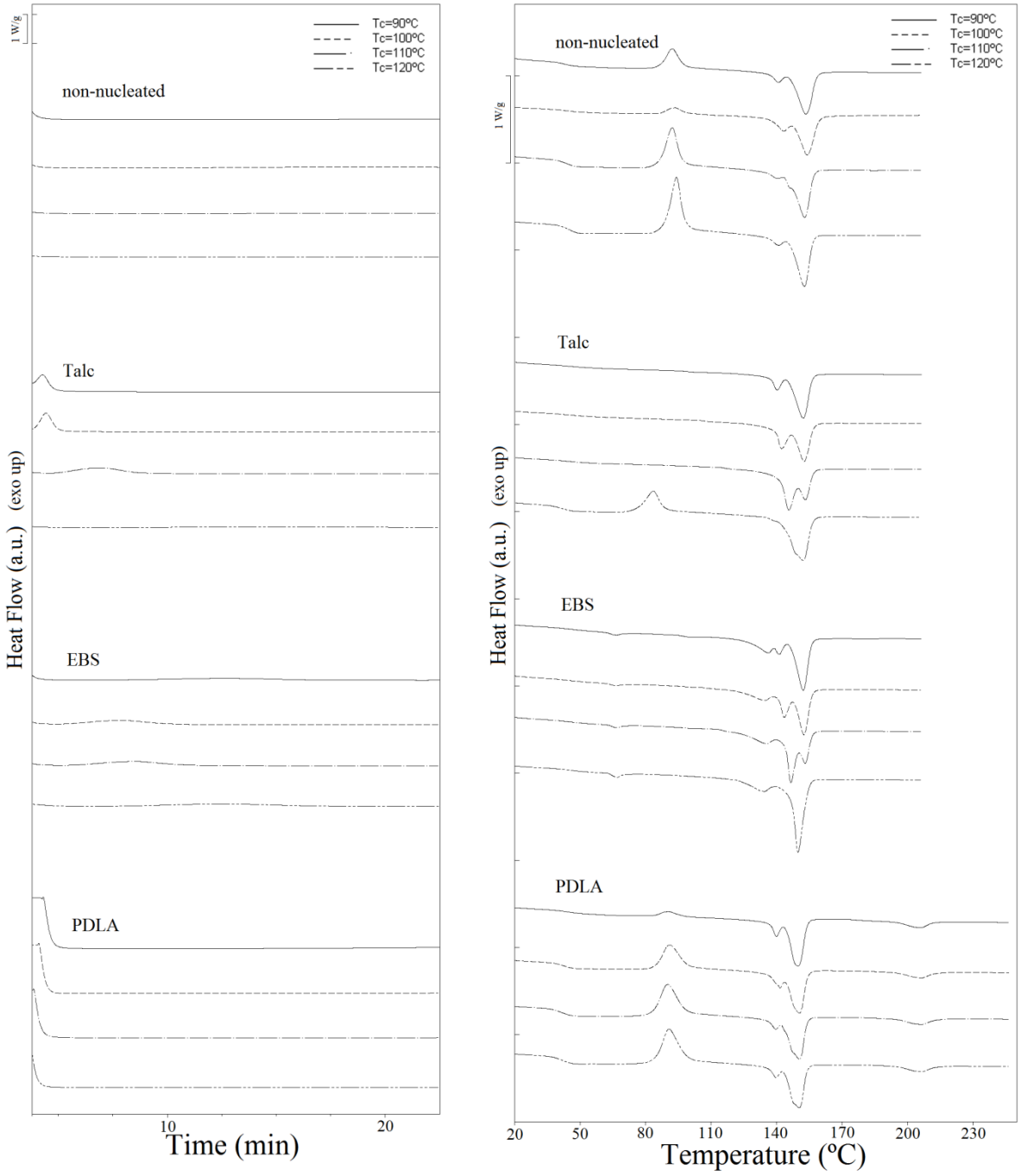

Fig. 4-2. DSC thermograms of the isothermal crystallization step (a) and the subsequent heating thermograms (b) for plasticized and nucleated PLA_{96} crystallized at different temperatures.

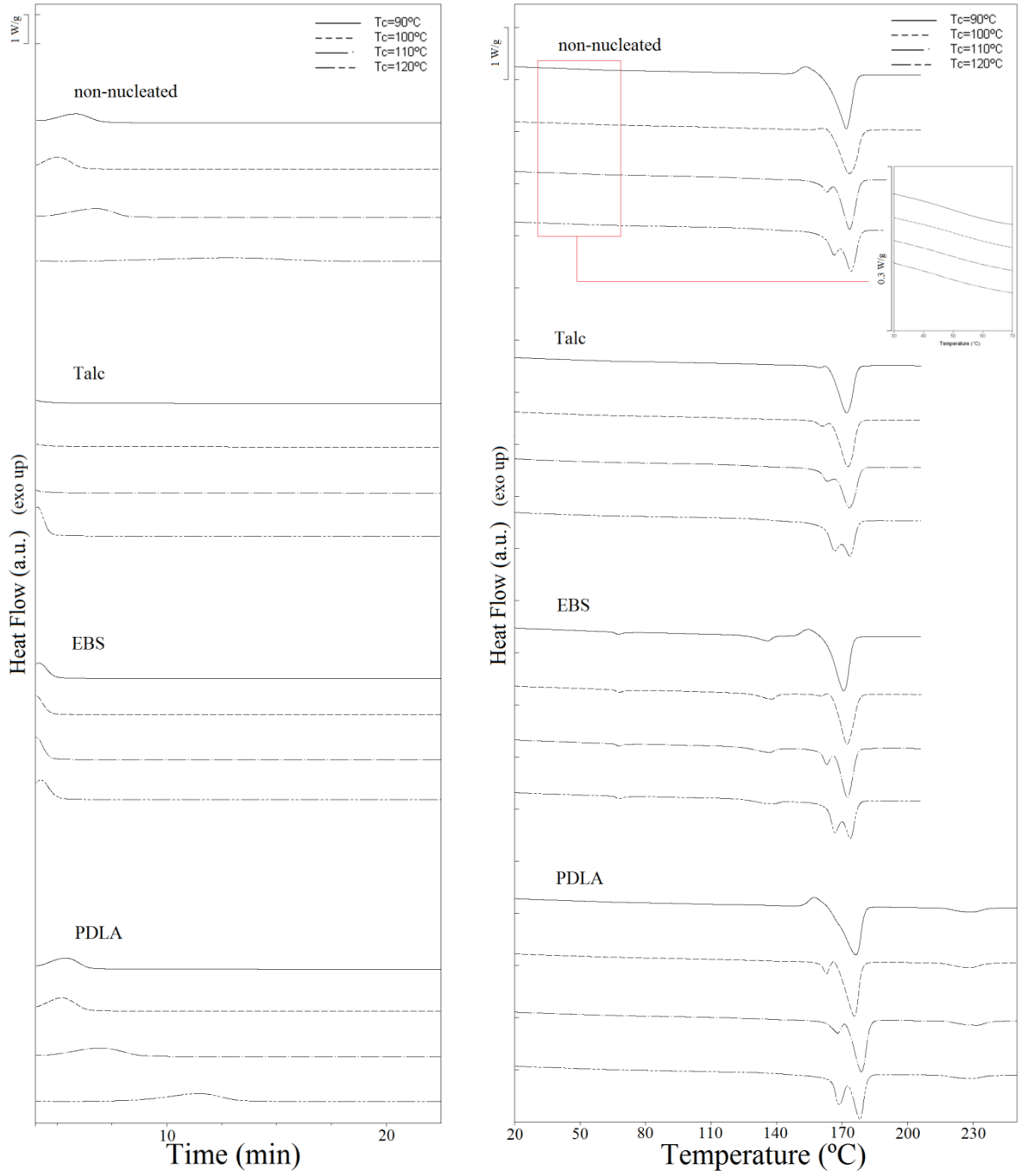

(a) (b)

Fig. 4-3. DSC thermograms of the isothermal crystallization step (a) and the subsequent heating thermograms (b) for plasticized and nucleated $PLA_{99.5}$ crystallized at different temperatures.

Fig. 4-2b and Fig. 4-3b show the subsequent heating scans. Some systems showed high crystallinity degrees, which led to very weak heat flow signal changes at T_g due to the limited presence of amorphous phase (insert in Fig. 4-3b resulting no possible the determination of reliable T_g values in some systems. For the cases that T_g can be determined, all systems showed the T_g at around 40-45ºC due to the plasticizing effect of DOA. In the systems based on plasticized PLA_{96} without nucleating agent, even though the chain mobility was increased, samples did not crystallize completely during the isothermal period. A double peak thermal transition was detected, defined by a low (T_{m2}) and a high (T_{m1}) temperature endotherms which have been attributed to the melting of original crystals and to the melting of the crystals formed through the melt-recrystallization process during the heating scan, respectively [253]. The peak height of T_{m2} increased relative to the height of T_{m1} by increasing the crystallization temperature selected, which is in agreement with the results reported by other authors [254]. The melt-recrystallization from α' to α involves a slight rearrangement of the macromolecular packing within the unit cell to a more energy-favourable state, corresponding to a reduction of lattice dimensions. This process has also been reported as a solid state crystal modification rather than a melting/recrystallization process in the literature [182]. This crystalline phase rearrangement can sometimes be detected as an exothermic peak instead of an endothermic one [255], as observed for example in $PLA_{99.5}$ crystallized at T_c=90ºC. The effect of the stereochemistry of PLA on the crystallization process was evident; at higher the L-lactic acid contents the ability to crystallize was higher and the crystallization rate increased, regardless the nucleating agent and crystallization temperature.

As shown in Fig. 4-2a and Fig. 4-3a, all systems showed the fastest crystallization in the temperature range of 90-100 ºC regardless the nucleating agent. Higher crystallization temperatures could have increased chain mobility, but at the same time diminished the supercooling degree determined by $\Delta T=T_m^0-T_c$. At temperatures above T_c=100 ºC, even though the mobility of PLA chains might be increased with temperature, the formation of crystal nuclei was slowed down. Hence, the overall crystallization process rate decreased. This optimum crystallization temperature range is lower than the temperature range reported for neat or nucleated PLA systems without plasticizer, i.e. T_c=105-115 ºC [169,256,257]. Thus, this decrease on the optimum crystallization temperature range could be attributed to

the presence of the plasticizer in the systems because the plasticizer improved the chain mobility of the polymer, as shown by the T_g value decrease.

Among the studied nucleating agents, talc showed to be the most efficient except at 120 ºC, at this temperature EBS induced a faster crystallization process than talc. The nucleation density of PLA obtained by EBS has been reported to be higher at higher crystallization temperatures [180]. Hence, even though the crystallization efficiency of inorganic nucleating agents like talc decreases considerably together with the supercooling degree, this is not the case of organic EBS. It was observed in the literature that some organic nucleating agents can lead to chemical nucleation. For example, organic sulfonic acid salts (e.g.: Lak 301 by Takemoto Oil) caused chain scission in polyesters and thus form ionic chain ends. These chain ends become ionic clusters that act as true nuclei [258,259]. Even though this effect has not been proved for EBS in the literature, might have an effect on its nucleating efficiency. In the systems nucleated by EBS, the small endothermic peak observed around 65 ºC was related to the polymorphic transition of the crystalline EBS [260]. The melting enthalpy of some samples was not easy to measure due to the overlapping of the melting peaks of the EBS crystals (≈138 ºC) and crystals of PLA_{96} (≈140-150 ºC). As the melting of EBS crystals did not overlap with T_{m2} in $PLA_{99.5}$ based systems, the melting enthalpy of EBS measured from these heating scans was used to estimate the melting enthalpy of PLA_{96} based systems when overlapped melting peaks were detected.

All PDLA nucleated systems showed melting peaks of the stereocomplex crystals around 206 and 222 ºC for PLA_{96} and $PLA_{99.5}$, respectively. The melting temperature and the enthalpy of the stereocomplex crystallites obtained from the DSC heating process could serve as indicators of the crystallite size and the amount of stereocomplex crystallites formed during the previous step [183]. Hence, a higher amount and bigger stereocomplex crystallites seemed to be created in $PLA_{99.5}$ based system than in PLA_{96} based ones as the melting enthalpy and temperature of stereocomplex crystallites was considerably higher in $PLA_{99.5}$ based systems. The cold crystallization peaks observed for PLA_{96} systems in the heating scans indicated that PLA_{96} nucleated with PDLA hardly crystallized during the isothermal period, especially at high crystallization temperatures. On the contrary, $PLA_{99.5}$ nucleated with PDLA crystallized completely at the selected conditions regardless the crystallization temperature.

Thermal transition temperatures, crystallization and melting enthalpies and the degree of crystallinity of different samples are reported in Table 4-3 and Table 4-4 for PLA_{96} and $PLA_{99.5}$ based systems, respectively. Standard deviations of measured transition enthalpies and temperatures were below 2.48 J/g and 0.73 ºC, respectively. The melting temperature T_{m2} increased with the applied isothermal crystallization temperature. However, the melting temperature T_{m1} remained roughly constant, which is in agreement with the results reported by Di Lorenzo for unplasticized PLA [254]. A possible explanation could be that the original α crystals created at higher crystallization temperatures are more perfect crystals, so increasing crystallization temperature resulted in higher T_{m2} value.

On the other hand, T_{m1} remained almost unaltered because the α crystals formed through the melt-recrystallization process during the heating scan happened at similar temperatures regardless the applied isothermal crystallization temperature.

Except for PLA_{96} systems crystallized at 120 ºC, talc nucleated and EBS nucleated systems showed similar melting temperature as well as crystallinity degree values. At this temperature the PLA_{96} based system crystallized completely when was nucleated with EBS due to the high nucleation efficiency of EBS at high crystallization temperatures, and consequently the crystallinity degree at 120 ºC was higher than that obtained by talc nucleated PLA_{96}. In all systems that were able to completely crystallize during the isothermal period, higher crystallization temperatures led to higher crystallinity degrees, which is in agreement with what Di Lorenzo reported for unplasticized PLA [254]. All nucleated systems that completely crystallized showed slightly higher crystallinity degrees than their non-nucleated counterparts.

	neat		plasticized				DOA+talc				DOA+EBS				DOA+PDLA			
T_c (ºC)	90	120	90	100	110	120	90	100	110	120	90	100	110	120	90	100	110	120
T_{cc} (ºC)	-	-	92	97	92	94	-	-	-	83	-	-	-	-	91	91	84	85
T_{m1} (ºC)	153	152	153	154	153	153	152	152	153	152	152	152	153	150	150	151	150	150
T_{m2} (ºC)	142	-	141	144	141/146	141	140	142	145	139/149	141	144	147	-	140	142	140	140
ΔH_{cc} (J/g)	-	-	11.2	4.3	23.7	29.8	-	-	-	13.4	-	-	-	-	3.1	17.8	24.2	25.0
ΔH_m (J/g)	5	1.6	28.8	29.5	29.9	29.8	31.9	32.7	32.8	31.9	32.0	34.1	35.4	35.7	30.1	29.4	27.9	28.0
$X_{c-\alpha}$ (%)	5.5	1.7	18.9	27.0	6.6	0.0	36.0	36.9	37.0	20.9	36.1	38.5	39.9	40.3	30.0	12.9	4.1	3.3
T_{m-sc} (ºC)															206	206	206	206
ΔH_{m-sc} (J/g)															5.2	5.3	5.5	5.2
X_{c-sc} (%)															36.6	37.3	38.7	36.6

Table 4-3. Summary of crystallization/melting temperatures and enthalpies of PLA_{96}: neat, plasticized with DOA, DOA+talc, DOA+EBS, and DOA+PDLA.

	neat		plasticized				DOA+talc				DOA+EBS				DOA+PDLA			
T_c (ºC)	90	120	90	100	110	120	90	100	110	120	90	100	110	120	90	100	110	120
T_{cc} (ºC)	109	110	-	-	-	-	-	-	-	-	-	-	-	-	-	-	-	-
T_{m1} (ºC)	175	176	172	173	173	174	172	173	173	173	171	172	172	174	169	169	172	171
T_{m2} (ºC)	156	169	153	162	163	166	160	161	163	167	155	161	163	167	151	157	161	162
ΔH_{cc} (J/g)	29	8	-	-	-	-	-	-	-	-	-	-	-	-	-	-	-	-
ΔH_m (J/g)	48	49	47.3	48.8	53.5	55.0	47.8	49.7	54.0	54.3	46.8	49.4	53.0	54.1	43.3	45.5	49.9	53.0
$X_{c-\alpha}$ (%)	20	44	50.7	52.3	57.3	58.9	53.9	56.1	60.9	61.3	52.8	55.7	59.8	61.0	48.6	51.2	56.1	59.2
T_{m-sc} (ºC)															220	220	222	221
ΔH_{m-sc} (J/g)															6.5	6.8	6.6	5.8
X_{c-sc} (%)															45.8	47.9	46.5	40.8

Table 4-4. Summary of crystallization/melting temperatures and enthalpies of $PLA_{99.5}$: neat, plasticized with DOA, DOA+talc, DOA+EBS, and DOA+PDLA.

Systems nucleated by PDLA showed slightly lower melting temperatures values than their counterpart systems nucleated by talc, EBS or without nucleating agent. Regarding the stereocomplex crystals, $PLA_{99.5}$ based systems showed higher stereocomplex crystallinity degree ($X_{c\text{-}sc}$) than PLA_{96} based ones. Moreover, the melting temperature of stereocomplex crystals was 14 ºC higher for $PLA_{99.5}$ based systems than for PLA_{96} based ones. This difference in melting temperature of the stereocomplex crystals suggested that the crystal perfection and/or size were not similar in PLA_{96} and $PLA_{99.5}$ based systems. Probably the lower L/D lactic acid ratio of PLA_{96} may hinder the formation of stereocomplex crystals with the capability to nucleate homochiral crystals. DSC results indicated that PLA_{96} nucleated with PDLA showed similar or even slower crystallization rates than the systems without nucleating agent. This behaviour suggested that stereocomplex crystals could constrain the homochiral crystallization of PLA rather than accelerate it, which is an effect that Xiong et al. recently detected and suggested to be dependent on the content of stereocomplex crystals [182].

The effect of pressure on the crystallization rate was studied by PVT measurements in talc nucleated systems because they showed the fastest crystallizing process in the DSC thermograms. T_c=120ºC was selected because the crystallization rate was the slowest at this temperature and so it enabled to better analize the effect of the pressure. Hence, Fig. 4-4 shows the variation of the specific volume of both systems during an isothermal process at 120 ºC and 200 bar pressure and the subsequent DSC heating scans. The specific volume decreases during crystallization due to the lower specific volume of the crystalline regions. $PLA_{99.5}$ nucleated with talc seemed to crystallize almost completely during the cooling process because the observed volume variation during the isothermal process was insignificant. On the other hand, the volume of PLA_{96} nucleated by talc seemed to stabilize after 20 minutes. The DSC heating scans performed after the PVT measurements (Fig. 4-4b) showed that both systems had crystallized completely. The crystallization behaviour monitored by PVT and DSC were in agreement in the case of talc nucleated $PLA_{99.5}$. However, PLA_{96} nucleated with talc crystallized completely under 200 bar pressure (PVT) in contrast to what seen by DSC at atmospheric pressure. Therefore, the increase of pressure considerably accelerated the crystallization process of this system. Yu et al. studied the isothermal crystallization of neat PLA and talc nucleated PLA under pressurization (5 bar) by compressed CO_2 [261]. In contrast to our results, in samples crystallized isothermally at

120 ºC after cooling from the melt, they observed that the crystallization time increased with pressure for both neat PLA and talc nucleated PLA. As the compressed CO_2 acts as a plasticizer and enhances polymer chain movement [262,263], Yu et al. suggested that the highly mobilized chains may have dissolved nuclei and hindered the formation of new nucleation sites, which decreased the overall crystallization rate [261]. In our work PLA was plasticized with dioctyl adipate and a higher pressure was applied during the PVT study (200 bar), which led to a higher crystallization rate. Hence, our results suggested that PLA systems plasticized by dioctyl adipate might show a higher crystallization rate when processed by processing techniques such as injection moulding than what measured in the DSC study.

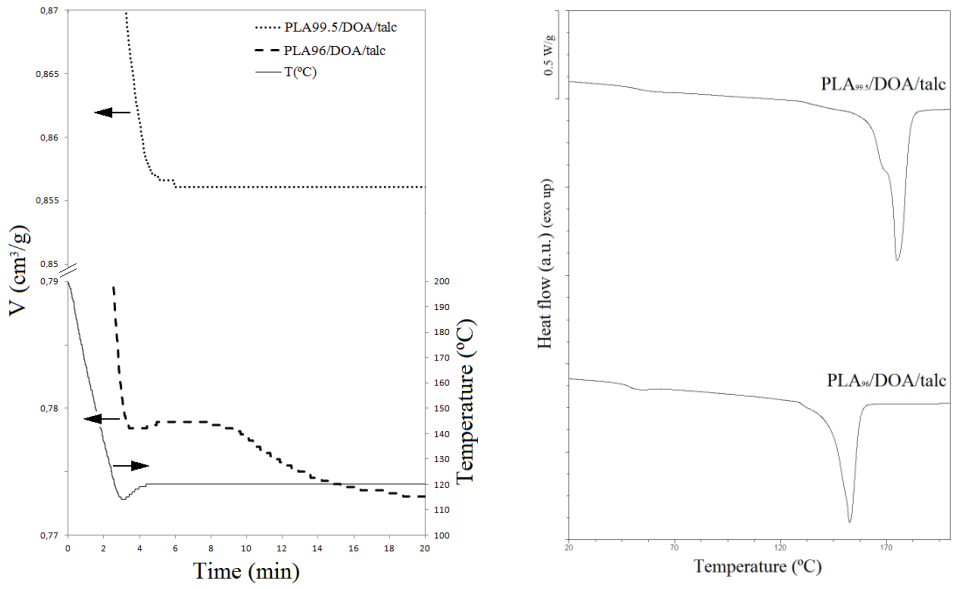

(a) (b)

Fig. 4-4. PVT (a) and subsequent heating DSC (b) diagrams for systems crystallized at Tc=120ºC and P=200 bar after cooling from the melt.

4.3.2. Crystalline structure

WAXS spectra of isothermally crystallized systems at 90 and 120 ºC are shown in Fig. 4-5 and Fig. 4-6, respectively. Spectra of neat polymers showed an amorphous structure in both cases. Even though in DSC the thermogram some degree of crystallinity was observed in neat $PLA_{99.5}$, no crystal structure was detected by WAXS. After the addition of plasticizer

non-nucleated systems crystallized and showed two peaks at $2\theta \approx 16.3^{\circ}$ and 18.6º related to diffractions of (110/200) and (203) planes of α' or α forms of PLLA homo-crystallites [184]. Besides, two tiny peaks at around 2θ=14.5º and 22º were also detected, related to diffractions of (010) and (015) planes, respectively [264,265]. The latter has been reported to be characteristic of α crystals [253], hence suggesting the coexistence of α and α' crystal forms. The peaks were more intense for higher L-lactic acid content polymer than low L-lactic acid content polymer, regardless the added nucleating agent. In general, after the addition of nucleating agents the WAXS diffractogram peaks were more intense than in systems without nucleating agents being the intensity increment more considerable in PLA_{96} based systems than for $PLA_{99.5}$. Regarding PLA_{96} based systems, talc seemed to be the most efficient among all the nucleating agents because talc nucleated system showed the peaks with highest intensity, which is in agreement with the DSC results. It should be mentioned that the diffraction spectra of talc nucleated systems showed three peaks related to the crystalline structure of talc, i.e. one peak at 2θ=12.2º and two overlapped peaks at around 18.3º and 18.6º [266]. Therefore, in talc nucleated PLA systems the peak at 18.6º is related to both talc crystals and α' PLLA homo-crystals. The other main peaks of PLA at 16.3º, 14.5º and 22º were detected in all talc nucleated PLA systems suggesting the coexistence of α and α' crystal forms. Regarding systems nucleated with EBS, no diffraction peak related to EBS crystals was detected in the analyzed 2θ range. Similar to systems nucleated with talc, α and α' crystal forms were observed, which was evidenced by the presence of the main peak at 16.3º and the tiny peak at 22º. Even though only 5 wt% of PDLA was present in the compounds, WAXS results of PLA nucleated with PDLA showed small diffraction peaks at 2θ=11.5, 20.2 and 23.5º, which are characteristic of stereocomplex PLA crystals [264]. These peaks were less intense for the samples crystallized at 120 ºC being hardly detectable for PLA_{96}, indicating that the system was almost amorphous, which is in agreement with the DSC data reported.

On the other hand, in $PLA_{99.5}$ based nucleated systems, the diffractogram differences between different systems were not so evident. WAXS results suggested that, within the selected crystallization temperature range, the crystalline phase of all samples was constituted by a mixture of α' and α crystals. Previous works suggested that crystallization temperatures above 110 ºC were needed to create α crystals in neat PLA samples [253,264].

In this work the existence of α crystals was observed in samples crystallized below 110ºC, which could be attributed to the presence of the plasticizer in the systems. In the samples crystallized at 90 ºC the intensity of the peak at 22º seemed to be lower than in the samples crystallized at 120 ºC. This fact suggested that at higher crystallization temperatures the presence of α crystals in the mixture seemed to increase. The coexistence of α and α' crystals is very common in semicrystalline PLA for a wide crystallization temperature range, being the α/α' ratio increased at higher crystallization temperatures [267].

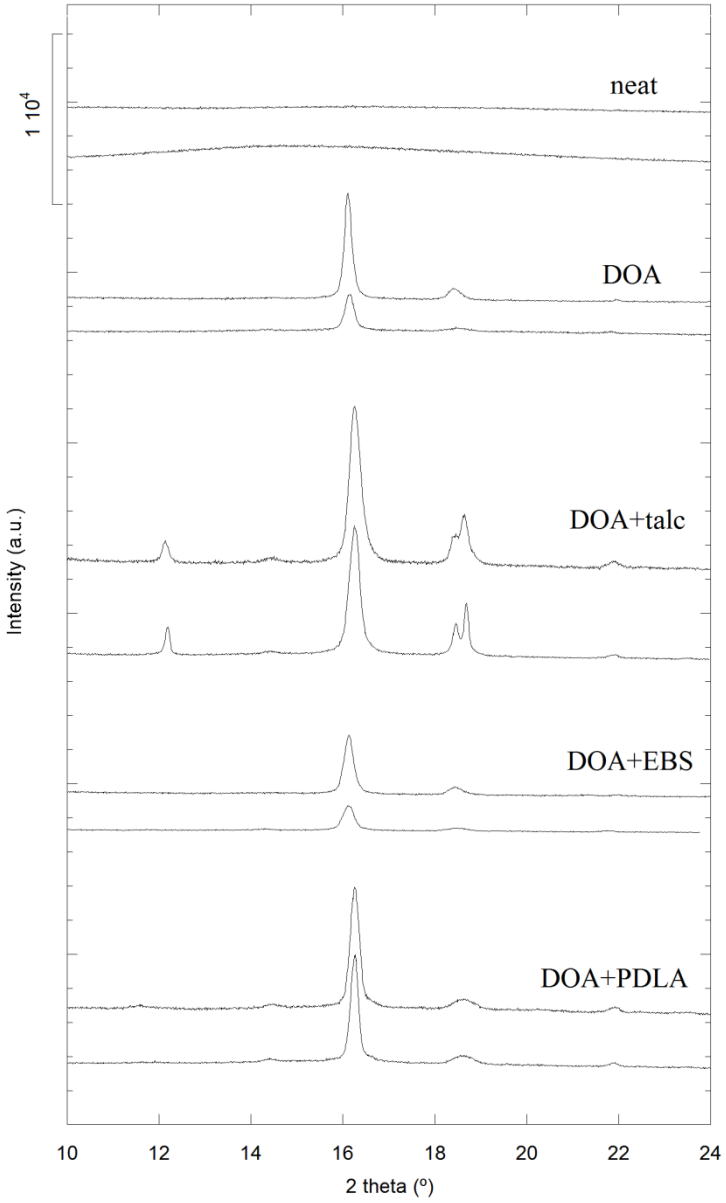

Fig. 4-5. X-ray scattering patterns for plasticized and nucleated $PLA_{99.5}$ (above) and PLA_{96} (below) crystallized at 90ºC.

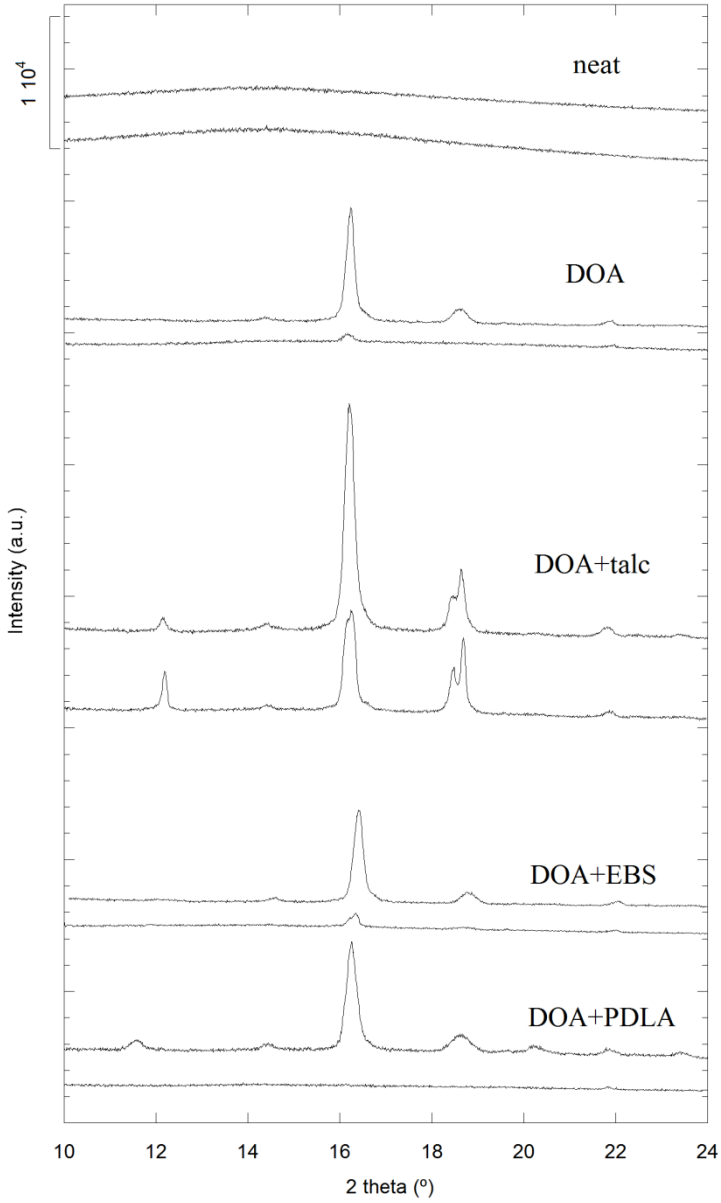

Fig. 4-6. X-ray scattering patterns for plasticized and nucleated $PLA_{99.5}$ (above) and PLA_{96} (below) crystallized at 120ºC.

4.3.3. Crystallization kinetics

As a representative example, the effect of nucleating agents on the isothermal induction time of PLA_{96} based systems is plotted in Fig. 4-7. PLA nucleated with talc showed the shortest induction times among the four studied systems. At low crystallization temperatures, 90 and 100 ºC, the isothermal induction time of both PLA based systems nucleated by talc remained below one minute. Systems nucleated by EBS showed higher induction times than talc

nucleated ones, especially at low crystallization temperatures. Regarding L-lactic acid content, $PLA_{99.5}$ based systems showed shorter induction times than PLA_{96} based ones regardless the used nucleating agent. After the addition of PDLA, even though the presence of stereocomplex crystals during the homo-crystallization was confirmed by DSC technique, no significant differences in the crystallization process were observed respect to systems without PDLA.

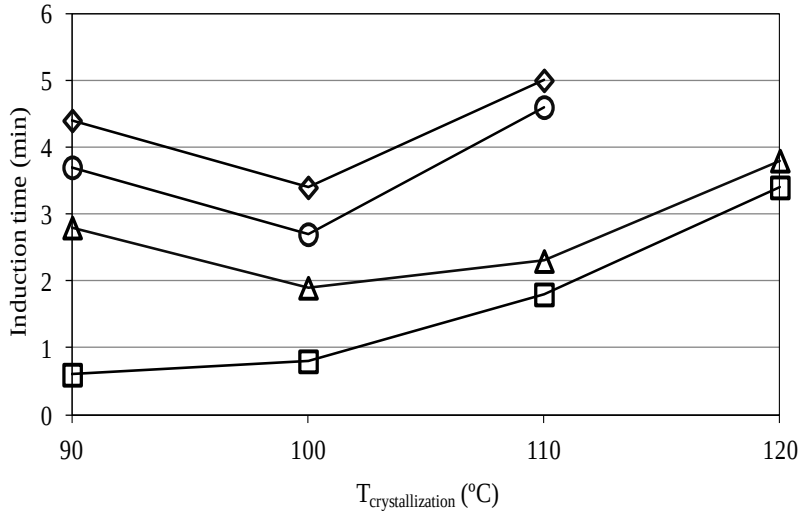

Fig. 4-7. Effect of different nucleating agents on the isothermal induction time of PLA_{96} plotted against crystallization temperature. Symbols: ◊ non-nucleated, □ talc, Δ EBS, ○ PDLA.

Half-crystallization times ($t_{1/2}$) were calculated from the experimental DSC data. For the systems which started the crystallization process during the cooling step, the time to achieve half of the melting enthalpy (measured during the heating step) was estimated as $t_{1/2}$. Fig. 4-8 shows the inverse of half-crystallization time of the different systems as a function of the crystallization temperature. The effect of the D-lactic acid content is obvious, but talc is able to considerably increase the crystallization rate of PLA_{96}, leading to faster crystallization rates than non-nucleated or PDLA nucleated $PLA_{99.5}$.

Concerning $PLA_{99.5}$, the effect of PDLA in the overall crystallization time is almost negligible, while EBS and talc showed a huge effect. Due to the fast crystallization shown by talc nucleated systems, only the half-crystallization time at T_c=120 ºC could be estimated. DSC traces show that $t_{1/2}$ of talc nucleated systems crystallized at lower temperatures (i.e. 90-110 ºC) should be shorter than the value observed at T_c=120 ºC. Actually, $t_{1/2}$ measured

for $PLA_{99.5}$ crystallized at 120 ºC and nucleated with talc or EBS were 0.74 and 0.86 min, respectively. Therefore, values as low as or lower than those obtained by EBS ($t_{1/2}$=0.34 min at Tc=90 ºC) are expected for talc nucleated systems. Half crystallization times of PLA based systems have been extensively reported in the literature [268–272]. However, values below 1 minute have been reported recently, e.g. achieved by the addition of modified montmorillonite ($t_{1/2}$=0.62 min) [185], layered zinc phenylphosphonates ($t_{1/2}$=0.57 min) [273], polyethylene glycol and dibenzylidene sorbitol ($t_{1/2}$=0.56 min) [247], polyethylene glycol and talc ($t_{1/2}$<1 min) [241], high melting point PLLA crystallites ($t_{1/2}$≈0.4 min) [274] and triphenyl phosphate and talc ($t_{1/2}$=0.7 min) [242], all of them obtained at isothermal conditions at crystallization temperatures ranging from 113 ºC to 131 ºC. This indicates the interesting improvement on crystallization rate which can be obtained by the combination of high aspect ratio talc, an efficient plasticizer and high L-lactic acid content PLLA.

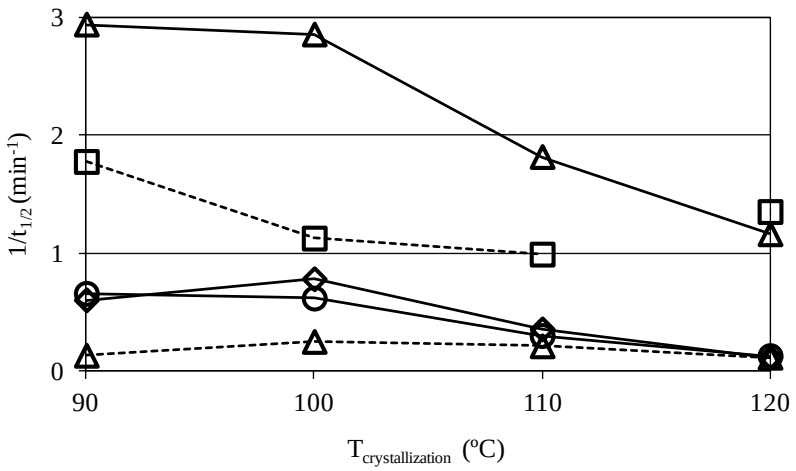

Fig. 4-8. Inverse of half-crystallization time of PLA_{96} (dash) and $PLA_{99.5}$ (solid line) plotted against crystallization temperature. Symbols: ◊ non-nucleated, □ talc, Δ EBS, ○ PDLA.

The systems which showed pure isothermal crystallization were fitted to Avrami kinetic model to evaluate the effect of the L-lactic acid content, crystallization temperature and nucleating agents on the rate constant (*k*) and the type of geometrical growth mechanism (*n*). In its simplest form, Avrami equation can be expressed as [275]:

$$1-V_c(t)=e^{(-kt^n)} \qquad \text{Eq. 4-6}$$

Where V_c is the relative volumetric crystallinity fraction, n is the Avrami exponent (related to the growth geometry of the crystals) and k is the overall crystallization rate constant (associated to both nucleation and growth contributions). Density values of crystalline and amorphous PLA were found in literature [45]. The linear form of this equation can be expressed as follows:

$$\log\left(-\ln\left(1-V_c(t)\right)\right) = \log k + n\log t \qquad \text{Eq. 4-7}$$

The Avrami parameters *n* and *k* can be obtained from the slopes and the intercepts of Eq. 4-7, respectively. Following the recommendations stated by Lorenzo et al. [275], the systems which showed an incomplete isothermal crystallization curve could not be fitted to Avrami equation. A conversion range from 3-60% of relative volumetric crystalline fraction was applied for the Avrami fittings of all analyzed systems, which lead to excellent correlation coefficients (Table 4-5 and Table 4-6). The correlation coefficients of the fits of all studied systems are 0.9990 or larger, as recommended by Lorenzo et al. [275].

Fig. 4-9 shows the relative volumetric crystallinity as a function of crystallization time (Fig. 4-9a) and the linear Avrami plots (Fig. 4-9b) for $PLA_{99.5}$ crystallized at T_c=120 ºC with and without nucleating agents. Even though the crystallization curve corresponding to EBS could not be analyzed because it started during the cooling step, talc and EBS showed to be more efficient nucleating agents than PDLA. Avrami parameters (k and n) are summarized in Table 4-5 and Table 4-6. Regarding the Avrami rate constant (k), the highest values have been calculated for talc nucleated systems. Plasticized $PLA_{99.5}$ nucleated by talc showed a k=1.23 min^{-n}. In the literature, only Shusheng et al. [273] and Hongwei et al. [185] have reported k values higher than the values reported in Table 4-6 for PLA based systems. However, in both cases the crystallization temperature selected was 130ºC, higher than for our systems.

	No Nucleating Agent				5% talc				5% EBS				5% PDLA			
T_c (ºC)	90	100	110	120	90	100	110	120	90	100	110	120	90	100	110	120
k (min^{-n})	**	**	**	**	*	*	0.317	**	0.084	0.227	0.186	0.076	**	**	**	**
n	**	**	**	**	*	*	2.71	**	2.82	2.82	2.92	3.05	**	**	**	**
R^2	**	**	**	**	*	*	0.9999	**	0.9990	0.9999	0.9999	0.9998	**	**	**	**

Table 4-5. Avrami constants (k and n) and coefficient of determination of the fit for PLA_{96} without nucleating agent, nucleated with talc, EBS and PDLA. Only the compounds which showed a completely isothermal crystallization were measured: *crystallization started during the cooling step, **crystallization did not finish during the studied isothermal period.

	No Nucleating Agent				5% talc				5% EBS				5% PDLA			
T_c (ºC)	90	100	110	120	90	100	110	120	90	100	110	120	90	100	110	120
k (min^{-n})	*	*	0.300	0.070	*	*	*	1.230	*	*	*	*	*	*	0.270	0.063
n	*	*	2.83	2.88	*	*	*	2.71	*	*	*	*	*	*	2.75	2.91
R^2	*	*	0.9994	0.9993	*	*	*	0.9994	*	*	*	*	*	*	0.9996	0.9994

Table 4-6. Avrami constants (k and n) and coefficient of determination of the fit for $PLA_{99.5}$ without nucleating agent, nucleated with talc, EBS and PDLA. Only the compounds which showed a completely isothermal crystallization were measured: *crystallization started during the cooling step; **crystallization did not finish during the studied isothermal period.

Avrami exponent n ranged from 2.71 to 3.05 indicating that the crystallization mechanism may have not changed. The obtained *n* values were similar to those reported for unplasticized PLA systems and were related to a three-dimensional spherulitic growth of crystals [169,256,276]. Therefore, equivalent geometrical crystal growth behaviour is supposed for all compounds regardless T_c, nucleating agent and stereochemistry of the matrix.

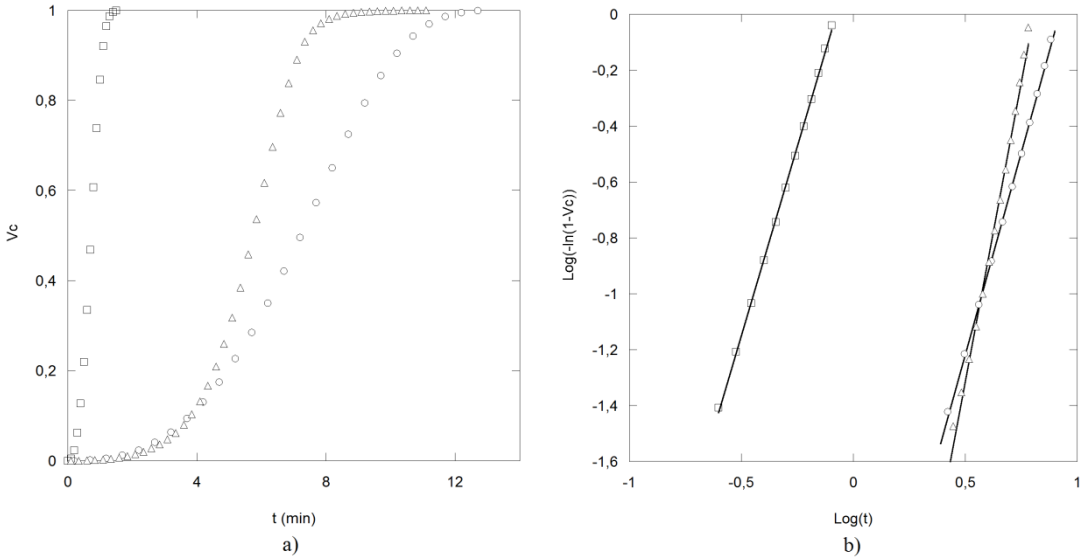

Fig. 4-9. (a) Volumetric crystalline fraction as a function of time during isothermal crystallization and (b) Avrami plots of $PLA_{99.5}$ crystallized at T_c=120ºC and nucleated by different agents: without nucleating agent (○), talc (□), and PDLA (Δ).

4.3.4. Crystal morphology and spherulite radial growth rate

The evolution of the crystal morphology was analyzed by POM. Fig. 4-10 shows images of plasticized PLA systems without nucleating agent after the isothermal crystallization period (20 minutes). POM images confirmed that nucleation density was higher at low crystallization temperatures, resulting in tiny spherulites as observed at samples crystallized at T_c=90-100 ºC. He et al. studied this type of small spherulites with irregularly arranged lamellae in neat PLLA, and concluded that when nucleation density was significantly high, a large number of nucleation sites could be formed in the same growth layer of a lamella, which contributed to the formation of defects in the crystal [277]. On the contrary, samples crystallized at higher temperatures (T_c=110-120 ºC) showed nice circular spherulites (until impingement). $PLA_{99.5}$ based systems showed higher crystallinity degree at high

crystallization temperatures than PLA_{96} ones, which is in agreement with previous studies which concluded that the crystallization behaviour and morphology are function of the stereochemistry of the matrix [168].

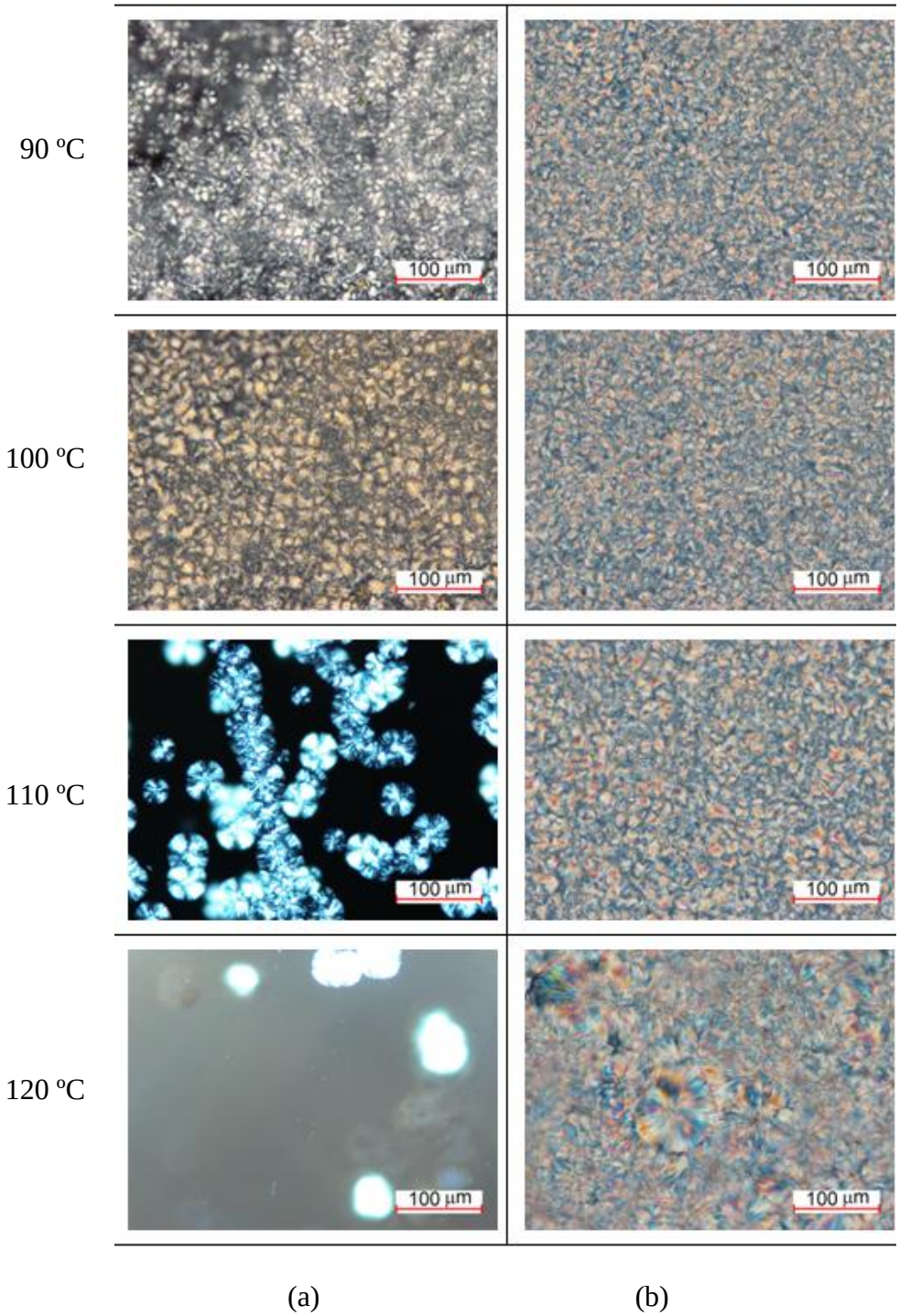

Fig. 4-10. POM images of different plasticized PLA crystallized at different temperatures: a) PLA_{96} and b) $PLA_{99.5}$

Fig. 4-11 shows POM images of neat PLA and plasticized PLA nucleated with different agents after 20 minutes at 120 ºC. Talc is a very efficient nucleating agent and 5wt% was enough to dramatically increase the nucleation density, hindering the growth of big spherulites even at 120 ºC. This is in agreement with the fast crystallization kinetics measured for the talc nucleated systems by DSC technique. One of the main reasons for the huge nucleation efficiency might be the high aspect ratio of the used laminar talc [278]. Similar results concerning the morphology and the crystal size were obtained when plasticized PLA was nucleated with EBS crystals. EBS crystals were quickly created at around 120-130 ºC during the cooling step and then acted as nucleating agents for the epitaxial growth of PLA crystals.

Regarding $PLA_{99.5}$ nucleated by PDLA, formation and melting of stereocomplex crystals was detected by POM as a change in light transmission at around 220 ºC (not shown in the figures). However, due to the low content of PDLA in these systems (i.e. 5% in weight), the size and morphology of stereocomplex crystals could not be analyzed. Concerning the formation of homochiral crystals, their size greatly depended on the crystallization temperature. Tiny crystals were formed at low temperatures whereas bigger spherulites were observed at high crystallization temperatures. Results indicated that the nucleation density obtained by the addition of PDLA at high crystallization temperatures was lower than that obtained by talc and EBS. Higher crystallization temperatures led to bigger spherulites because nucleation density was lower and, therefore, each nucleation site had more space to grow before spherulites impinge on each other.

Radial growth rate of spherulites was measured from POM images at different crystallization times. It could not be measured in systems containing talc or EBS due to the high nucleation density and tiny size of the crystals. $PLA_{99.5}$ based systems showed higher growth rates than PLA_{96} ones. Results of systems nucleated by PDLA showed that it does not only affect the nucleation step, but also the growing rate (Fig. 4-12). Both PLA matrices showed faster spherulitic growing rate in presence of PDLA. Similar results were reported by Yamane et al. [250], who observed that PDLA increased the radial growth rate of PLLA, even though this effect was hugely dependant on the temperature at which the blend had been previously heated up.

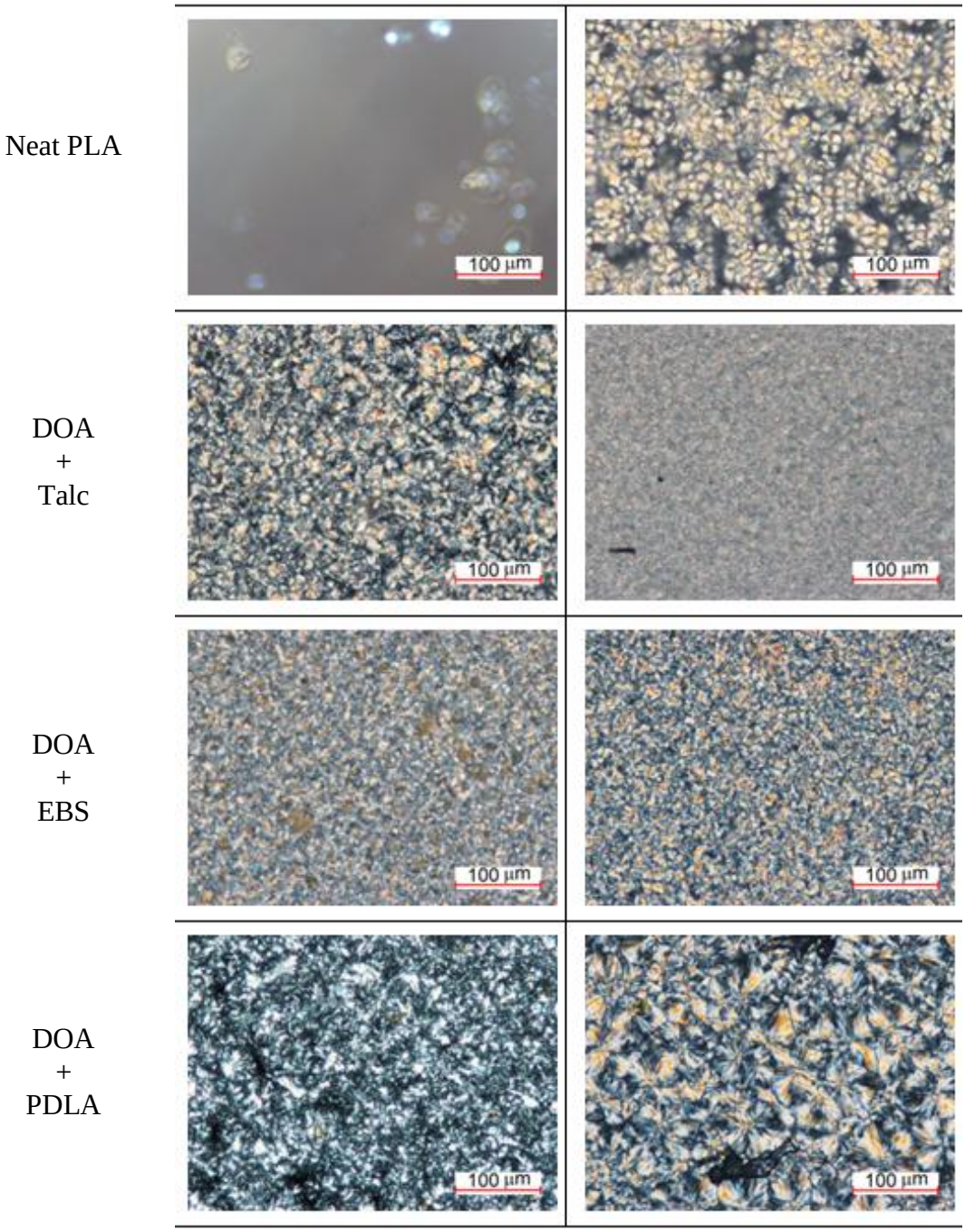

Fig. 4-11. POM images of neat PLA and plasticized and nucleated PLA crystallized at T_c=120ºC: a) PLA_{96} and b) $PLA_{99.5}$

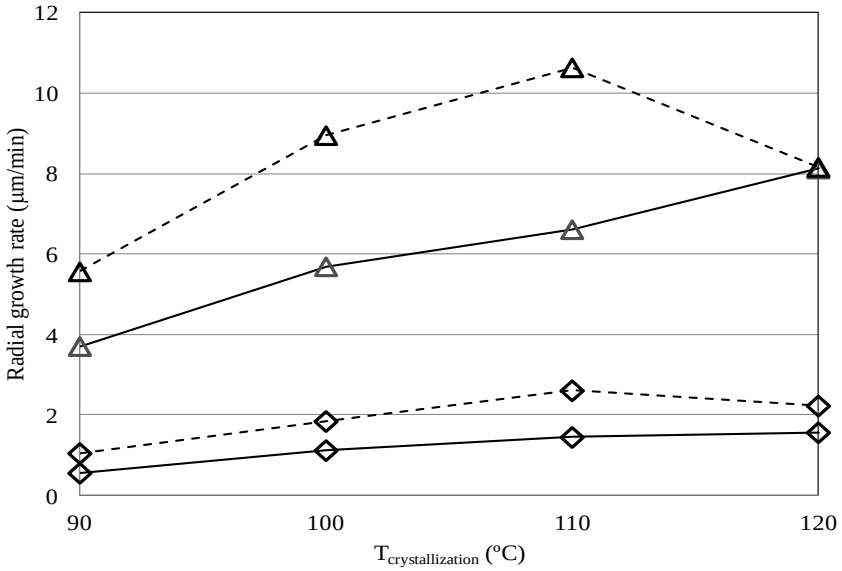

Fig. 4-12. Radial growth rate vs. T_c (after cooling from the melt) of systems without nucleating agent (solid line)) and with PDLA (dash). Symbols: ◊ PLA_{96}, Δ $PLA_{99.5}$.

Tsuji et al [175] studied the effects of the addition of different contents of PDLA on the crystallization behaviour of PLLA from the melt. They carried out the estimation of the radius growth rate of PLLA films having different contents of PDLA at crystallization temperatures above 125 ºC because at lower crystallization temperatures the high density of PLLA spherulites disturbed the estimation. They observed that the radius growth rate was approximately constant irrespective to PDLA content when compared at the same crystallization temperature. Moreover, they observed the maximum radius growth rate at 125 ºC, and it decreased as the crystallization temperature increased. In our work, probably due to the effect of the plasticiser, the maximum radius growth rate was observed around 110 ºC, and it decreased as the crystallization temperature increased. Tsuji et al. [175] suggested that the effect of PDLA on the spherulitic growing rate of PLA crystals might be dependent on the amount of stereocomplex crystals contained by the homochiral PLA crystals. If a significant amount of stereocomplex crystallites were contained in the homochiral spherulites other than their centres, the enormously high radial growth rates values observed for stereocomplex spherulites should increase the overall growing rate values.

Regarding crystallization temperature, the highest radial growth rate of spherulites was observed around 110-120 ºC. However, as the amount of nucleation sites was smaller, this temperature did not match with the crystallization temperature at which fastest overall crystallization was observed by DSC technique (i.e. T_c=90-100 ºC), which is in agreement with the results reported by Miyata et al. for neat PLA [279]. Thus, a better balance between nucleation density and growth rate was obtained at lower temperatures than at those where fastest spherulite growth happened.

4.3.5. Increase of the melting temperature due to the presence of stereocomplex crystals

During the study, some particular tests were carried out using a PLA grade with a 1.5% D-lactic acid content ($PLA_{98.5}$), including DSC scans. This grade was Natureworks' Ingeo 6201 (Mn=97000, Đ=1.6). The general behaviour of the systems based on $PLA_{98.5}$ was similar to that of those based on PLA_{96}. However, unlike with the other nucleating agents, a singular behaviour was noticed on $PLA_{98.5}$ systems nucleated with PDLA ($PLA_{98.5}$/DOA/PDLA). This system showed higher crystallization rate than PLA_{96}/DOA/PDLA. Furthermore, no cold crystallization was observed in the heating scans of $PLA_{98.5}$ crystallized at 90, 100 and 110ºC, indicating that the samples crystallized completely at the selected conditions during the isothermal period (Fig. 4-13).

Besides, when plasticized $PLA_{98.5}$ was nucleated with PDLA, both T_{m1} and T_{m2} were detected at higher temperatures than with other nucleating agents or without any nucleating agent. T_{m1} of $PLA_{98.5}$ increased from 154 to 165ºC. This behaviour was not observed in systems based on PLA_{96} or $PLA_{99.5}$ (Fig. 4-2 and Fig. 4-3).

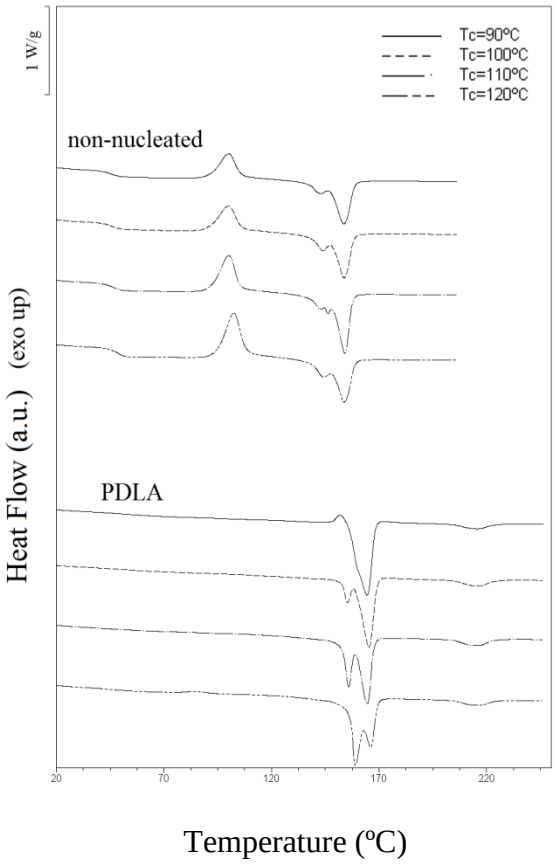

Fig. 4-13. DSC heating thermograms for plasticized PLA_{96} without nucleating agent and with PDLA crystallized at different temperatures.

For the best of the author's knowledge, this increase of the melting temperature of homochiral crystals of PLA due to the presence of stereocomplex crystals has not been reported previously. Therefore, authors believe that this is an effect that deserves more experimental work and a deeper analysis, which has not been carried out during this thesis.

4.3.6. Processing of semicrystalline PLA based compound into a heated mould

In order to study the technical feasibility of in situ crystallized PLA based compounds during injection moulding, the compound which showed the fastest crystallization rate was injection moulded to obtain test specimens. Hence, $PLA_{99.5}$/DOA/talc was injection moulded into a mould previously heated up to 95-100ºC, which was the temperature at which fastest crystallization rates were obtained by DSC. Hence, the applied injection moulding

conditions were not in accordance with those commonly recommended for amorphous PLA [104]. After several trials, the optimized injection moulding parameters for in situ complete crystallization of the compound were defined (Fig. 4-14). At these conditions, a full injection cycle took around 76 seconds. In order to ensure complete crystallization the cooling time was set for 50 seconds, but trials carried out later on showed that set cooling time could be shortened below 20 seconds, hence decreasing the full injection cycle of a 4 mm thick part below 36 seconds. This value is in the range of cost effective injection moulding timings.

Equipment	DEMAG IntElect 100
Mould	Tensile specimens (halterio)
Material	$PLLA_{99.5}$/DOA/talc

	nozzle	*barrel3*	*barrel2*	*barrel1*
Barrel T (ºC)	210	200	190	175
Mould T (ºC)	95-100			

Inj. speed (mm/s)	100
Measured P (esp. bar)	331

Holding t (s)	20
Holding P (esp. bar)	400

Cooling t (s)	50
ω (rpm)	150
Suction (mm)	62
Backpressure (esp. bar)	50

Fig. 4-14. Optimized injection moulding parameters for in situ complete crystallization of $PLA_{99.5}$/DOA/talc.

The complete crystallization was confirmed by DSC, where no cold crystallization was observed before the melting transition showing an enthalpy of 46.2 J/g (X_c=52%).

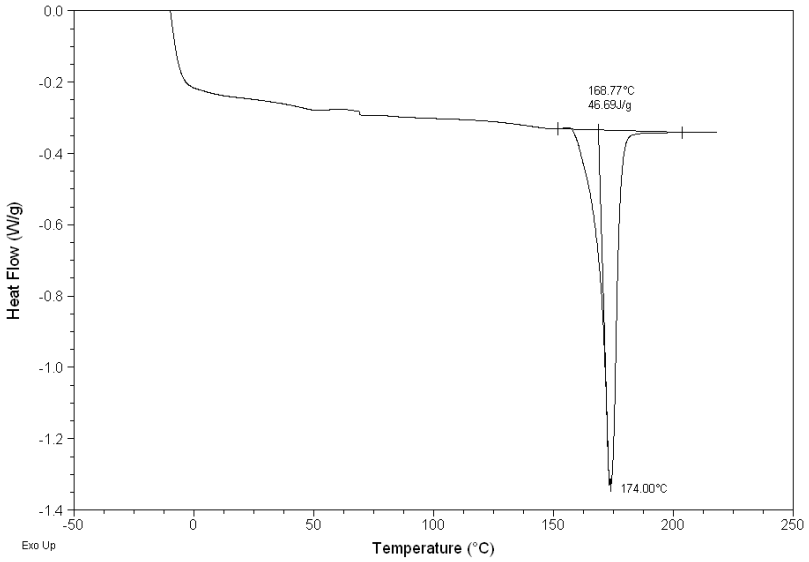

Fig. 4-15. DSC heating scan of injection moulded $PLA_{99.5}$/DOA/talc.

4.4. Conclusions

The combination of plasticizer and nucleating agents was proved to be a very effective approach to improve crystallization rates of PLA with different L-lactic acid content. Systems based on $PLA_{99.5}$ showed the fastest kinetics regardless the used nucleating agent. Results showed a stronger correlation of the crystallization kinetics to the L-lactic acid content of polylactide than to the selected nucleating agent or crystallization temperature. Talc showed to be the most efficient among the different studied nucleating agents. Plasticized $PLA_{99.5}$ nucleated with talc showed half-crystallization times below 1 minute, which make these compounds very interesting to achieve crystallized PLA products. It was concluded from PVT measurements that the increase of pressure considerably accelerated the crystallization process. Therefore, for polymer processing techniques where melted polymer crystallizes under high pressure (e.g.: injection moulding), the crystallization times obtained by DSC technique under atmospheric pressure should be taken only as illustrative values. The highest crystallization rate was observed between 90 and 100 ºC for all systems, regardless the presence or absence of nucleating agent. Avrami exponent remained constant around $n \approx 2.7\text{-}3.0$ for all compounds suggesting equivalent three-dimensional spherulitic growth regardless crystallization temperature, nucleating agent and polymer L-lactic acid

content. WAXS results of crystallized systems showed the coexistence of α and α' crystals. Among the studied parameters, the melting temperature of α crystals depend on the L-lactic acid content, whereas the achieved crystallinity degree and melting temperature of α' crystals were also influenced by the crystallization temperature and the nucleating agent.

A staggering behaviour was detected when plasticized PLA with 98.5% L-lactic acid content was nucleated with PDLA. This system showed increased melting temperatures of the homochiral crystals, which was not detected for PLA_{96} or $PLA_{99.5}$. However, this effect was not further studied within the frame of this thesis.

Chapter 5. Estimation of the useful lifespan of PLA based compounds

5.1. Introduction

Measuring the ageing of PLA based compounds is of great interest because they directly affect the properties of the polymer. The performance of PLA in terms of durability depends on multiple ageing mechanisms such as physical ageing, thermal decomposition [280–282], hydrolysis [283–285], oxidative degradation without the presence of water and UV light [286], photooxidation [287,288], natural weathering [289] and thermo-oxidation at high temperature [290,291]. Frequently several of these mechanisms take place concurrently and the resulting complex degradation mechanism becomes very hard to deconvolute [292].

The useful lifespan of PLA based compounds is variable and its prediction needs to be studied independently in each case, as it depends on the formulation of the compound. One of the major objectives of the current study was to predict the lifespan of the PLA based compounds developed during this thesis work by measuring the loss of mechanical properties while accelerated ageing at temperatures below T_m. Hence, the ageing was extended over a longer time period to avoid the pitfalls associated with high temperature range Arrhenius extrapolations to room temperature. At high temperatures the degradation mechanism can be different of that occurring at lower temperatures. In such instances a simple Arrhenius extrapolation of the high temperature data could lead to incorrect predicted lifetimes at lower temperatures. Even though some chemical and physical complications underlying a typical Arrhenius analysis of accelerated aging data have been reported [293], it is still one of the most known and used approaches for ageing data analysis. The chosen

ageing temperatures were close to those asked for durable applications like, for example, the automotive sector.

One of the most important ageing mechanisms of PLA is the degradation at thermo-oxidative conditions. Concerning kinetics of this kind of degradation, different assessments of activation energy (E_a) can be found in the literature. However, it is noteworthy that these experimental data are based on thermogravimetric measurements, which might not fit with activation energies calculated from mechanical property loss curves. For example, Gupta and Deshmukh reported that the overall activation energy of degradation of PLA was 104–125 kJ/mol from isothermal TGA measurements in air at different temperatures from 70 to 105 ºC [294]. McNeill and Leiper investigated the degradation of PLLA under both controlled heating conditions and isothermal conditions in an inert atmosphere. A first-order kinetic model enabled them to obtain an apparent activation energy of 119 ± 4 kJ/mol in the temperature range of 240–270 ºC [295,296]. Babanalbandi et al. reported E_a values for PLLA using isothermal gravimetric analysis over the temperature range 180–280 ºC under nitrogen and air. Their results showed that E_a for isothermal weight loss rate was between 72 and 103 kJ/mol depending on the weight loss fraction selected for the study [297]. Their hypothesis was that the degradation process of PLLA followed complex kinetics, even at low conversion. Liu et al. reported that the degradation of PLA at processing temperatures (i.e. 170–200 ºC under air or nitrogen) follows a random chain scission mechanism, with two to three degradation stages depending on atmosphere and exposure temperature. They identified that change of E_a from 137 kJ/mol to 142 kJ/mol can be associated with the various degradation stages [298]. Other studies have previously reported that the thermo-oxidative degradation mechanism of PLA at low temperatures (T<150 ºC) leads to a random chain scission process [286].

Lifespan predictions involve performing accelerated aging studies. Time-temperature superposition can be carried out using the data obtained at different aging temperatures when each increase in temperature increases the overall degradation rate by a constant multiplicative factor, which is the assumed principle underlying accelerated aging. When the assumption is valid, the data from each elevated temperature can be superposed at a reference temperature by multiplying the aging time at an elevated temperature by a constant, referred to as the multiplicative shift factor a_T. If the empirically derived shift factors lead to superposition of the data from all accelerated temperatures they can then be

plotted on an Arrhenius plot (log a_T versus 1/T) to see if a linear plot (Arrhenius behaviour) is obtained [293,299]. Despite Gillen et al. and Hoang et al. have published alternative models for the ageing analysis, these models have been mainly developed for polyolefins [293,300]. Therefore, the method applied within this study corresponds to that described in ISO 2578 [301]. This standard aims the determination of thermal endurance limits of plastics in general. This method is based on the direct application of the tensile strength or strain at break criteria to the Arrhenius relationship. First, for each ageing temperature, the value of the chosen property, tensile strength or strain at break, is plotted as a function of the logarithm of the time. Based on the recommendations indicated in the ISO 2578 Standard and other studies [299], the time to reach a 50% loss in tensile strength or strain at break was chosen as the end-point criteria. These points determined the times to failure at each ageing temperature. In this chapter we have focused our efforts on the prediction of the lifespan of two compounds developed during this thesis work under thermo-oxidative conditions. For this purpose, tensile tests were performed at room temperature on un-aged and aged samples using tensile strength and strain at break values as a performance indicator for the degree of ageing.

5.2. Experimental

5.2.1. Materials

The useful lifespan of two formulations obtained during this thesis and reported in 0 and 0 was studied. The selected two formulations were 1) PLA/PMMA blend 80/20 %wt, which showed the highest tensile strength and elastic modulus among all physical blend compositions studied in 0 and 2) $PLA_{99.5}$/DOA/talc, which showed the fastest crystallization kinetics in 0. Even though PLA/PMMA blend 80/20 %wt modified with 3pph of (P(S-co-GMA)) copolymer showed very interesting properties, this blend was not selected for this study because its high viscosity during reactive extrusion hindered the production of high quantities using the same equipments as in Chapter 3.

For ease of reading, the two systems, PLA/PMMA blend 80/20 %wt and $PLA_{99.5}$/DOA/talc were renamed in the next sections as PLAblend and PLAcryst, respectively.

5.2.2. Characterization techniques

Tensile tests were carried out following the specifications of ISO 527 standard, at 23ºC and 1mm/min rate by means of a MTS Insight electromechanical tensile test machine equipped with a contact mechanical extensometer. Tensile strength, modulus and strain at break were registered for each sample.

For the purpose of the lifespan estimation, tensile strength and strain at break values were of relevance. However, due to the critical importance of the impact resistance of PLA based compounds, notched Charpy tests were also carried out following the specifications of ISO 179-1 using the same specimens as for tensile testing (80x10x4 mm^3). Two heating DSC scans were performed from -10 to 250 ºC at a heating rate of 10 ºC/min using a TA Instruments Q100 model, previously calibrated by indium and sapphire standards. Finally, Dynamic Mechanical Analysis (DMA) was carried out in a Rheometrics Solid Analyzer RSA II applying a 2% deformation at a 1Hz frequency by dual cantilever bending method. Specimens with 50x4x3 mm^3 dimensions cut from injection moulded platelets were heated from 35 to 140 ºC at a rate of 2 ºC/min.

5.2.3. Sample preparation and ageing

The extrusion processes described at 3.2.2 and 4.2.2 sections were replicated in order to obtain pellets of PLAblend and PLAcryst, respectively. Dumb-bell type specimens (according to ISO 527) were injection moulded for the subsequent characterization. PLAblend pellets were injection moulded at a mould temperature of 30 ºC. On the contrary, the mould temperature was set to 100 ºC before injecting PLAcryst in order to obtain the maximum crystallinity degree during the process.

Test specimens were aged at different temperatures in air. Two ovens (Memmert UF-75 and Memmert UFE-400) set at different temperatures were used simultaneously. Five test specimens were removed from the oven at different ageing periods and conditioned to room temperature in a desiccant chamber for 24 hours before tensile testing at room temperature.

The selected ageing temperatures were 23, 50, 70, 90 and 110 ºC; the former being a temperature below the T_g of the studied systems, 50 ºC was close to the T_g and the other ageing temperatures were above T_g, but in all cases below the melting temperature (T_m).

5.3. Results and discussion

Fig. 5-1 shows the first heating DSC traces of the selected materials after injection moulding. PLAblend showed the T_g at 60 ºC and very low crystallinity degree (< %3). PLAcryst showed a melting enthalpy of 46.2 J/g (X_c=52%) and no cold crystallization process, indicating that it had been completely crystallized during injection moulding. Two T_g are observed around 42 and 71 ºC which could correspond to the mobile amorphous fraction (MAF) and rigid amorphous fraction (RAF) of the semicrystalline PLA, respectively. In both cases, the DSC results were similar to those reported in the previous chapters of this thesis except for the cold crystallization shown by PLAblend in Fig. 3-5. This system showed the same low crystallinity degree in both cases (< %3). However, the cooling rate suffered by the 2 mm thick platelet injection moulded for the analysis in Chapter 3 might be higher than for the 4 mm thick Dumb-bell type specimen for this study.

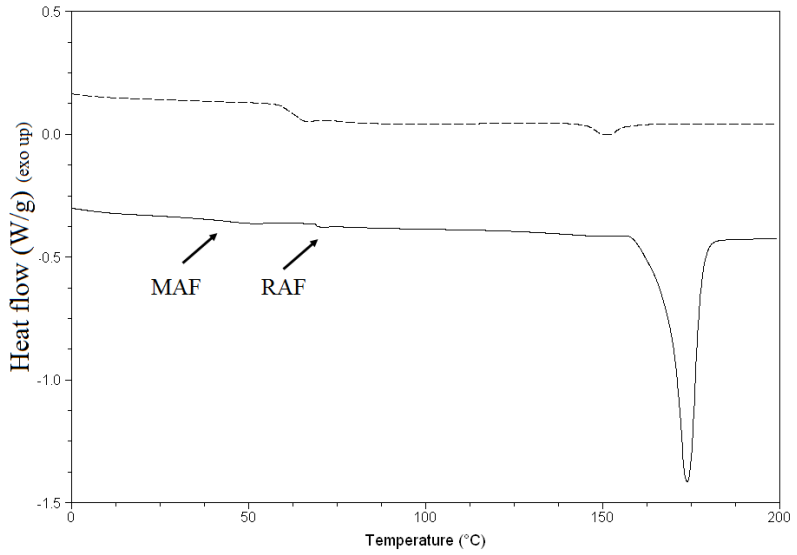

Fig. 5-1. First DSC heating scans of PLAblend (dash) and PLAcryst (solid) specimens after injection moulding.

In order to compare the dynamic mechanical behaviour of PLAblend and PLAcryst, Fig. 5-2 shows the evolution of the storage modulus of both compounds during a heating scan. Both compounds showed similar modulus at room temperature (≈2x10^9 Pa). Due to its amorphous microstructure, PLAblend showed a pronounced loss of stiffness, of around two orders of

magnitude, during T_g (≈68ºC). Hence, the maximum useful temperature of PLAblend is determined by the T_g. The slight increase of the modulus value above 100ºC is due to the cold crystallization process. However, the increase in stiffness due to the cold crystallization was not enough to withstand the dynamic bending so the test had to be stopped around 120ºC.PLAcryst showed two T_g transitions but the loss of stiffness was much smaller than for PLAblend, due to its semicrystalline structure. This compound retained the storage modulus above $2x10^8$ Pa until around 135ºC, which is a value that has been correlated to the HDT-B value (ISO 75) of PLA based compounds and therefore indicative of the maximum useful temperature.

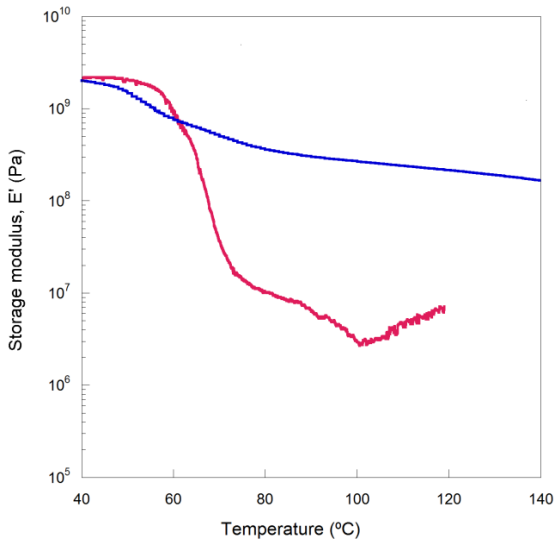

Fig. 5-2. Dynamo-mechanical behaviour of PLAblend (red line) and PLAcryst (blue line).

This indicates that PLAcryst, due to its high crystalline degree (X_c=52%), is a compound which can be used at temperatures above T_g, range at which it starts to become rubbery but still keeping a high enough stiffness.

5.3.1. Lifespan estimation of PLAblend. Tensile strength and strain at break.

The useful lifespan of PLAblend and PLAcryst has been estimated by two criteria: the loss of tensile strength and strain at break. Fig. 5-3 and Fig. 5-4 show the evolution of the tensile strength and strain at break of PLAblend while ageing at different temperatures. The remaining tensile strength and strain at break have been plotted as a function of the

logarithm of the time. The time to failure is defined as the time at which the curve intersects the horizontal line, which represents the end-point criterion. The time to failure has been reached faster for the strain at break than for the tensile strength. Hence, the loss in strain at break will lead to shorter lifespan predictions than tensile strength. For tensile strength the drop is very slow at 23 and 50 ºC, which are temperatures below the glass transition temperature. Above this temperature the effect of the ageing on the tensile strength is accelerated. On the contrary, in the case of strain at break the ageing at 23 and 50 ºC is more pronounced than for tensile strength.

A reasonable time-temperature superposition was obtained when the curves were shifted (T_{ageing}=90 ºC was selected as reference), which indicated an Arrhenius behaviour of PLAblend. It should be noted that data obtained at 23 ºC was not included in the time-temperature superposition analysis of both tensile strength and strain at break due to the lack of a sufficient amount of loss to generate a plausible shift factor.

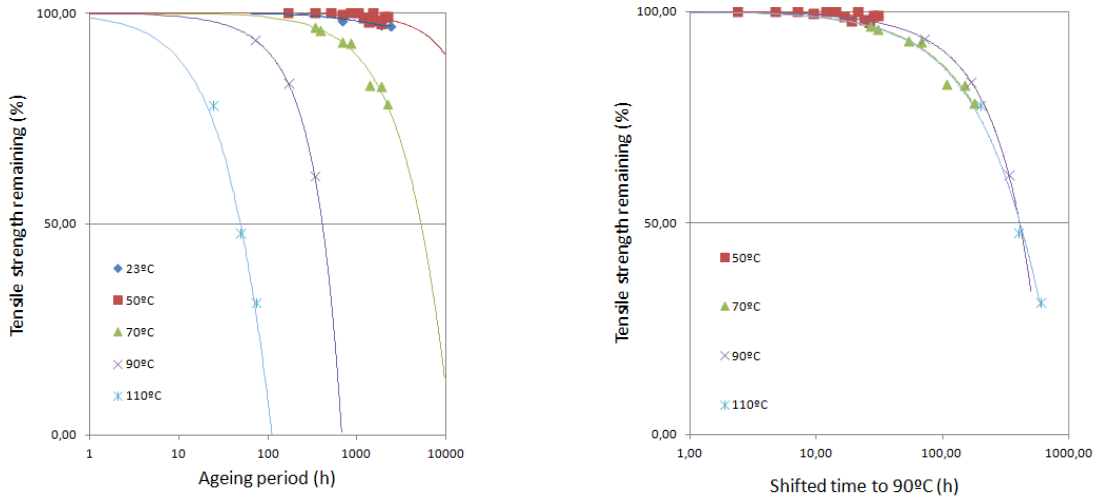

(a) (b)

Fig. 5-3. Tensile strength loss of PLAblend (a) at different ageing temperatures and (b) time-shifted curves (reference temperature: 90 ºC).

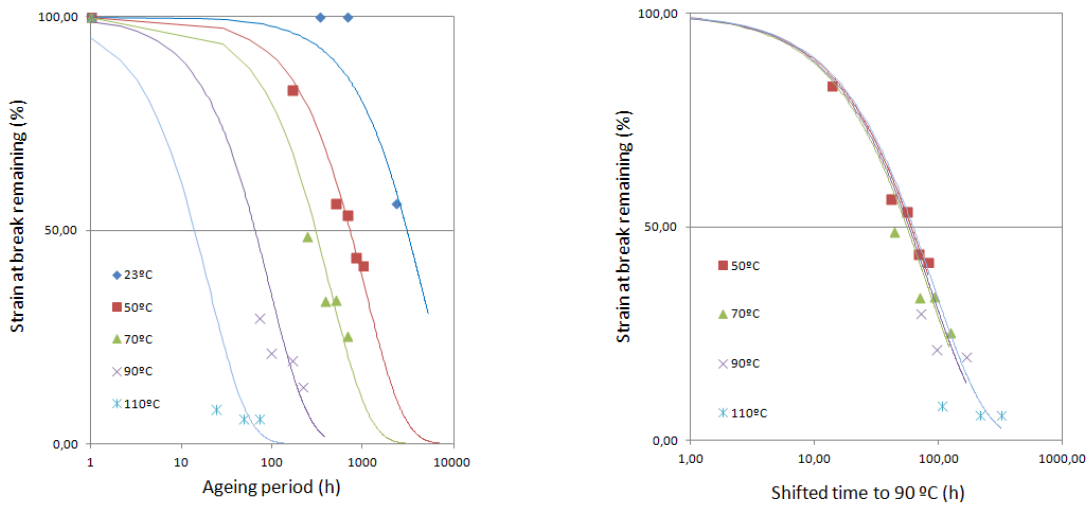

(a) (b)

Fig. 5-4. Strain at break loss of PLAblend (a) at different ageing temperatures and (b) time-shifted curves (reference temperature: 90 ºC).

.

The calculation of the *thermal endurance plot* is based on these times to achieve the end point criterion and the respective exposure temperatures. The times to achieve the end point criterion at each temperature are plotted in a logarithmic time scale as the ordinate and an abscissa based on the reciprocal of the absolute temperature showing the correlated values in degrees Celsius. A first-order regression line is then drawn through the points plotted on the graph, which thus represents the thermal endurance of the studied material [301]. The reliability of the extrapolation of the graph depends on obtaining an acceptable Arrhenius plot. This is defined in ISO 2578 as the value of the correlation coefficient R^2 to be higher than 0.95. Fig. 5-5 shows the endurance plots obtained for PLAblend. The correlation coefficient correspondent to the two linear regressions were R^2=0.988 and 0.967 for tensile strength and strain at break, respectively. This confirmed that the ageing behaviour of PLAblend obeys an Arrhenius law.

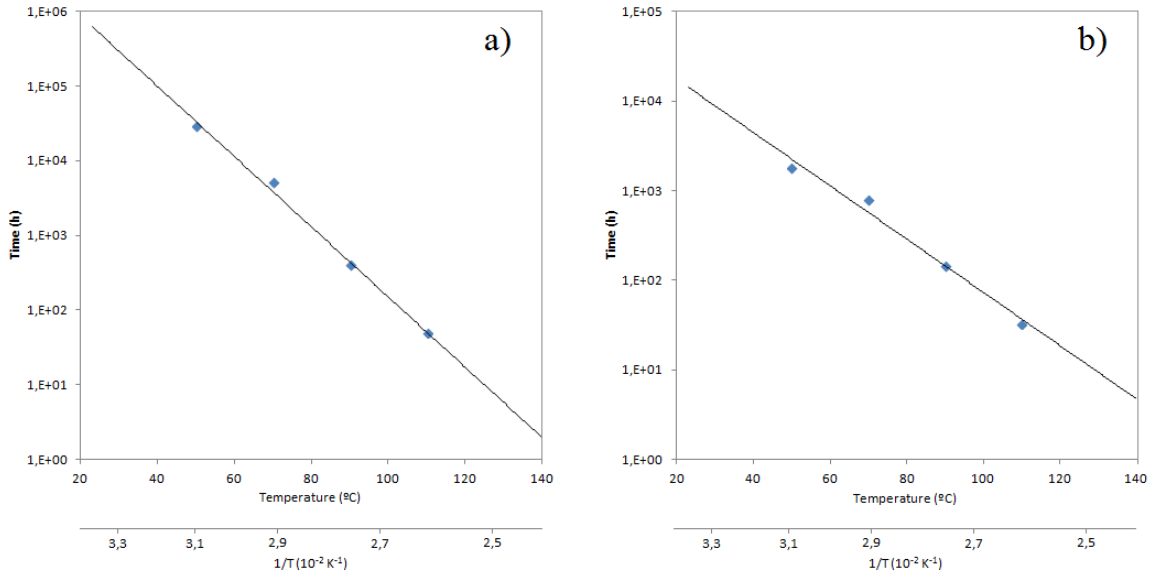

Fig. 5-5. Thermal endurance plot of PLAblend calculated for 50% loss of a) tensile strength and b) strain at break.

The lifespan varies significantly depending on the selected criterion. The strain at break has shown to be more sensitive to ageing than the tensile strength due to the inherent brittleness of this PLA based compound (Table 5-1). The blend has been predicted to be able to stand from 1 to 4 months at 70 ºC, but the lifespan is reduced to a few hours from 90 ºC on. At temperatures below T_g, i.e. 23 and 50 ºC, the lifespan estimation gives interesting values. PLAblend seems to be very stable at 23 ºC concerning the tensile strength, but the strain at break reaches a 50% loss in two years and a half, so the stability of the compound might have its limitations even at 23 ºC. Even though at 50 ºC the compound is below the T_g, the lifespan is limited to 3 months in terms of strain at break loss. It has to be noted that, although the regression line obtained from the endurance plots is within the range required by the ISO 2578, the T_g is a second order transition which might disrupt the proper extrapolation of the estimated lifespan below T_g. Therefore, probably the values estimated for temperatures below T_g are lower than the real ones, as they have been estimated by a regression line which includes three data obtained above T_g.

Time / T(ºC)	Tensile strength		Strain at break	
	h	months	h	months
23	1435653	1994	21474	30
50	33298	46	2000	3
70	3003	4	439	0.6
90	353	0.5	114	0
110	52	0	34	0

Table 5-1. Lifespan of PLAblend estimated for a 50% loss of tensile strength or strain at break.

Finally, the activation energy (E_a) of PLAblend was calculated by the equation of the endurance plot Eq. 5-1 [302]:

$$\ln t_{endurance} = \ln(A) + \frac{1}{T} E_a \qquad \text{Eq. 5-1}$$

Where $t_{endurance}$ represents the endurance time, A is a material constant, T is the absolute temperature in K, and E_a is the activation energy in J/mol.

E_a of PLAblend is 13 kJ/mol and 8.4 kJ/mol for tensile strength and strain at break, respectively. This indicates that the stability of the mechanical properties of these PLA based compounds is far lower than other conventional engineering thermoplastics like polycarbonate (PC) (229-272 kJ/mol) [302] or polyamide (PA) (77 kJ/mol) [299]. Rasselet et al. reported that PLA can suffer chain scission under thermo-oxidative conditions at temperatures from 70 ºC to the melting temperature and that the effect of hydrolysis can be neglected at those conditions [286]. They detected a decrease of T_g value which was attributed to the chain scission and molecular weight loss of PLA due to oxidation. They also reported a linear relationship between $1/M_n$ and the T_g for samples aged at 110-150ºC. Concerning PLAblend, Fig. 5-6 shows the second heating DSC scans of PLAblend before and after ageing at 50 and 110 ºC for the maximum tested time period, where no decrease of T_g value is noticed. On the contrary, T_g is increased around 4 ºC regardless the ageing temperature. These results suggested that the ageing mechanism is similar at both temperatures and that there is no important molecular weight loss due to oxidation, which would have induced a reduction of the glass transition temperature. The ageing periods applied in our study did not exceed 72 hours at 110 ºC because it was enough to reach the

selected end-point criteria (50% loss of the mechanical property) whereas Rasselet et al. extended their research for 500 hours, until they reached 1% strain at break. It is noteworthy that they did not detect any significant T_g decrease in the temperature and time range that we used in our study, which is in agreement with the results reported in this work. Hence, probably the same degradation mechanisms might have led the degradation in our study, the difference being that we stopped the ageing tests before reaching a molecular weight loss that would have led to a T_g value decrease.

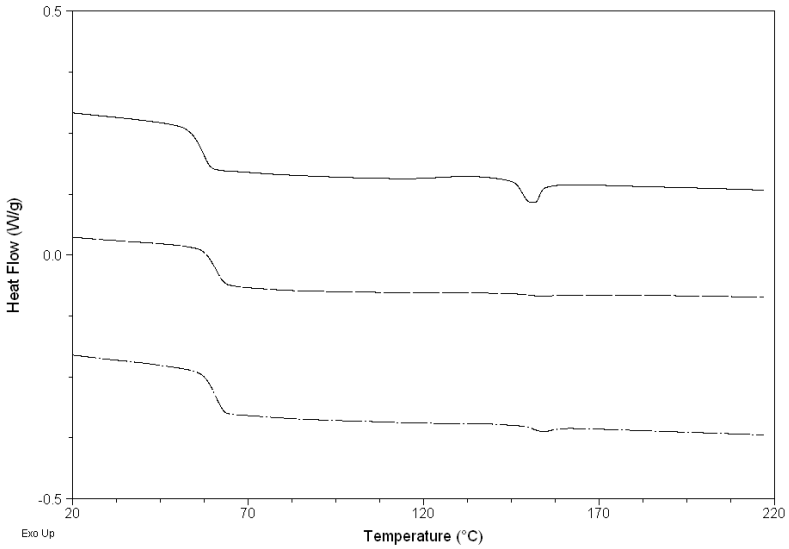

Fig. 5-6. Second DSC heating scans of PLAblend aged at different temperatures.
Un-aged (solid line), 50 ºC (dash), 110 ºC (dash-dot).

Regarding the tensile modulus of PLAblend, it remained constant at around 3.5 GPa after ageing at different temperatures. This indicates that despite ageing decreases the ability of the material to elongate increasing brittleness, the elastic range, where the modulus is measured, remains unaltered. Regarding the impact properties, PLAblend showed an impact resistance of 1.7 kJ/m^2 for notched specimens before ageing. After 3 months of ageing at different temperatures the impact resistance value was still the same.

5.3.2. Lifespan estimation of PLAcryst. Tensile strength and strain at break.

Again, a 50% loss in the selected property has been defined as the end-point criterion. Fig. 5-7 shows the evolution of the strain at break of PLAcryst while ageing at different

temperatures. Due to the fast loss of strain at break, which we realized after obtaining the results, the amount of data points above 50% of loss was not enough to obtain a reliable fit. Therefore, in the case of PLAcryst, the lifespan estimation study has only been carried out using tensile strength data.

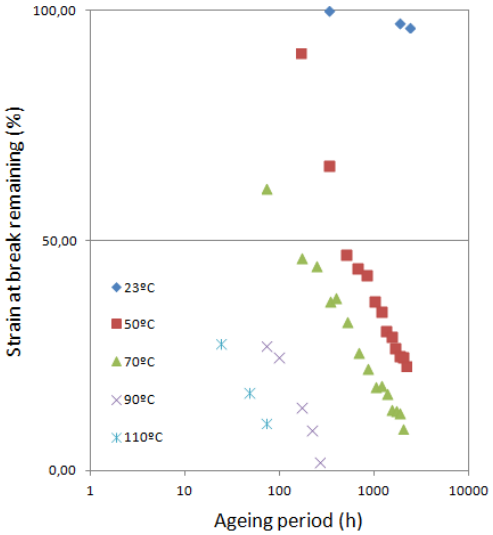

Fig. 5-7. Strain at break loss of PLAcryst at different ageing temperatures.

Fig. 5-8 shows the evolution of the tensile strength of PLAcryst while ageing at different temperatures. The drop is slow at 23 ºC, which is below the glass transition temperature of this compound (≈45 ºC). Above this temperature the effect of the ageing is quickly accelerated. It should be mentioned that it was observed an increase of tensile strength above 100% for the system aged at 50 and 70 ºC. Similar to PLAblend, a reasonable time-temperature superposition was obtained for PLAcryst when the curves were shifted (T_{ageing}=90 ºC was selected as reference), which indicated the Arrhenius behaviour (Fig. 5-8). It should be noted that data obtained at 23 ºC was not included in the time-temperature superposition analysis due to the lack of a sufficient amount of tensile strength loss to generate a plausible shift factor. Fig. 5-9 shows the endurance plot obtained for PLAcryst. The correlation coefficient correspondent to the linear regression was R^2=0.953, which confirmed that the ageing behaviour of PLAcryst obeys an Arrhenius law.

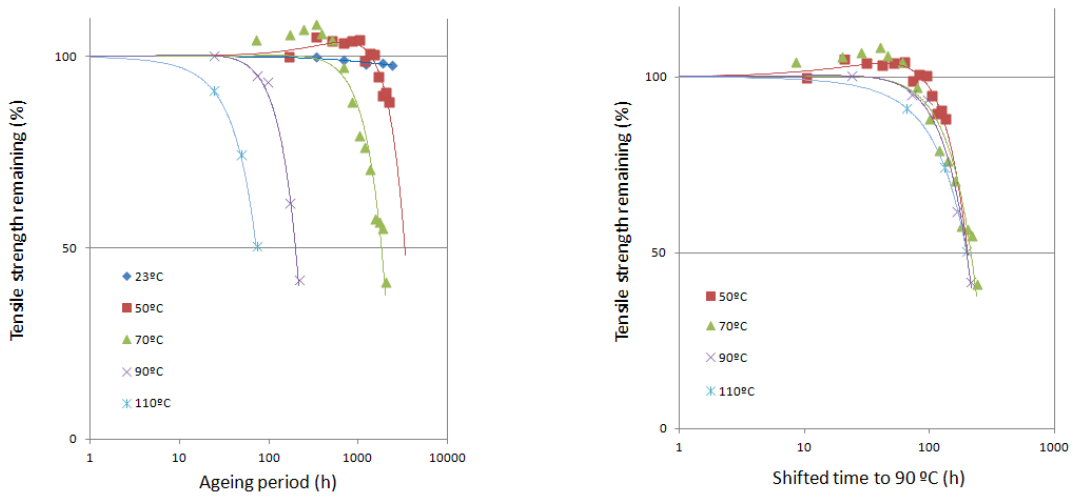

(a) (b)

Fig. 5-8. Tensile strength loss of PLAcryst at different ageing temperatures (left) and time-shifted curves (reference temperature: 90 ºC).

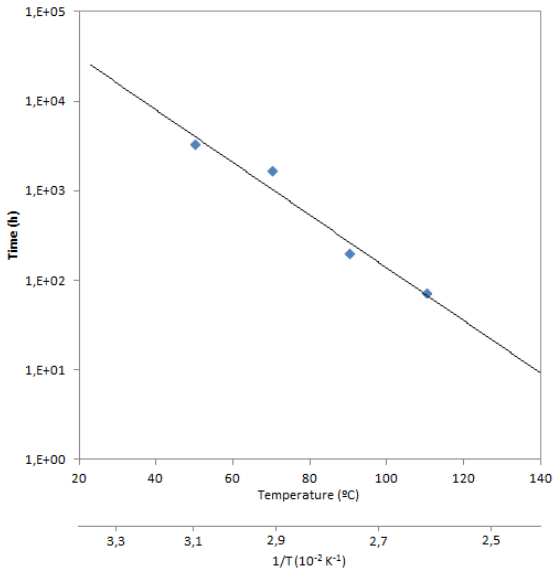

Fig. 5-9. Thermal endurance plot of PLAcryst calculated for 50% loss of tensile strength.

PLAcryst has been predicted to be able to stand around 1 month and a half at 70 ºC (Table 5-2), but the lifespan is reduced to a few hours form 90 ºC on. Compared to PLAblend, using the tensile strength loss criteria for both compounds, PLAcryst shows a shorter usage

lifespan, probably due to the lower T_g, which accelerates ageing. At 23 ºC, which is below the T_g of the compound, PLAcryst is supposed to withstand almost 3 years before it loses half of its tensile strength. At 50 ºC the lifespan is reduced to 7 months. Probably, the values estimated for temperatures below T_g (i.e. 23 ºC) are lower than the real ones, as they have been estimated by a regression line carried out on data obtained above T_g.

Time / T(ºC)	h	months
23	50512	70
50	4802	7
70	1067	1
90	280	0
110	84	0

Table 5-2. Lifespan of PLAcryst estimated for a 50% loss of tensile strength.

On the other hand, the activation energy (E_a) of PLAcryst was calculated by the equation of the endurance plot Eq. 5-1 [302]. E_a calculated by loss in tensile strength of PLAcryst is 8.3 kJ/mol, a value which is very close to those obtained for PLAblend, suggesting that the stability of the mechanical properties of these PLA based compounds is far lower than other conventional engineering thermoplastics [299,302]. Fig. 5-10 shows the second heating DSC scans of PLAcryst before and after ageing at 50 and 110 ºC for the maximum tested time period. Due to the high crystallinity, the T_g of PLAcryst was not easy to measure by DSC. However, it was estimated that it increased around 6-7 ºC regardless the ageing temperature, a bit more than the T_g increase of PLAblend at the same conditions, probably due to the loss of DOA plasticiser during ageing. Like for PLAblend, this increase suggested that the ageing mechanism is similar at both temperatures and there is no important molecular weight loss due to oxidation, which would have induced a reduction of the glass transition temperature. Hence, the same degradation mechanisms as PLAblend might have been suffered by PLAcryst.

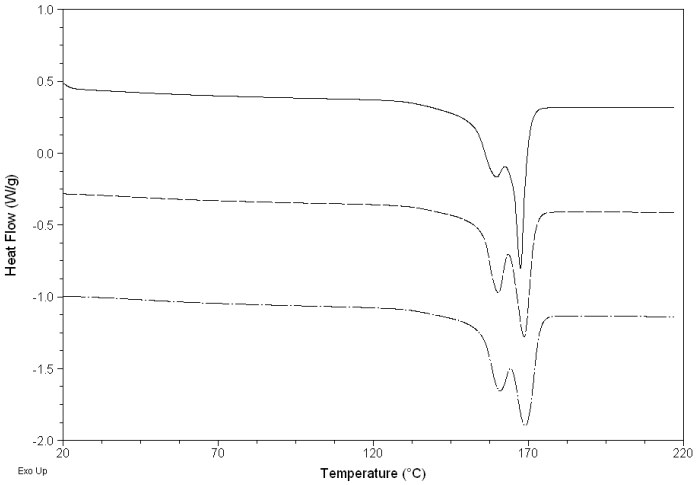

Fig. 5-10. Second DSC heating scans of PLAcryst aged at different temperatures: Un-aged (solid line), 50 ºC (dash), 110 ºC (dash-dot).

Similar to what was seen for PLAblend, the tensile modulus of PLAcryst remained constant at around 3.5 GPa after ageing at different temperatures. This indicates that despite ageing increases brittleness, the elastic range, where the modulus is measured, remains unaltered for amorphous and semicrystalline PLA compounds.

Impact resistance measurements showed a fast embrittlement of PLAcryst (Fig. 5-11), coming down from 6 to 3 kJ/m^2 after two months ageing at 50 ºC, less than one at 70 ºC and just a few days at 90-110 ºC.

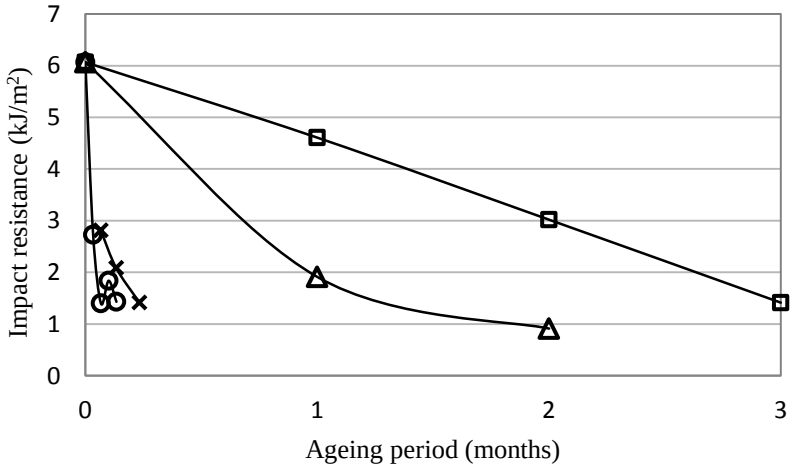

Fig. 5-11. Evolution of impact resistance of PLAcryst while ageing at different temperatures: □ 50 ºC, Δ 70 ºC, × 90 ºC and ○ 110 ºC.

These results fit with the fast ageing detected for strain at break. Even though the tensile modulus is stable and tensile strength is kept over 50% for some months at 23 and 50 ºC, the embrittlement of this compound is very fast above its T_g, which is around 45 ºC.

5.3.2.1. Increase in tensile strength: stability of DOA in the compound.

Results showed an increase in tensile strength after a certain ageing time for systems aged at 50 and 70 ºC. This effect was not noticed at 23 ºC and above 70 ºC. Thus, DSC analysis was carried out to a sample aged at 50 ºC during 42 days, which was one of the tests that showed the highest tensile strength. Fig. 5-12 shows the DSC thermograms of this sample and an un-aged PLAcryst sample. The melting enthalpy is around 46 J/g in both curves, and the peaks show no important variations except a little displacement of the melting peak at T_{m2}. However, there is a clear variation at the glass transition temperature. Before ageing, two T_g are observed at 42 and 71 ºC which could correspond to the mobile amorphous fraction (MAF) and rigid amorphous fraction (RAF) of the semicrystalline PLA, respectively. The low value of the T_g of the MAF suggests that DOA plasticizer is mainly concentrated in this fraction. However, after an ageing of 42 days at 50 ºC a single T_g is detected at 55 ºC, which is close to the T_g of the unplasticized PLA. Therefore, the ageing seems to lead to a reorganization of the amorphous phase and a partial/complete migration of the plasticizer, which could increase the tensile strength.

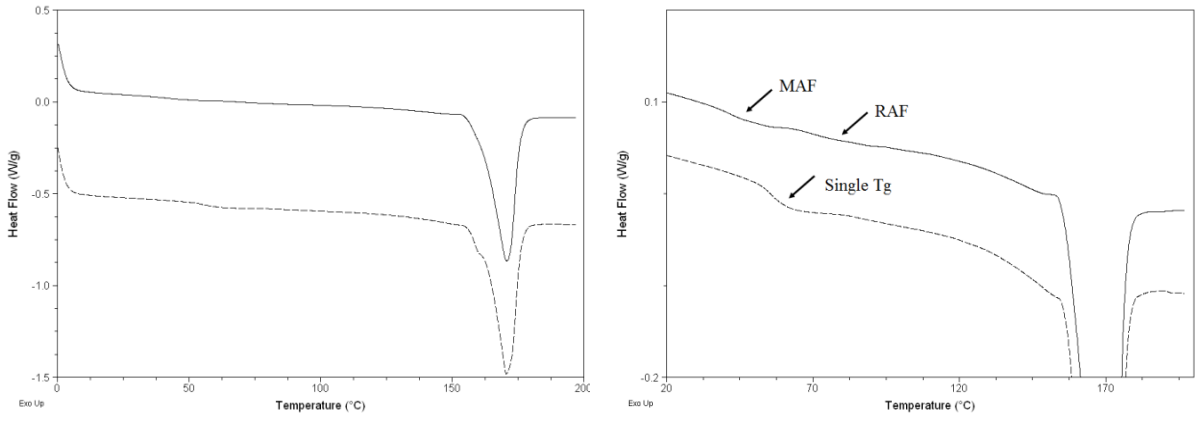

(a) (b)

Fig. 5-12. a) DSC first heating scans of PLAcryst before (solid line) and after ageing for 42 days at 50 ºC (dash) and b) magnification of the region of the glass transition.

The increase of the tensile strength above 100% was not detected at 90 and 110 ºC probably because the migration process was faster at temperatures above 70 ºC, same as the loss in tensile strength or strain at break due to ageing. Hence, at those temperatures the increase in strength due to the migration of plasticizer could be compensated by the loss due to ageing, or perhaps the frequency of testing was not enough to detect the effect of the plasticizer loss on the tensile strength values. On the other hand, concerning ageing at 23 ºC, the plasticizer might be more stable in the compound, so it might not migrate or do it at a very slow rate.

5.4. Conclusions

The useful lifespans of PLA/PMMA 80/20 (%wt) and PLA/DOA/talc have been estimated based on the stability of mechanical properties while ageing. The studied PLA based systems showed low activation energies, around 8-20 kJ/mol, far lower than the mechanical test based activation energies reported for other thermoplastics. This indicates that the stability of the mechanical properties of these compounds is lower than other conventional engineering thermoplastics.

Estimations predicted longer lifespans for PLA/PMMA than for PLA/DOA/talc. However, both compounds showed short lifespans when aged at temperatures above their corresponding glass transition.

On the other hand, PLA/PMMA showed a drastic loss in stiffness at T_g due to its almost amorphous structure. Hence, it should be used below its glass transition temperature. On the contrary, due to its semicrystalline structure, PLA/DOA/talc showed acceptable mechanical properties above its glass transition temperature, in the range of 50 to 90 ºC. Therefore, this compound would also be an interesting option for applications which require being occasionally heated up to 90 ºC for short periods.

On the other hand, the low stability of DOA plasticiser in PLAcryst has been reported. It should be noted that the plasticizer has been added to these compounds with the aim of accelerating the crystallization process. However, its presence in the compound is not that interesting in terms of thermal properties, as it decreases the glass transition temperature.

Therefore, after accelerating the crystallization process, once a semicrystalline PLA based compound is produced, the migration of the plasticizer can be, if controlled, a positive point for this kind of compounds.

Chapter 6. Conclusions

6.1. General conclusions

PLA is a biobased and biodegradable polymer with interesting mechanical properties. However, in its amorphous state, the brittleness and the moderate thermal resistance have been the limiting factors to use this polymer in semidurable and durable applications. In this PhD thesis new PLA-based formulations with enhanced properties were developed and comprehensively studied. Physical blending, reactive blending and accelerated crystallization approaches were proved to be interesting ways to achieve this aim. The mechanical and thermal properties together with the estimated lifespan of the developed compounds suggested that each of them could be useful for a different durable/semidurable application.

The blending approach.

A clear displacement to higher values of the T_g of PLA was noticed when it was blended with high molecular weight PMMA, hence slightly increasing the thermal resistance. The miscibility of PLA/PMMA blends prepared via melt processing seemed to be dependent on the mixing processing conditions (temperature and screw rotation speed) and the molecular weights of the polymers. The impact resistance increased at least 78 % when the presence of PMMA in the blend was 50 wt% or higher, probably due to a phase inversion in the blend. These blends are easy to produce by extrusion and also to be injection moulded.

However, the impact resistance exhibited by these blends was similar to that of the neat polymer they were rich in. Thus, those with a high presence of PLA showed a low impact resistance. This limited level of impact resistance of neat PLA was overcome by reactive blending PLA with PMMA at 80/20 wt% modified by 3pph of the reactive poly(styrene-co-glycidyl methacrylate) copolymer. This way a ductile compound with a high PLA content was developed by reactive extrusion due to the improved interfacial adhesion. The overall properties of this blend are unique: toughness combined with high tensile stiffness and strength, all together in a high PLA containing blend (>75%). However, the reactive extrusion leads to an important increase of viscosity; therefore, the amount of added reactive copolymer to the blend is a key factor in order to achieve melt-processable modified PLA/PMMA blends.

The accelerated crystallization approach.

PLA with different L-lactic acid content were studied in combination of a plasticizer (DOA) and different nucleating agents in order to accelerate the crystallization rate to injection moulding timings. The results showed a stronger correlation of the crystallization kinetics to the L-lactic acid content of polylactide than to the selected nucleating agent or crystallization temperature. Among talc, EBS and PDLA, talc showed to be the most efficient nucleating agent in the studied crystallization temperature range. Therefore, PLA with ≈99.5 L-lactic acid content plasticized with 5% of DOA and nucleated with another 5% of a specific laminar talc (B.E.T.=19.5m^2/g) showed the fastest crystallization rates, crystallizing at half-crystallization times below 1 minute. Besides, it was shown that the increase of pressure considerably accelerated the crystallization process, which indicates that this compound is very interesting to achieve crystallized PLA products by injection moulding. The highest crystallization rates were observed between 90 and 100 ºC by DSC, which is an interesting guideline to define the best mould temperature to shorten the injection cycle.

After compounding by extrusion, the only handicap to properly process this compound by injection moulding is that the mould should be heated up to 95-100 ºC, which is not a big technical deal for any engineering plastic processor. At these conditions, plastic parts can be

moulded at cycle times below 40 seconds for a 4 mm thick part, which is within the economically feasible range for injection moulding.

Lifespan estimation of the studied PLA based compounds

The lifespan estimation of PLA/PMMA 80/20 (%wt) when aged below T_g, temperature range at which amorphous thermoplastics are supposed to be used, indicates that this compound would retain its properties for more than two years and a half in terms of strain at break, and a great amount of years concerning tensile strength. Hence, this material could be potentially used in applications where high stiffness and impact resistance are asked at a limited working temperature (<60ºC).

On the contrary, the PLA/DOA/talc becomes brittle much faster than PLA/PMMA 80/20 (%wt) when aged. However, this system shows better mechanical properties than PLA/PMMA 80/20 (%wt) in the range of 50 to 90 ºC due to its high crystallinity, which allows this compound to be used above its T_g. Therefore, PLA/DOA/talc would be an interesting option for applications which require for slight mechanical resistance around 50-90 ºC, the limiting factor being that spending long periods (weeks) at these temperatures will accelerate the ageing and so the embrittlement of the compound.

As a general conclusion, these compounds are not suitable for demanding durable applications like automotive, household appliances etc. were 8-12 years long lifespans are required. However, they can be suitable for semi-durable consumer goods like mobile-covers, keyboards... which demand for shorter, 2-3 years long, lifespans. In those cases, PLA/PMMA 80/20 (%wt) will be a better choice than PLAcryst due to its better ageing stability for products which require application temperatures below 60 ºC. If, on the contrary, the plastic part might suffer for some brief hot situations (60-80 ºC), PLA/DOA/talc will be a better option, due to its better properties above T_g.

6.2. Prospects for future research

Some interesting topics were put aside while the researching period of this thesis. Besides, some others have arisen from the obatined results. A summary of the most interesting ones is briefly considered in this section.

The study of the increase of the melting temperature of PDLA nucleated PLA systems.

During the experimental work reported in Chapter 4, some particular tests were carried out using a PLA grade with a 1.5% D-lactic acid content. The general behaviour of the systems based on this PLA was similar to that of those based on PLA_{96}. However, unlike with the other nucleating agents, a singular behaviour was noticed on $PLA_{98.5}$ systems nucleated with PDLA ($PLA_{98.5}$/DOA/PDLA). Both T_{m1} and T_{m2} were detected at higher temperatures than with other nucleating agents or without any nucleating agent. T_{m1} of $PLA_{98.5}$ increased from 154 to 165ºC.

As mentioned before, for the best of the author's knowledge, this increase of the melting temperature of homochiral crystals of PLA due to the presence of stereocomplex crystals has not been reported previously. Therefore, authors believe that this is an effect that deserves more experimental work and a deeper analysis, which is planned to be studied in the near future.

Estimation of the useful lifespan of PLA/PMMA 80/20 (%wt) blend modified with 3pph of (P(S-co-GMA)) copolymer, together with neat PLA and ABS as intercomparative references.

Chapter 5 reports the study concerning the useful lifespan estimation of PLA/PMMA 80/20 (%wt) and PLA/DOA/talc compounds. However, the properties of the mentioned PLA/PMMA blend were considerably improved when it was modified with the reactive (P(S-co-GMA)) copolymer. The study of this blend was discarded from the planned experimental work because its high viscosity during reactive extrusion hindered the production of the high quantities of compound needed for the ageing tests. The interesting properties of this compound compared to the non-reactive one makes interesting to estimate

its useful lifespan. Indeed, its modified molecular arquitecture (branched) might improve its stability.

Besides, the estimation of the lifespan of neat PLA will enable to analize whether the developed compounds have a shorter or larger lifespan than the neat polymer. Moreover, the same information regarding a petrochemical thermoplastic (i.e.: ABS) will add context to evaluate the lifespans of these PLA based compounds against conventional plastics.

Identification of the main mechanisms behind the ageing of PLA based compounds.

The lifespans of two PLA based systems have been estimated and reported in Chapter 5 of this thesis. But the mechanisms behind the the ageing had not been studied. This is a very interesting but complicated issue to be solved, especially because various mechanisms might take place concurretly, leading to a very complex solution. However, the monitoring of the molecular weight loss during ageing by GPC is method that has given interesting results for other systems found in literature, so we believe there is plenty of interesting research which could be carried out in this sense.

6.3. List of publications

Anakabe, J., Zaldua Huici, A. M., Eceiza, A., & Arbelaiz, A. (2015). Melt blending of polylactide and poly (methyl methacrylate): Thermal and mechanical properties and phase morphology characterization. *Journal of Applied Polymer Science*, 132(42).

Anakabe, J., Zaldua Huici, A. M., Eceiza, A., & Arbelaiz, A. (2016). The effect of the addition of poly (styrene-co-glycidyl methacrylate) copolymer on the properties of polylactide/poly (methyl methacrylate) blend. *Journal of Applied Polymer Science*, 133(37).

Anakabe, J., Zaldua Huici, A. M., Eceiza, A., Arbelaiz, A., & Avérous, L. (2017). Combined effect of nucleating agent and plasticizer on the crystallization behaviour of polylactide. *Polymer Bulletin* (accepted, DOI: 10.1007/s00289-017-1989-z).

Anakabe, J., Eceiza, A., Arbelaiz, A. & Zaldua Huici, A. M. (2017). Evolution of the mechanical properties and the estimation of useful lifespan of PLA based compounds. *Polymer testing* (submitted).

6.4. List of communications

Anakabe, J., Zaldua Huici, A. M., & Mondragon, I. (2012). Study of phase morphology and mechanical properties of PLA/PMMA blends. *11th European Symposium on Polymer Blends* (Donostia-San Sebastian, Spain)

Anakabe, J., Zaldua Huici, A. M., Eceiza, A., & Arbelaiz, A. (2015). Effect of epoxy functionalised poly (styrene-co-acrylate) copolymer on high PLA content PLA/PMMA blends. *5th International Conference on Biobased and Biodegradable Polymers* (Donostia-San Sebastian, Spain)

Annex I: Index of Figures

Annex II: Index of Tables

Annex III: Abbreviations

Materials

A-PLA	Amorphous Polylactide
ABS	Acrylonitrile-Butadiene-Styrene polymer
CNC	Cellulose Nanocrystals
DMF	Dimethylformamide
EBS	Ethylene bis-stearamide
EPDM	Ethylene Propylene Diene Monomer rubber
E-PLA	Expanded Polylactide
EPS	Expanded polystyrene
MMT	Montmorillonite clay
PA	Polyamide
PBAT	Poly(butylene-adipate-terephthalate)
PBS	Poly(butylene succionate)
PBT	Poly(butylene terephthalate)
PC	Polycarbonate
PCL	Polycaprolactone
PDLA	Poly D-lactide
PE	Polyethylene

PEF	Poly(ethylene furanoate)
PET	Poly(ethylene terephthalate)
PHA	Poly(hydroxyalkanoate)
PHB	Poly(hydroxybutyrate)
PHBV	Poly(hydroxybutyrate-valerate)
PMMA	Poly(methyl methacrylate)
PLA	Polylactide, Poly(lactic acid)
PLLA	Poly L-lactide
PP	Polypropylene
PS	Polystyrene
P(S-co-GMA)	Poly(styrene-co-glycidyl methacrylate)
PTT	Poly(trimethylene terephthalate)
PU	Polyurethane
PVC	Poly(vinyl chloride)
sc-PLA	Stereocomplex polylactide
THF	Tetrahydrofurane

Techniques

DMA	Dynamic Mechanical Analysis
DSC	Differential Scanning calorimetry
FTIR	Fourier Transform Infrared
GPC	Gas Permeation Chromatography
NMR	Nuclear Magnetic Resonance
SEM	Scanning Electron Microscopy

REx	Reactive Extrusion
WAXS	Wide Angle X-ray Scattering

Others

ASTM	American Society for Testing and Materials
CAGR	Compound Annual Growth Rate
CAS	Chemical Abstract Service
FWHM	Full Width at Half Maximum
GMO	Genetically Modified Organisms
LAB	Lactic Acid Bacteria
LCA	Life-Cycle Assessment
PDI	Polydispersity Index
pph	parts per hundred
ppm	parts per million
RH	Relative Humidity

Annex IV: Symbols

C_p	Heat capacity
E	Elastic Modulus (Young's)
E_{coh}	Cohesive energy
F	Molar attraction constant
k	Avrami rate constant
M_n	Number average molecular weight
M_w	Weight average molecular weight
n	Avrami type geometrical growth mechanism
Đ	Polydispersity index
R	Univesal gas constant
T_c	Crystallization temperature
T_g	Glass transition temperature
T_m	Melting temperature
X_c	Degree of crystallinity
V	Molar volume of the repeating unit
V_c	Volumetric crystallinity fraction
ΔH_c	Cold crystallization enthlapy
ΔH_m	Melting enthalpy

ΔH_0	Theoretical melting enthalpy of a 100% crystalline polymer
η	Viscosity
$\dot{\gamma}$	Shear rate
Ø	Diameter
σ	Tensile strength
ω	Weight fraction
δ	Solubility parameter
χ_{12}	Flory-Huggins interaction parameter
2θ	Angle in X-ray diffraction

References

[1] D.R. Dodds, R.A. Gross, Chemicals from Biomass, Science. 318 (2007) 1250–1251. doi:10.1126/science.1146356.

[2] R. Narayan, Carbon footprint of bioplastics using biocarbon content analysis and life-cycle assessment, MRS Bull. 36 (2011) 716–721.

[3] Marcel Darlee, Sophisticated blends for durable biopolymers, Bioplastics Mag. 8 (2013) 20–21.

[4] A.U. Queiroz, F.P. Collares-Queiroz, Innovation and industrial trends in bioplastics, J. Macromol. Sci. Part C Polym. Rev. 49 (2009) 65–78.

[5] R Narayan, 3rd International Conference on Biodegradable and Biobased Polymers, in: Strassbourg, 2011.

[6] L. Avérous, Polylactic acid: synthesis, properties and applications, in: Monomers Polym. Compos. Renew. Resour., Elsevier: Oxford, UK, 2008. https://books.google.es/books?hl=es&lr=&id=N-byhCZyTn0C&oi=fnd&pg=PA433&dq=averous+2008&ots=HavSDry8ut&sig=gFcPt4ovPOnMFwEMy97mpfOArps (accessed September 14, 2016).

[7] Market study and Trend Reports on "Bio-based Building Blocks and Polymers in the World – Capacities, Production and Applications: Status Quo and Trends Towards 2020″ - Bio-based News - The portal for bio-based economy and industrial biotechnology, Bio-Based News. (n.d.). http://news.bio-based.eu/market-study-and-trend-reports-on-bio-based-building-blocks-and-polymers-in-the-world-capacities-production-and-applications-status-quo-and-trends-towards-2020-2/ (accessed May 11, 2015).

[8] Tomi Nyman, News for "drop-in" bioplastics, Bioplastics Mag. 9 (2014) 12–13.

[9] Harald Kaeb, Florence Aeschelmann, Lara Dammer, Michael Carus, Market Study on Consumption of biodegradable and compostable plastic products in Europe, European Bioplastics, 2016.

[10] The Coca-Cola Company, Coca-Cola Produces World's First PET Bottle Made Entirely From Plants, 2015. http://www.coca-colacompany.com/stories/coca-cola-produces-worlds-first-pet-bottle-made-entirely-from-plants (accessed September 26, 2016).

[11] Michael Carus, nova-newsletter March 2015, (2015).

[12] François de Bie, Global bioplastics production capacities continue to grow despite low oil price, in: Berlin, 2015.

[13] Purac Biochem bv, Corbion Purac successfully develops PLA resin from second generation feedstocks, (2015). http://www.corbion.com/media/press-releases?newsId=1955535.

[14] Bio-based economy - Services of the nova-Institut GmbH, Bio-Based Econ. (n.d.). http://bio-based.eu/ (accessed November 28, 2016).

[15] D. Almeida, M. de F. Marques, Thermal and catalytic pyrolysis of plastic waste, Polímeros. 26 (2016) 44–51.

[16] E. Sevigné-Itoiz, C.M. Gasol, J. Rieradevall, X. Gabarrell, Contribution of plastic waste recovery to greenhouse gas (GHG) savings in Spain, Waste Manag. 46 (2015) 557–567.

[17] D.K.A. Barnes, F. Galgani, R.C. Thompson, M. Barlaz, Accumulation and fragmentation of plastic debris in global environments, Philos. Trans. R. Soc. Lond. B Biol. Sci. 364 (2009) 1985–1998. doi:10.1098/rstb.2008.0205.

[18] The Ocean Cleanup, developing technologies to extract, prevent and intercept plastic pollution, Ocean Cleanup. (n.d.). http://www.theoceancleanup.com/ (accessed January 22, 2016).

[19] H.A. Leslie, Microplastic litter in the Dutch Marine Environment, Institute for Environmental Studies, Deltares, 2011. http://www.ivm.vu.nl/en/Images/Deltares-IVM_rapport_microplastics-2_tcm234-409861.pdf (accessed January 20, 2016).

[20] S.L. Wright, R.C. Thompson, T.S. Galloway, The physical impacts of microplastics on marine organisms: a review, Environ. Pollut. 178 (2013) 483–492.
[21] J.R. Jambeck, R. Geyer, C. Wilcox, T.R. Siegler, M. Perryman, A. Andrady, R. Narayan, K.L. Law, Plastic waste inputs from land into the ocean, Science. 347 (2015) 768–771.
[22] Maarten van der Wal, Myra van der Meulen, Gijsbert Tweehuijsen, Monika Peterlin, Andreja Palatinus, Manca Kovač Viršek, Lucia Coscia, Andrej Kržan, SFRA0025: Identification and Assessment of Riverine Input of (Marine) Litter, European Comission DG Environment, 2015.
[23] Microplastics in the environment - sources, impacts & solutions, in: Cologne, germany, 2015. http://microplastic-conference.eu/.
[24] ASTM Subcomittee D20.96, D7991-15, Standard Test Method for Determining Aerobic Biodegradation of Plastics Buried in Sandy Marine Sediment under Controlled Laboratory Conditions, ASTM, West Conshohocken, PA, 2015. http://www.astm.org/Standards/D7991.htm.
[25] Ramani Narayan, Biodegradable-compostable plastics -a primer vis-à-vis recycling and end-of-life issues, Bioplastics Mag. 9 (2014) 56–57.
[26] E.T. Vink, K.R. Rabago, D.A. Glassner, P.R. Gruber, Applications of life cycle assessment to NatureWorks™ polylactide (PLA) production, Polym. Degrad. Stab. 80 (2003) 403–419.
[27] E.T. Vink, S. Davies, Life cycle inventory and impact assessment data for 2014 Ingeo™ polylactide production, Ind. Biotechnol. 11 (2015) 167–180.
[28] NatureWorks LLC, Revised NatureWorks INGEO biopolymer life cycle assesment data passes rigurous third party peer-review, Minnetonka, MN, USA, 2015. http://www.natureworksllc.com/News-and-Events/Press-Releases/2015/07-22-15-Ingeo-Biopolymer-Life-Cycle-Assessment.
[29] NatureWorks LLC., New PLA formulations to replace ABS, Bioplastics Mag. (2015) 16–17.
[30] M.H. Hartmann, High Molecular Weight Polylactic Acid Polymers, in: D.D.L. Kaplan (Ed.), Biopolym. Renew. Resour., Springer Berlin Heidelberg, 1998: pp. 367–411. http://link.springer.com/chapter/10.1007/978-3-662-03680-8_15 (accessed May 15, 2015).
[31] www.corbion.com, Under the microscope: lactic acid, (n.d.). http://www.corbion.com/about-corbion/corbion-stories/lactic-acid-the-lifeblood-of-our-business/under-the-microscope-lactic-acid (accessed June 1, 2015).
[32] R. Datta, M. Henry, Lactic acid: recent advances in products, processes and technologies — a review, J. Chem. Technol. Biotechnol. 81 (2006) 1119–1129. doi:10.1002/jctb.1486.
[33] J. Lunt, Large-scale production, properties and commercial applications of polylactic acid polymers, Polym. Degrad. Stab. 59 (1998) 145–152. doi:10.1016/S0141-3910(97)00148-1.
[34] R.P. John, K.M. Nampoothiri, A. Pandey, Fermentative production of lactic acid from biomass: an overview on process developments and future perspectives, Appl. Microbiol. Biotechnol. 74 (2007) 524–534. doi:10.1007/s00253-006-0779-6.
[35] K. Madhavan Nampoothiri, N.R. Nair, R.P. John, An overview of the recent developments in polylactide (PLA) research, Bioresour. Technol. 101 (2010) 8493–8501. doi:10.1016/j.biortech.2010.05.092.
[36] K. Okano, T. Tanaka, C. Ogino, H. Fukuda, A. Kondo, Biotechnological production of enantiomeric pure lactic acid from renewable resources: recent achievements, perspectives, and limits, Appl. Microbiol. Biotechnol. 85 (2009) 413–423. doi:10.1007/s00253-009-2280-5.
[37] R.P. John, K.M. Nampoothiri, A. Pandey, Simultaneous saccharification and fermentation of cassava bagasse for l-(+)-lactic acid production using Lactobacilli, Appl. Biochem. Biotechnol. 134 (2006) 263–272. doi:10.1385/ABAB:134:3:263.
[38] C. Idler, J. Venus, B. Kamm, Microorganisms for the Production of Lactic Acid and Organic Lactates, in: B. Kamm (Ed.), Microorg. Biorefineries, Springer Berlin Heidelberg, 2015: pp. 225–273. http://link.springer.com/chapter/10.1007/978-3-662-45209-7_9 (accessed January 29, 2015).
[39] W.H. Carothers, G.L. Dorough, F.J. van Natta, Studies of polymerization and ring formation. X. The reversible polymerization of six-membered cyclic esters, J. Am. Chem. Soc. 54 (1932) 761–772. doi:10.1021/ja01341a046.
[40] Kulkarni RK, Pani KC, Neuman CC, Leonard FF, Polylactic acid for surgical implants, Arch. Surg. 93 (1966) 839–843. doi:10.1001/archsurg.1966.01330050143023.
[41] K. Enomoto, M. Ajioka, A. Yamaguchi, Polyhydroxycarboxylic acid and preparation process thereof, Google Patents, 1994. https://www.google.com/patents/US5310865 (accessed September 14, 2016).
[42] T. Kashima, T. Kameoka, C. Higuchi, M. Ajioka, A. Yamaguchi, Aliphatic polyester and preparation process thereof, Google Patents, 1995. https://www.google.com/patents/US5428126 (accessed September 14, 2016).

[43] K. Hiltunen, M. Härkönen, J.V. Seppälä, T. Väänänen, Synthesis and characterization of lactic acid based telechelic prepolymers, Macromolecules. 29 (1996) 8677–8682.
[44] S.-H. Hyon, K. Jamshidi, Y. Ikada, Synthesis of polylactides with different molecular weights, Biomaterials. 18 (1997) 1503–1508.
[45] D. Garlotta, A literature review of poly (lactic acid), J. Polym. Environ. 9 (2001) 63–84.
[46] K. Hiltunen, J.V. Seppälä, M. Härkönen, Effect of catalyst and polymerization conditions on the preparation of low molecular weight lactic acid polymers, Macromolecules. 30 (1997) 373–379.
[47] P.R. Gruber, E.S. Hall, J.J. Kolstad, M.L. Iwen, R.D. Benson, R.L. Borchardt, Continuous process for manufacture of lactide polymers with controlled optical purity, Google Patents, 1992. https://www.google.com/patents/US5142023 (accessed September 14, 2016).
[48] P.R. Gruber, E.S. Hall, J.J. Kolstad, M.L. Iwen, R.D. Benson, R.L. Borchardt, Continuous process for manufacture of lactide polymers with purification by distillation, Google Patents, 1994. https://www.google.com/patents/US5357035 (accessed September 14, 2016).
[49] S. Kobayashi, A. Makino, Enzymatic polymer synthesis: an opportunity for green polymer chemistry, Chem. Rev. 109 (2009) 5288–5353.
[50] A.-C. Albertsson, R.K. Srivastava, Recent developments in enzyme-catalyzed ring-opening polymerization, Adv. Drug Deliv. Rev. 60 (2008) 1077–1093.
[51] S. Matsumura, K. Mabuchi, K. Toshima, Lipase-catalyzed ring-opening polymerization of lactide, Macromol. Rapid Commun. 18 (1997) 477–482.
[52] P. Degee, P. Dubois, R. Jérôme, S. Jacobsen, H.-G. Fritz, New catalysis for fast bulk ring-opening polymerization of lactide monomers, in: Macromol. Symp., Wiley Online Library, 1999: pp. 289–302. http://onlinelibrary.wiley.com/doi/10.1002/masy.19991440126/abstract (accessed September 14, 2016).
[53] S. Jacobsen, H.-G. Fritz, P. Degée, P. Dubois, R. Jérôme, Continuous reactive extrusion polymerisation of L-lactide—an engineering view, in: Macromol. Symp., Wiley Online Library, 2000: pp. 261–273. http://onlinelibrary.wiley.com/doi/10.1002/1521-3900(200003)153:1%3C261::AID-MASY261%3E3.0.CO;2-9/abstract (accessed September 14, 2016).
[54] J.-M. Raquez, R. Narayan, P. Dubois, Recent Advances in Reactive Extrusion Processing of Biodegradable Polymer-Based Compositions, Macromol. Mater. Eng. 293 (2008) 447–470.
[55] R. Auras, B. Harte, S. Selke, An overview of polylactides as packaging materials, Macromol. Biosci. 4 (2004) 835–864.
[56] I.W. Hamley, V. Castelletto, R.V. Castillo, A.J. Müller, C.M. Martin, E. Pollet, P. Dubois, Crystallization in Poly(l-lactide)-b-poly(ε-caprolactone) Double Crystalline Diblock Copolymers: A Study Using X-ray Scattering, Differential Scanning Calorimetry, and Polarized Optical Microscopy, Macromolecules. 38 (2005) 463–472. doi:10.1021/ma0481499.
[57] A.M. Harris, E.C. Lee, Improving mechanical performance of injection molded PLA by controlling crystallinity, J. Appl. Polym. Sci. 107 (2008) 2246–2255.
[58] G. Perego, G.D. Cella, C. Bastioli, Effect of molecular weight and crystallinity on poly(lactic acid) mechanical properties, J. Appl. Polym. Sci. 59 (1996) 37–43. doi:10.1002/(SICI)1097-4628(19960103)59:1<37::AID-APP6>3.0.CO;2-N.
[59] Robert Haan, Unique Purac Lactides for improved production and properties, in: UK, 2009.
[60] R.E. Drumright, P.R. Gruber, D.E. Henton, Polylactic Acid Technology, Adv. Mater. 12 (2000) 1841–1846.
[61] L.-T. Lim, R. Auras, M. Rubino, Processing technologies for poly(lactic acid), Prog. Polym. Sci. 33 (2008) 820–852. doi:10.1016/j.progpolymsci.2008.05.004.
[62] D.E. Henton, P. Gruber, J. Lunt, J. Randall, Polylactic Acid technology, Nat. Fibers Biopolym. Biocomposites Taylor Francis FL USA. (2005) 527–577.
[63] J.R. Dorgan, J. Janzen, M.P. Clayton, S.B. Hait, D.M. Knauss, Melt rheology of variable L-content poly (lactic acid), J. Rheol. 1978-Present. 49 (2005) 607–619.
[64] A. Celli, M. Scandola, Thermal properties and physical ageing of poly (L-lactic acid), Polymer. 33 (1992) 2699–2703.
[65] H. Cai, V. Dave, R.A. Gross, S.P. McCarthy, Effects of physical aging, crystallinity, and orientation on the enzymatic degradation of poly (lactic acid), J. Polym. Sci. Part B Polym. Phys. 34 (1996) 2701–2708.
[66] E.W. Fischer, H.J. Sterzel, G. Wegner, Investigation of the structure of solution grown crystals of lactide copolymers by means of chemical reactions, Kolloid-Z. Z. Für Polym. 251 (1973) 980–990.
[67] M. Pyda, R.C. Bopp, B. Wunderlich, Heat capacity of poly (lactic acid), J. Chem. Thermodyn. 36 (2004) 731–742.

[68] A. Södergård, M. Stolt, Properties of lactic acid based polymers and their correlation with composition, Prog. Polym. Sci. 27 (2002) 1123–1163. doi:10.1016/S0079-6700(02)00012-6.
[69] NatureWorks LLC, Solubility of Ingeo Biopolymer in Various Solvents, n.d. http://www.natureworksllc.com/~/media/Technical_Resources/Properties_Documents/PropertiesDocument_Solubility-Test-Results_pdf.pdf (accessed August 2, 2016).
[70] Q. Fang, M.A. Hanna, Rheological properties of amorphous and semicrystalline polylactic acid polymers, Ind. Crops Prod. 10 (1999) 47–53.
[71] J.J. Cooper-White, M.E. Mackay, Rheological properties of poly (lactides). Effect of molecular weight and temperature on the viscoelasticity of poly (l-lactic acid), J. Polym. Sci. Part B Polym. Phys. 37 (1999) 1803–1814.
[72] P. Gruber, JJ. Kolstad, D.R. Witzke, Viscosity-modified lactide polymer composition and process for manufacture thereof, US5594095 A, n.d. http://www.google.com/patents/US5594095 (accessed August 2, 2016).
[73] D.W. Grijpma, A.J. Nijenhuis, P.G.T. Van Wijk, A.J. Pennings, High impact strength as-polymerized PLLA, Polym. Bull. 29 (1992) 571–578.
[74] L. Fambri, A. Pegoretti, R. Fenner, S.D. Incardona, C. Migliaresi, Biodegradable fibres of poly (L-lactic acid) produced by melt spinning, Polymer. 38 (1997) 79–85.
[75] S. Jacobsen, H.-G. Fritz, Plasticizing polylactide—the effect of different plasticizers on the mechanical properties, Polym. Eng. Sci. 39 (1999) 1303–1310.
[76] P. Törmälä, Biodegradable self-reinforced composite materials; manufacturing structure and mechanical properties, Clin. Mater. 10 (1992) 29–34.
[77] H. Tsuji, Y. Ikada, Stereocomplex formation between enantiomeric poly (lactic acid) s. XI. Mechanical properties and morphology of solution-cast films, Polymer. 40 (1999) 6699–6708.
[78] I. Engelberg, J. Kohn, Physico-mechanical properties of degradable polymers used in medical applications: a comparative study, Biomaterials. 12 (1991) 292–304.
[79] Y. Ikada, H. Tsuji, others, Biodegradable polyesters for medical and ecological applications, Macromol. Rapid Commun. 21 (2000) 117–132.
[80] D.W. Grijpma, C.A. Joziasse, A.J. Pennings, Star-shaped polylactide-containing block copolymers, Makromol. Chem. Rapid Commun. 14 (1993) 155–161.
[81] D.W. Grijpma, A.J. Pennings, (Co) polymers of L-lactide, 2. Mechanical properties, Macromol. Chem. Phys. 195 (1994) 1649–1663.
[82] M. Ajioka, K. Enomoto, K. Suzuki, A. Yamaguchi, The basic properties of poly (lactic acid) produced by the direct condensation polymerization of lactic acid, J. Environ. Polym. Degrad. 3 (1995) 225–234.
[83] J.E. Bergsma, W.C. De Bruijn, F.R. Rozema, R.R.M. Bos, G. Boering, Late degradation tissue response to poly (L-lactide) bone plates and screws, Biomaterials. 16 (1995) 25–31.
[84] S. Li, H. Garreau, M. Vert, Structure-property relationships in the case of the degradation of massive poly (α-hydroxy acids) in aqueous media, J. Mater. Sci. Mater. Med. 1 (1990) 198–206.
[85] K.I. Park, M. Xanthos, A study on the degradation of polylactic acid in the presence of phosphonium ionic liquids, Polym. Degrad. Stab. 94 (2009) 834–844.
[86] G.G. Pitt, M.M. Gratzl, G.L. Kimmel, J. Surles, A. Sohindler, Aliphatic polyesters II. The degradation of poly (DL-lactide), poly (ε-caprolactone), and their copolymers in vivo, Biomaterials. 2 (1981) 215–220.
[87] C.C. Chu, Degradation phenomena of two linear aliphatic polyester fibres used in medicine and surgery, Polymer. 26 (1985) 591–594.
[88] L.S. Liu, V.L. Finkenstadt, C.-K. Liu, T. Jin, M.L. Fishman, K.B. Hicks, Preparation of poly (lactic acid) and pectin composite films intended for applications in antimicrobial packaging, J. Appl. Polym. Sci. 106 (2007) 801–810.
[89] Saskia Nuijten, Corbion makes next step in entering the PLA market, (2015). http://www.corbion.com/media/press-releases?newsId=1919551 (accessed June 1, 2015).
[90] Karin Roeleveld, Total and Corbion form a Joint Venture in bioplastics, (2016). http://www.corbion.com/media/press-releases?newsId=2057215 (accessed November 17, 2016).
[91] Synbra Tecnology b.v., (n.d.). http://www.synbratechnology.nl/.
[92] Paul Charteris, High temperature resistant PLA foams, Bioplastics Mag. 8 (2013) 28–29.
[93] Y. Zhao, Z. Wang, J. Wang, H. Mai, B. Yan, F. Yang, Direct synthesis of poly (D, L-lactic acid) by melt polycondensation and its application in drug delivery, J. Appl. Polym. Sci. 91 (2004) 2143–2150.
[94] R. Mehta, V. Kumar, H. Bhunia, S.N. Upadhyay, Synthesis of poly (lactic acid): a review, J. Macromol. Sci. Part C Polym. Rev. 45 (2005) 325–349.
[95] S. Viju, G. Thilagavathi, Recent developments in PLA fibers, Chem. Fibers Int. 59 (2009) 154.

[96] Rainer hagen, The potential of PLA for the fiber market, Bioplastics Mag. 8 (n.d.) 12–14.
[97] Chung-Jen Wu, Bioplastics for high-end consumer electronics, Bioplastics Mag. 8 (2013) 38–40.
[98] Francesca Brunori, PLA compounds for the automotive sector, Bioplastics Mag. 9 (2014) 16–17.
[99] C.J. Weber, V. Haugaard, R. Festersen, G. Bertelsen, Production and applications of biobased packaging materials for the food industry, Food Addit. Contam. 19 (2002) 172–177.
[100] V. Siebott, PLA - the future of rigid packaging?, Bioplastics Mag. 2 (2007) 28–29.
[101] Making preforms for PLA bottles, Bioplastics Mag. 2 (2006) 16–18.
[102] NatureWorks LLC, Crystallizing and Drying Ingeo Biopolymer, n.d. http://www.natureworksllc.com/~/media/Technical_Resources/Processing_Guides/ProcessingGuide_Crystallizing-and-Drying_pdf.pdf (accessed August 1, 2016).
[103] NatureWorks LLC, NatureWorks. Sheet Extrusion Processing Guide, Minnetonka, MN, USA, 2005. http://www.natureworksllc.com/~/media/Technical_Resources/Processing_Guides/ProcessingGuide_Sheet-Extrusion_pdf.pdf.
[104] NatureWorks LLC, NatureWorks. Injection Molding Process Guide for Ingeo 3051D, Minnetonka, MN, USA, 2006. http://www.natureworksllc.com/~/media/Technical_Resources/Technical_Data_Sheets/TechnicalDataSheet_3052D_injection-molding_pdf.pdf.
[105] R. Colombo, Method and apparatus for manufacturing by extrusion structural members from thermoplastic synthetic resins, US2563396 A, 1951. https://www.google.com/patents/US2563396 (accessed February 2, 2016).
[106] R. Colombo, Screw press for extruding plastic materials, US2968836 (A), 1961. http://worldwide.espacenet.com/publicationDetails/biblio?FT=D&date=19610124&DB=worldwide.espacenet.com&locale=en_EP&CC=US&NR=2968836A&KC=A&ND=4 (accessed February 2, 2016).
[107] Y. Wang, Compounding in co-rotating twin-screw extruders, iSmithers Rapra Publishing, 2000. https://books.google.es/books?hl=es&lr=&id=IUi8gUmU-SsC&oi=fnd&pg=PA3&dq=compounding+in+co-rotating+twin+screw+extruders+yeh+wang&ots=4XElM77qxU&sig=YWgd5y0-n1t4liWCU_XmAwerp2Y (accessed February 2, 2016).
[108] R. Von Oepen, W. Michaeli, Injection moulding of biodegradable implants, Clin. Mater. 10 (1992) 21–28.
[109] J. Ren, Biodegradable poly (lactic acid): synthesis, modification, processing and applications, Springer Science & Business Media, 2011. https://books.google.es/books?hl=es&lr=&id=JC-zMTB8YVIC&oi=fnd&pg=PP3&dq=Biodegradable+poly+(lactic+acid):+synthesis,+modification,+processing+and+applications&ots=uTn-4s0jpG&sig=GtkipS-681lYYu5mzRYrLC6Hi74 (accessed January 20, 2017).
[110] K. Cink, R. Bopp, K. Sikkema, Injection stretch blow molding process using polylactide resins, 2005. https://www.google.com/patents/US20070187876 (accessed August 3, 2016).
[111] NatureWorks LLC, Injection Stretch Blow Molding Ingeo™ Biopolymer, NatureWorks LLC, USA, n.d. http://www.natureworksllc.com/~/media/Technical_Resources/Processing_Guides/ProcessingGuide_ISBM-Bottle_pdf.pdf (accessed August 3, 2016).
[112] NatureWorks LLC, Processing Guide for Thermoforming Articles, NatureWorks LLC, USA, n.d. http://www.iraplast.com/guia-bio/processingguides_thermoformingarticles_pdf.ashx.pdf (accessed August 3, 2016).
[113] L. BOSIERS, S. ENGELMANN, Thermoformed packaging made of PLA, Kunststoffe Plast Eur. 93 (2003) 21–23.
[114] L.M. Mathieu, T.L. Mueller, P.-E. Bourban, D.P. Pioletti, R. Müller, J.-A.E. M\a anson, Architecture and properties of anisotropic polymer composite scaffolds for bone tissue engineering, Biomaterials. 27 (2006) 905–916.
[115] V. Maquet, D. Martin, B. Malgrange, R. Franzen, J. Schoenen, G. Moonen, R. Jérôme, Peripheral nerve regeneration using bioresorbable macroporous polylactide scaffolds, J. Biomed. Mater. Res. 52 (2000) 639–651.
[116] W. Busby, N.R. Cameron, C.A.B. Jahoda, Tissue engineering matrixes by emulsion templating, Polym. Int. 51 (2002) 871–881.
[117] J. Guan, K.M. Eskridge, M.A. Hanna, Acetylated starch-polylactic acid loose-fill packaging materials, Ind. Crops Prod. 22 (2005) 109–123.
[118] BioFoam Moulded products | Synbra Technology, (n.d.). http://www.synbratechnology.com/biofoam/biofoam-moulded-products/ (accessed August 3, 2016).

[119] Y. Di, S. Iannace, E. Di Maio, L. Nicolais, Reactively modified poly (lactic acid): properties and foam processing, Macromol. Mater. Eng. 290 (2005) 1083–1090.
[120] A.G. Mikos, A.J. Thorsen, L.A. Czerwonka, Y. Bao, R. Langer, D.N. Winslow, J.P. Vacanti, Preparation and characterization of poly (L-lactic acid) foams, Polymer. 35 (1994) 1068–1077.
[121] Jim Nangeroni, Ingeo™ Resin Fundamentals & Applications, in: Thailand, 2013.
[122] Carlos F. Jasso-Gastinel, José M. Kenny, Modification of Polymer Properties, 1st ed., Elsevier Inc., 2016. http://store.elsevier.com/Modification-of-Polymer-Properties/isbn-9780323443531/.
[123] M.Y. Jo, Y.J. Ryu, J.H. Ko, J.-S. Yoon, Effects of compatibilizers on the mechanical properties of ABS/PLA composites, J. Appl. Polym. Sci. 125 (2012) E231–E238.
[124] A.M. Gajria, V. Dave, R.A. Gross, S.P. McCarthy, Miscibility and biodegradability of blends of poly (lactic acid) and poly (vinyl acetate), Polymer. 37 (1996) 437–444.
[125] B. Riedl, R.E. Prud'Homme, Thermodynamic study of poly (vinyl chloride)/polyester blends by inverse-phase gas chromatography at 120° C, J. Polym. Sci. Part B Polym. Phys. 24 (1986) 2565–2582.
[126] B.O. Leung, A.P. Hitchcock, J.L. Brash, A. Scholl, A. Doran, Phase Segregation in Polystyrene-Polylactide Blends, Macromolecules. 42 (2009) 1679–1684.
[127] A. Mohamed, S.H. Gordon, G. Biresaw, Poly (lactic acid)/polystyrene bioblends characterized by thermogravimetric analysis, differential scanning calorimetry, and photoacoustic infrared spectroscopy, J. Appl. Polym. Sci. 106 (2007) 1689–1696.
[128] J.B. Lee, Y.K. Lee, G.D. Choi, S.W. Na, T.S. Park, W.N. Kim, Compatibilizing effects for improving mechanical properties of biodegradable poly (lactic acid) and polycarbonate blends, Polym. Degrad. Stab. 96 (2011) 553–560.
[129] K. Hashima, S. Nishitsuji, T. Inoue, Structure-properties of super-tough PLA alloy with excellent heat resistance, Polymer. 51 (2010) 3934–3939.
[130] Y.F. Kim, C.N. Choi, Y.D. Kim, K.Y. Lee, M.S. Lee, Compatibilization of immiscible poly (l-lactide) and low density polyethylene blends, Fibers Polym. 5 (2004) 270–274.
[131] K. Hamad, M. Kaseem, F. Deri, Melt rheology of poly (lactic acid)/low density polyethylene polymer blends, Adv. Chem. Eng. Sci. 1 (2011) 208.
[132] K.S. Anderson, S.H. Lim, M.A. Hillmyer, Toughening of polylactide by melt blending with linear low-density polyethylene, J. Appl. Polym. Sci. 89 (2003) 3757–3768.
[133] O. Martin, L. Averous, Poly (lactic acid): plasticization and properties of biodegradable multiphase systems, Polymer. 42 (2001) 6209–6219.
[134] A.N. Gaikwad, E.R. Wood, T. Ngai, T.P. Lodge, Two calorimetric glass transitions in miscible blends containing poly (ethylene oxide), Macromolecules. 41 (2008) 2502–2508.
[135] R.A. Zoppi, E.A.R. Duek, D.C. Coraça, P.P. Barros, Preparation and characterization of poly (L-lactic acid) and poly (ethylene oxide) blends, Mater. Res. 4 (2001) 117–125.
[136] A.J. Nijenhuis, E. Colstee, D.W. Grijpma, A.J. Pennings, High molecular weight poly (L-lactide) and poly (ethylene oxide) blends: Thermal characterization and physical properties, Polymer. 37 (1996) 5849–5857.
[137] Y. Hu, Y.S. Hu, V. Topolkaraev, A. Hiltner, E. Baer, Crystallization and phase separation in blends of high stereoregular poly (lactide) with poly (ethylene glycol), Polymer. 44 (2003) 5681–5689.
[138] Y. Hu, M. Rogunova, V. Topolkaraev, A. Hiltner, E. Baer, Aging of poly (lactide)/poly (ethylene glycol) blends. Part 1. Poly (lactide) with low stereoregularity, Polymer. 44 (2003) 5701–5710.
[139] Y. Hu, Y.S. Hu, V. Topolkaraev, A. Hiltner, E. Baer, Aging of poly (lactide)/poly (ethylene glycol) blends. Part 2. Poly (lactide) with high stereoregularity, Polymer. 44 (2003) 5711–5720.
[140] J.-S. Yoon, S.-H. Oh, M.-N. Kim, I.-J. Chin, Y.-H. Kim, Thermal and mechanical properties of poly (l-lactic acid)–poly (ethylene-co-vinyl acetate) blends, Polymer. 40 (1999) 2303–2312.
[141] H.M. Burt, J.K. Jackson, S.K. Bains, R.T. Liggins, A.M.C. Oktaba, A.L. Arsenault, W.L. Hunter, Controlled delivery of taxol from microspheres composed of a blend of ethylene-vinyl acetate copolymer and poly (d, l-lactic acid), Cancer Lett. 88 (1995) 73–79.
[142] T. Yokohara, M. Yamaguchi, Structure and properties for biomass-based polyester blends of PLA and PBS, Eur. Polym. J. 44 (2008) 677–685.
[143] S.-Y. Gu, K. Zhang, J. Ren, H. Zhan, Melt rheology of polylactide/poly (butylene adipate-co-terephthalate) blends, Carbohydr. Polym. 74 (2008) 79–85.
[144] I. Noda, E.B. Bond, D.H. Melik, Polyhydroxyalkanoate copolymer and polylactic acid polymer compositions for laminates and films, Google Patents, 2004. https://www.google.com/patents/US6808795 (accessed September 30, 2016).

[145] W. Amass, A. Amass, B. Tighe, A review of biodegradable polymers: uses, current developments in the synthesis and characterization of biodegradable polyesters, blends of biodegradable polymers and recent advances in biodegradation studies, Polym. Int. 47 (1998) 89–144.
[146] G. Rohman, F. Lauprêtre, S. Boileau, P. Guérin, D. Grande, Poly (d, l-lactide)/poly (methyl methacrylate) interpenetrating polymer networks: Synthesis, characterization, and use as precursors to porous polymeric materials, Polymer. 48 (2007) 7017–7028.
[147] J.L. Eguiburu, J.J. Iruin, M.J. Fernandez-Berridi, J. San Roman, Blends of amorphous and crystalline polylactides with poly (methyl methacrylate) and poly (methyl acrylate): a miscibility study, Polymer. 39 (1998) 6891–6897.
[148] H. Tsuji, Y. Ikada, Crystallization from the melt of poly (lactide) s with different optical purities and their blends, Macromol. Chem. Phys. 197 (1996) 3483–3499.
[149] S.J. De Jong, W.N.E. van Dijk-Wolthuis, J.J. Kettenes-Van den Bosch, P.J.W. Schuyl, W.E. Hennink, Monodisperse enantiomeric lactic acid oligomers: preparation, characterization, and stereocomplex formation, Macromolecules. 31 (1998) 6397–6402.
[150] T. Okihara, M. Tsuji, A. Kawaguchi, K.-I. Katayama, H. Tsuji, S.-H. Hyon, Y. Ikada, Crystal structure of stereocomplex of poly (L-lactide) and poly (D-lactide), J. Macromol. Sci. Part B Phys. 30 (1991) 119–140.
[151] S. Brochu, R.E. Prud'Homme, I. Barakat, R. Jerome, Stereocomplexation and morphology of polylactides, Macromolecules. 28 (1995) 5230–5239.
[152] Y. Wang, J.F. Mano, Stereocomplexation and morphology of enantiomeric poly (lactic acid) s with moderate-molecular-weight, J. Appl. Polym. Sci. 107 (2008) 1621–1627.
[153] L.A. Utracki, A. Ajji, Chapter 4. Interphase and compatibilization by addition of a compatibilizer., in: Polym. Blends Handb., Springer, 2002. http://link.springer.com/content/pdf/10.1007/0-306-48244-4.pdf (accessed September 30, 2016).
[154] W.E. Baker, C.E. Scott, G.-H. Hu, M.K. Akkapeddi, Reactive polymer blending, Hanser Munich, 2001. http://sutlib2.sut.ac.th/sut_contents/69612.pdf (accessed September 30, 2016).
[155] Y. Li, H. Shimizu, Improvement in toughness of poly (l-lactide)(PLLA) through reactive blending with acrylonitrile–butadiene–styrene copolymer (ABS): Morphology and properties, Eur. Polym. J. 45 (2009) 738–746.
[156] L. Wang, W. Ma, R.A. Gross, S.P. McCarthy, Reactive compatibilization of biodegradable blends of poly (lactic acid) and poly (ε-caprolactone), Polym. Degrad. Stab. 59 (1998) 161–168.
[157] T. Semba, K. Kitagawa, U.S. Ishiaku, H. Hamada, The effect of crosslinking on the mechanical properties of polylactic acid/polycaprolactone blends, J. Appl. Polym. Sci. 101 (2006) 1816–1825.
[158] T. Semba, K. Kitagawa, U.S. Ishiaku, M. Kotaki, H. Hamada, Effect of compounding procedure on mechanical properties and dispersed phase morphology of poly (lactic acid)/polycaprolactone blends containing peroxide, J. Appl. Polym. Sci. 103 (2007) 1066–1074.
[159] J.-F. Zhang, X. Sun, Mechanical properties of poly (lactic acid)/starch composites compatibilized by maleic anhydride, Biomacromolecules. 5 (2004) 1446–1451.
[160] H. Wang, X. Sun, P. Seib, Strengthening blends of poly (lactic acid) and starch with methylenediphenyl diisocyanate, J. Appl. Polym. Sci. 82 (2001) 1761–1767.
[161] N. Wang, J. Yu, X. Ma, Preparation and characterization of thermoplastic starch/PLA blends by one-step reactive extrusion, Polym. Int. 56 (2007) 1440–1447.
[162] H. Wang, X. Sun, P. Seib, Mechanical properties of poly (lactic acid) and wheat starch blends with methylenediphenyl diisocyanate, J. Appl. Polym. Sci. 84 (2002) 1257–1262.
[163] J.-F. Zhang, X. Sun, Mechanical and thermal properties of poly (lactic acid)/starch blends with dioctyl maleate, J. Appl. Polym. Sci. 94 (2004) 1697–1704.
[164] D. Carlson, L. Nie, R. Narayan, P. Dubois, Maleation of polylactide (PLA) by reactive extrusion, J. Appl. Polym. Sci. 72 (1999) 477–485.
[165] H. Wang, X. Sun, P. Seib, Effects of starch moisture on properties of wheat starch/poly (lactic acid) blend containing methylenediphenyl diisocyanate, J. Polym. Environ. 10 (2002) 133–138.
[166] M.-B. Coltelli, C. Toncelli, F. Ciardelli, S. Bronco, Compatible blends of biorelated polyesters through catalytic transesterification in the melt, Polym. Degrad. Stab. 96 (2011) 982–990.
[167] A. Södergård, J.-F. Selin, J.H. Näsman, Hydrolytic degradation of peroxide modified poly(L-lactide), Polym. Degrad. Stab. 51 (1996) 351–359. doi:10.1016/0141-3910(95)00271-5.
[168] S. Saeidlou, M.A. Huneault, H. Li, C.B. Park, Poly (lactic acid) crystallization, Prog. Polym. Sci. 37 (2012) 1657–1677.
[169] J.J. Kolstad, Crystallization kinetics of poly (L-lactide-co-meso-lactide), J. Appl. Polym. Sci. 62 (1996) 1079–1091.

[170] Y. Liu, L. Wang, Y. He, Z. Fan, S. Li, Non-isothermal crystallization kinetics of poly (L-lactide), Polym. Int. 59 (2010) 1616–1621.
[171] C. Courgneau, V. Ducruet, L. Averous, J. Grenet, S. Domenek, Nonisothermal crystallization kinetics of poly (lactide)—effect of plasticizers and nucleating agent, Polym. Eng. Sci. 53 (2013) 1085–1098.
[172] C. Courgneau, S. Domenek, R. Lebosse, A. Guinault, L. Averous, V. Ducruet, Effect of crystallization on barrier properties of formulated polylactide, Polym. Int. 61 (2012) 180–189.
[173] J.Y. Nam, S. Sinha Ray, M. Okamoto, Crystallization behavior and morphology of biodegradable polylactide/layered silicate nanocomposite, Macromolecules. 36 (2003) 7126–7131.
[174] J.-Z. Liang, L. Zhou, C.-Y. Tang, C.-P. Tsui, Crystalline properties of poly (L-lactic acid) composites filled with nanometer calcium carbonate, Compos. Part B Eng. 45 (2013) 1646–1650.
[175] H. Tsuji, H. Takai, S.K. Saha, Isothermal and non-isothermal crystallization behavior of poly (L-lactic acid): Effects of stereocomplex as nucleating agent, Polymer. 47 (2006) 3826–3837.
[176] S.C. Schmidt, M.A. Hillmyer, Polylactide stereocomplex crystallites as nucleating agents for isotactic polylactide, J. Polym. Sci. Part B Polym. Phys. 39 (2001) 300–313.
[177] X. Shi, G. Zhang, T.V. Phuong, A. Lazzeri, Synergistic Effects of Nucleating Agents and Plasticizers on the Crystallization Behavior of Poly(lactic acid), Molecules. 20 (2015) 1579–1593. doi:10.3390/molecules20011579.
[178] H.-S. Xu, X.J. Dai, P.R. Lamb, Z.-M. Li, Poly (L-lactide) crystallization induced by multiwall carbon nanotubes at very low loading, J. Polym. Sci. Part B Polym. Phys. 47 (2009) 2341–2352.
[179] H. Tsuji, H. Takai, N. Fukuda, H. Takikawa, Non-Isothermal Crystallization Behavior of Poly (L-lactic acid) in the Presence of Various Additives, Macromol. Mater. Eng. 291 (2006) 325–335.
[180] J.Y. Nam, M. Okamoto, H. Okamoto, M. Nakano, A. Usuki, M. Matsuda, Morphology and crystallization kinetics in a mixture of low-molecular weight aliphatic amide and polylactide, Polymer. 47 (2006) 1340–1347.
[181] J. Sun, H. Yu, X. Zhuang, X. Chen, X. Jing, Crystallization behavior of asymmetric PLLA/PDLA blends, J. Phys. Chem. B. 115 (2011) 2864–2869.
[182] Z. Xiong, G. Liu, X. Zhang, T. Wen, S. de Vos, C. Joziasse, D. Wang, Temperature dependence of crystalline transition of highly-oriented poly (L-lactide)/poly (D-lactide) blend: In-situ synchrotron X-ray scattering study, Polymer. 54 (2013) 964–971.
[183] J. Narita, M. Katagiri, H. Tsuji, Highly Enhanced Accelerating Effect of Melt-Recrystallized Stereocomplex Crystallites on Poly (L-lactic acid) Crystallization, 2–Effects of Poly (D-lactic acid) Concentration, Macromol. Mater. Eng. 298 (2013) 270–282.
[184] J. Narita, M. Katagiri, H. Tsuji, Highly enhanced accelerating effect of melt-recrystallized stereocomplex crystallites on poly (L-lactic acid) crystallization: effects of molecular weight of poly (D-lactic acid), Polym. Int. 62 (2013) 936–948.
[185] H. Zhao, Y. Bian, M. Xu, C. Han, Y. Li, Q. Dong, L. Dong, Enhancing the crystallization of poly (l-lactide) using a montmorillonitic substrate favoring nucleation, CrystEngComm. 16 (2014) 3896–3905.
[186] M.S. Huda, L.T. Drzal, A.K. Mohanty, M. Misra, Chopped glass and recycled newspaper as reinforcement fibers in injection molded poly (lactic acid)(PLA) composites: a comparative study, Compos. Sci. Technol. 66 (2006) 1813–1824.
[187] L. Shen, H. Yang, J. Ying, F. Qiao, M. Peng, Preparation and mechanical properties of carbon fiber reinforced hydroxyapatite/polylactide biocomposites, J. Mater. Sci. Mater. Med. 20 (2009) 2259–2265.
[188] A. Orue, A. Jauregi, C. Peña-Rodriguez, J. Labidi, A. Eceiza, A. Arbelaiz, The effect of surface modifications on sisal fiber properties and sisal/poly (lactic acid) interface adhesion, Compos. Part B Eng. 73 (2015) 132–138.
[189] A. Arbelaiz, B. Fernandez, J.A. Ramos, A. Retegi, R. Llano-Ponte, I. Mondragon, Mechanical properties of short flax fibre bundle/polypropylene composites: Influence of matrix/fibre modification, fibre content, water uptake and recycling, Compos. Sci. Technol. 65 (2005) 1582–1592.
[190] T. Lu, S. Liu, M. Jiang, X. Xu, Y. Wang, Z. Wang, J. Gou, D. Hui, Z. Zhou, Effects of modifications of bamboo cellulose fibers on the improved mechanical properties of cellulose reinforced poly (lactic acid) composites, Compos. Part B Eng. 62 (2014) 191–197.
[191] Y. Yu, X. Huang, W. Yu, A novel process to improve yield and mechanical performance of bamboo fiber reinforced composite via mechanical treatments, Compos. Part B Eng. 56 (2014) 48–53.
[192] A. Orue, A. Jauregi, U. Unsuain, J. Labidi, A. Eceiza, A. Arbelaiz, The effect of alkaline and silane treatments on mechanical properties and breakage of sisal fibers and poly (lactic acid)/sisal fiber composites, Compos. Part Appl. Sci. Manuf. 84 (2016) 186–195.

[193] A.N. Netravali, R.B. Henstenburg, S.L. Phoenix, P. Schwartz, Interfacial shear strength studies using the single-filament-composite test. I: Experiments on graphite fibers in epoxy, Polym. Compos. 10 (1989) 226–241.
[194] M. Narkis, E.J.H. Chen, R.B. Pipes, Review of methods for characterization of interfacial fiber-matrix interactions, Polym. Compos. 9 (1988) 245–251.
[195] Aitor arbelaiz, Iñaki Mondragon, Testing the effect of processing and surface treatment on the interfacial adhesion of single fibers in natural fiber composites, in: Interface Eng. Nat. Fibre Compos. Maximum Perform., Woodhead Publishing Ltd, Cambridge, 2011. https://books.google.es/books?hl=es&lr=&id=w6JgAgAAQBAJ&oi=fnd&pg=PP1&dq=arbelaiz+Testing+the+effect+of+processing+and+surface+treatment+on+the+interfacial+adhesion+of+single+fibers+in+natural+fiber+composites.+In:+Zafeiropoulos+N,+editor.+From+interface+engineering+of+natural+fibre+composites+for+maximum+performance.+Cambridge&ots=pfInkPIxZH&sig=O8BZV6QFX3UfyNkxF-QnakEYe9M (accessed February 9, 2017).
[196] S. Kamel, Nanotechnology and its applications in lignocellulosic composites, a mini review, Express Polym. Lett. 1 (2007) 546–575.
[197] J.-M. Raquez, Y. Habibi, M. Murariu, P. Dubois, Polylactide (PLA)-based nanocomposites, Prog. Polym. Sci. 38 (2013) 1504–1542. doi:10.1016/j.progpolymsci.2013.05.014.
[198] G. Zhang, J. Zhang, S. Wang, D. Shen, Miscibility and phase structure of binary blends of polylactide and poly (methyl methacrylate), J. Polym. Sci. Part B Polym. Phys. 41 (2003) 23–30.
[199] S.-H. Li, E.M. Woo, Immiscibility–miscibility phase transitions in blends of poly (L-lactide) with poly (methyl methacrylate), Polym. Int. 57 (2008) 1242–1251.
[200] S. Hirota, T. Sato, Y. Tominaga, S. Asai, M. Sumita, The effect of high-pressure carbon dioxide treatment on the crystallization behavior and mechanical properties of poly (l-lactic acid)/poly (methyl methacrylate) blends, Polymer. 47 (2006) 3954–3960.
[201] B. Imre, K. Renner, B. Pukánszky, Interactions, structure and properties in poly (lactic acid)/thermoplastic polymer blends, Express Polym. Lett. 8 (2014) 2–14.
[202] C. Samuel, J.-M. Raquez, P. Dubois, PLLA/PMMA blends: A shear-induced miscibility with tunable morphologies and properties?, Polymer. 54 (2013) 3931–3939. doi:10.1016/j.polymer.2013.05.021.
[203] K.-P. Le, R. Lehman, J. Remmert, K. Vanness, P.M.L. Ward, J.D. Idol, Multiphase blends from poly (L-lactide) and poly (methyl mathacrylate), J. Biomater. Sci. Polym. Ed. 17 (2006) 121–137.
[204] J.R. Dorgan, J. Janzen, D.M. Knauss, S.B. Hait, B.R. Limoges, M.H. Hutchinson, Fundamental solution and single-chain properties of polylactides, J. Polym. Sci. Part B Polym. Phys. 43 (2005) 3100–3111.
[205] J.E. Mark, Physical properties of polymers handbook, Springer, 2007. http://link.springer.com/content/pdf/10.1007/978-0-387-69002-5.pdf (accessed September 11, 2014).
[206] T.A. Instruments, SDT Q series getting started guide, New Castle DE. 19720 (2007).
[207] H. Varela-Rizo, S. Bittolo-Bon, I. Rodriguez-Pastor, L. Valentini, I. Martin-Gullon, Processing and functionalization effect in CNF/PMMA nanocomposites, Compos. Part Appl. Sci. Manuf. 43 (2012) 711–721.
[208] M. Wei, A.E. Tonelli, Compatiblization of polymers via coalescence from their common cyclodextrin inclusion compounds, Macromolecules. 34 (2001) 4061–4065.
[209] J. Zhang, H. Tsuji, I. Noda, Y. Ozaki, Weak intermolecular interactions during the melt crystallization of poly (L-lactide) investigated by two-dimensional infrared correlation spectroscopy, J. Phys. Chem. B. 108 (2004) 11514–11520.
[210] G. Zhang, J. Zhang, X. Zhou, D. Shen, Miscibility and phase structure of binary blends of polylactide and poly (vinylpyrrolidone), J. Appl. Polym. Sci. 88 (2003) 973–979.
[211] K. Sakurai, T. Maegawa, T. Takahashi, Glass transition temperature of chitosan and miscibility of chitosan/poly (N-vinyl pyrrolidone) blends, Polymer. 41 (2000) 7051–7056.
[212] D.W. Van Krevelen, K. Te Nijenhuis, Properties of polymers: their correlation with chemical structure; their numerical estimation and prediction from additive group contributions, Elsevier, 2009. https://books.google.es/books?hl=es&lr=&id=bzRKwjZeQ2kC&oi=fnd&pg=PR7&dq=Van+Krevelen,+D.W.+and+Te+Nijenhuis,+K.+In+Properties+of+Polymers,+Elsevier+2009%3B+Chapter+7&ots=wYS4UZcuVh&sig=9Dm9lFfSdm0BMRaVmt4141o6HFY (accessed May 23, 2016).
[213] Evonic Industries, PLEXIGLAS® Molding Compounds, (n.d.). www.plexiglas-polymers.com (accessed May 23, 2016).
[214] M. Pluta, M. Murariu, A.-L. Dechief, L. Bonnaud, A. Galeski, P. Dubois, Impact-modified polylactide–calcium sulfate composites: Structure and properties, J. Appl. Polym. Sci. 125 (2012) 4302–4315.

[215] N. Petchwattana, S. Covavisaruch, N. Euapanthasate, Utilization of ultrafine acrylate rubber particles as a toughening agent for poly (lactic acid), Mater. Sci. Eng. A. 532 (2012) 64–70.
[216] K.A. Afrifah, L.M. Matuana, Impact modification of polylactide with a biodegradable ethylene/acrylate copolymer, Macromol. Mater. Eng. 295 (2010) 802–811.
[217] S. Sun, M. Zhang, H. Zhang, X. Zhang, Polylactide toughening with epoxy-functionalized grafted acrylonitrile–butadiene–styrene particles, J. Appl. Polym. Sci. 122 (2011) 2992–2999. doi:10.1002/app.34111.
[218] Racha Al-Itry, Abderrahim Maazouz, Improvement in melt strengthening of Poly (lactic acid) through reactive blending with poly (butylene adipate-co-terephthalate) (PBAT) and epoxy-functionalized chains, in: Strassbourg, 2011.
[219] M. Mihai, M.A. Huneault, B.D. Favis, Rheology and extrusion foaming of chain-branched poly (lactic acid), Polym. Eng. Sci. 50 (2010) 629–642.
[220] A. Jaszkiewicz, A.K. Bledzki, R. van der Meer, P. Franciszczak, A. Meljon, How does a chain-extended polylactide behave?: a comprehensive analysis of the material, structural and mechanical properties, Polym. Bull. 71 (2014) 1675–1690.
[221] Y.-M. Corre, J. Duchet, J. Reignier, A. Maazouz, Melt strengthening of poly (lactic acid) through reactive extrusion with epoxy-functionalized chains, Rheol. Acta. 50 (2011) 613–629. doi:10.1007/s00397-011-0538-1.
[222] S. Pilla, S.G. Kim, G.K. Auer, S. Gong, C.B. Park, Microcellular extrusion-foaming of polylactide with chain-extender, Polym. Eng. Sci. 49 (2009) 1653.
[223] N.A.I. Wei Kit Chee, Impact Toughness and Ductility Enhancement of Biodegradable Poly(lactic acid)/Poly(ε-caprolactone) Blends via Addition of Glycidyl Methacrylate, Adv. Mater. Sci. Eng. 2013 (2013). doi:10.1155/2013/976373.
[224] V. Ojijo, S.S. Ray, Super toughened biodegradable polylactide blends with non-linear copolymer interfacial architecture obtained via facile in-situ reactive compatibilization, Polymer. 80 (2015) 1–17. doi:10.1016/j.polymer.2015.10.038.
[225] N. Najafi, M.C. Heuzey, P.J. Carreau, Polylactide (PLA)-clay nanocomposites prepared by melt compounding in the presence of a chain extender, Compos. Sci. Technol. 72 (2012) 608–615. doi:10.1016/j.compscitech.2012.01.005.
[226] W. Li, D. Wu, S. Sun, G. Wu, H. Zhang, Y. Deng, H. Zhang, L. Dong, Toughening of polylactide with epoxy-functionalized methyl methacrylate–butyl acrylate copolymer, Polym. Bull. 71 (2014) 2881–2902. doi:10.1007/s00289-014-1228-9.
[227] Y. Hao, H. Liang, J. Bian, S. Sun, H. Zhang, L. Dong, Toughening of polylactide with epoxy-functionalized methyl methacrylate–butadiene copolymer, Polym. Int. 63 (2014) 660–666. doi:10.1002/pi.4561.
[228] N.C. Thanh, C. Ruksakulpiwat, Y. Ruksakulpiwat, Effect of Melt Mixing Time in Internal Mixer on Mechanical Properties and Crystallization Behavior of Glycidyl Methacrylate Grafted Poly (Lactic Acid), J. Mater. Sci. Chem. Eng. 03 (2015) 102. doi:10.4236/msce.2015.37013.
[229] Y.W. Wang, C. Fu, Y. Luo, C. Ruan, Y. Zhang, Y. Fu, Melt synthesis and characterization of poly(L-lactic acid) chain linked by multifunctional epoxy compound, J. Wuhan Univ. Technol.-Mater Sci Ed. 25 (2010) 774–779. doi:10.1007/s11595-010-0090-3.
[230] S. Japon, L. Boogh, Y. Leterrier, J.-A.E. Månson, Reactive processing of poly(ethylene terephthalate) modified with multifunctional epoxy-based additives, Polymer. 41 (2000) 5809–5818. doi:10.1016/S0032-3861(99)00768-5.
[231] K. Lamnawar, A. Baudouin, A. Maazouz, Interdiffusion/reaction at the polymer/polymer interface in multilayer systems probed by linear viscoelasticity coupled to FTIR and NMR measurements, Eur. Polym. J. 46 (2010) 1604–1622. doi:10.1016/j.eurpolymj.2010.03.019.
[232] Q.T. Nguyen, S. Japon, A. Luciani, Y. Leterrier, J.-A.E. Månson, Molecular characterization and rheological properties of modified poly(ethylene terephthalate) obtained by reactive extrusion, Polym. Eng. Sci. 41 (2001) 1299–1309. doi:10.1002/pen.10830.
[233] D.N. Bikiaris, G.P. Karayannidis, Chain extension of polyesters PET and PBT with two new diimidodiepoxides. II, J. Polym. Sci. Part Polym. Chem. 34 (1996) 1337–1342. doi:10.1002/(SICI)1099-0518(199605)34:7<1337::AID-POLA22>3.0.CO;2-9.
[234] H. Inata, S. Matsumura, Chain extenders for polyesters. I. Addition-type chain extenders reactive with carboxyl end groups of polyesters, J. Appl. Polym. Sci. 30 (1985) 3325–3337. doi:10.1002/app.1985.070300815.
[235] S.M. Aharoni, C.E. Forbes, W.B. Hammond, D.M. Hindenlang, F. Mares, K. O'Brien, R.D. Sedgwick, High-temperature reactions of hydroxyl and carboxyl PET chain end groups in the presence of

aromatic phosphite, J. Polym. Sci. Part Polym. Chem. 24 (1986) 1281–1296. doi:10.1002/pola.1986.080240614.
[236] J. Cailloux, O.O. Santana, E. Franco-Urquiza, J.J. Bou, F. Carrasco, J. Gámez Pérez, M.L. Maspoch, Sheets of branched poly (lactic acid) obtained by one step reactive extrusion calendering process: melt rheology analysis, Express Polym. Lett. 7 (2013) 304–318.
[237] A. Bouzouita, C. Samuel, D. Notta-Cuvier, J. Odent, F. Lauro, P. Dubois, J.-M. Raquez, Design of highly tough poly (l-lactide)-based ternary blends for automotive applications, J. Appl. Polym. Sci. 133 (2016). http://onlinelibrary.wiley.com/doi/10.1002/app.43402/full (accessed May 23, 2016).
[238] T. Patrício, P. Bártolo, Thermal Stability of PCL/PLA Blends Produced by Physical Blending Process, Procedia Eng. 59 (2013) 292–297. doi:10.1016/j.proeng.2013.05.124.
[239] D. Notta-Cuvier, J. Odent, R. Delille, M. Murariu, F. Lauro, J.M. Raquez, B. Bennani, P. Dubois, Tailoring polylactide (PLA) properties for automotive applications: Effect of addition of designed additives on main mechanical properties, Polym. Test. 36 (2014) 1–9.
[240] J. Anakabe, A.M. Zaldua Huici, A. Eceiza, A. Arbelaiz, Melt blending of polylactide and poly(methyl methacrylate): Thermal and mechanical properties and phase morphology characterization, J. Appl. Polym. Sci. 132 (2015) 42677. doi:10.1002/app.42677.
[241] H. Li, M.A. Huneault, Effect of nucleation and plasticization on the crystallization of poly (lactic acid), Polymer. 48 (2007) 6855–6866.
[242] H.W. Xiao, P. Li, X. Ren, T. Jiang, J.-T. Yeh, Isothermal crystallization kinetics and crystal structure of poly (lactic acid): Effect of triphenyl phosphate and talc, J. Appl. Polym. Sci. 118 (2010) 3558–3569.
[243] M. Pluta, Morphology and properties of polylactide modified by thermal treatment, filling with layered silicates and plasticization, Polymer. 45 (2004) 8239–8251.
[244] S. Gumus, G. Ozkoc, A. Aytac, Plasticized and unplasticized PLA/organoclay nanocomposites: Short- and long-term thermal properties, morphology, and nonisothermal crystallization behavior, J. Appl. Polym. Sci. 123 (2012) 2837–2848.
[245] H. Xiao, L. Yang, X. Ren, T. Jiang, J.-T. Yeh, Kinetics and crystal structure of poly (lactic acid) crystallized nonisothermally: effect of plasticizer and nucleating agent, Polym. Compos. 31 (2010) 2057–2068.
[246] G.-X. Zou, Q.-W. Jiao, X. Zhang, C.-X. Zhao, J.-C. Li, Crystallization behavior and morphology of poly (lactic acid) with a novel nucleating agent, J. Appl. Polym. Sci. 132 (2015). http://onlinelibrary.wiley.com/doi/10.1002/app.41367/full (accessed June 9, 2015).
[247] J. You, W. Yu, C. Zhou, Accelerated Crystallization of Poly (lactic acid): Synergistic Effect of Poly (ethylene glycol), Dibenzylidene Sorbitol, and Long-Chain Branching, Ind. Eng. Chem. Res. 53 (2014) 1097–1107.
[248] Y. Li, H. Wu, Y. Wang, L. Liu, L. Han, J. Wu, F. Xiang, Synergistic effects of PEG and MWCNTs on crystallization behavior of PLLA, J. Polym. Sci. Part B Polym. Phys. 48 (2010) 520–528.
[249] M. Murariu, A. Da Silva Ferreira, M. Alexandre, P. Dubois, Polylactide (PLA) designed with desired end-use properties: 1. PLA compositions with low molecular weight ester-like plasticizers and related performances, Polym. Adv. Technol. 19 (2008) 636–646.
[250] H. Yamane, K. Sasai, Effect of the addition of poly (D-lactic acid) on the thermal property of poly (L-lactic acid), Polymer. 44 (2003) 2569–2575.
[251] E.W. Fischer, H.J. Sterzel, G. Wegner, Investigation of the structure of solution grown crystals of lactide copolymers by means of chemical reactions, Kolloid-Z. Z. Für Polym. 251 (1973) 980–990.
[252] H. Tsuji, I. Fukui, Enhanced thermal stability of poly (lactide) s in the melt by enantiomeric polymer blending, Polymer. 44 (2003) 2891–2896.
[253] P. Pan, W. Kai, B. Zhu, T. Dong, Y. Inoue, Polymorphous crystallization and multiple melting behavior of poly (L-lactide): molecular weight dependence, Macromolecules. 40 (2007) 6898–6905.
[254] M.L. Di Lorenzo, The Crystallization and Melting Processes of Poly(L-lactic acid), Macromol. Symp. 234 (2006) 176–183. doi:10.1002/masy.200650223.
[255] P. Pan, Y. Inoue, Polymorphism and isomorphism in biodegradable polyesters, Prog. Polym. Sci. 34 (2009) 605–640. doi:10.1016/j.progpolymsci.2009.01.003.
[256] S. Iannace, L. Nicolais, Isothermal crystallization and chain mobility of poly (L-lactide), J. Appl. Polym. Sci. 64 (1997) 911–919.
[257] S. Barrau, C. Vanmansart, M. Moreau, A. Addad, G. Stoclet, J.-M. Lefebvre, R. Seguela, Crystallization behavior of carbon nanotube- polylactide nanocomposites, Macromolecules. 44 (2011) 6496–6502.

[258] R. Legras, C. Bailly, M. Daumerie, J.M. Dekoninck, J.P. Mercier, M.V. Zichy, E. Nield, Chemical nucleation, a new concept applied to the mechanism of action of organic acid salts on the crystallization of polyethylene terephthalate and bisphenol—A polycarbonate, Polymer. 25 (1984) 835–844.
[259] V. Nagarajan, K. Zhang, M. Misra, A.K. Mohanty, Overcoming the fundamental challenges in improving the impact strength and crystallinity of PLA biocomposites: influence of nucleating agent and mold temperature, ACS Appl. Mater. Interfaces. 7 (2015) 11203–11214.
[260] Marvin Rosen, LLoyd C. Franklin, Process for the interconversion of crystalline forms of ethylene bis-stearamide, EP0023088 A1, n.d. http://www.google.com/patents/EP0023088A1 (accessed February 3, 2015).
[261] L. Yu, H. Liu, K. Dean, L. Chen, Cold crystallization and postmelting crystallization of PLA plasticized by compressed carbon dioxide, J. Polym. Sci. Part B Polym. Phys. 46 (2008) 2630–2636.
[262] M. Takada, S. Hasegawa, M. Ohshima, Crystallization kinetics of poly (L-lactide) in contact with pressurized CO2, Polym. Eng. Sci. 44 (2004) 186–196.
[263] M. Mihai, M.A. Huneault, B.D. Favis, H. Li, Extrusion Foaming of Semi-Crystalline PLA and PLA/Thermoplastic Starch Blends, Macromol. Biosci. 7 (2007) 907–920.
[264] H. Tsuji, K. Tashiro, L. Bouapao, M. Hanesaka, Synchronous and separate homo-crystallization of enantiomeric poly(l-lactic acid)/poly(d-lactic acid) blends, Polymer. 53 (2012) 747–754. doi:10.1016/j.polymer.2011.12.023.
[265] T. Tabi, I.E. Sajó, F. Szabo, A.S. Luyt, J.G. Kovács, Crystalline structure of annealed polylactic acid and its relation to processing, Express Polym Lett. 4 (2010) 659–668.
[266] Y. Obata, T. Sumitomo, T. Ijitsu, M. Matsuda, T. Nomura, The effect of talc on the crystal orientation in polypropylene/ethylene-propylene rubber/talc polymer blends in injection molding, Polym. Eng. Sci. 41 (2001) 408–416.
[267] J. Zhang, K. Tashiro, H. Tsuji, A.J. Domb, Disorder-to-order phase transition and multiple melting behavior of poly (L-lactide) investigated by simultaneous measurements of WAXD and DSC, Macromolecules. 41 (2008) 1352–1357.
[268] H. Abe, Y. Kikkawa, Y. Inoue, Y. Doi, Morphological and kinetic analyses of regime transition for poly [(S)-lactide] crystal growth, Biomacromolecules. 2 (2001) 1007–1014.
[269] J. Sun, Z. Hong, L. Yang, Z. Tang, X. Chen, X. Jing, Study on crystalline morphology of poly (L-lactide)-poly (ethylene glycol) diblock copolymer, Polymer. 45 (2004) 5969–5977.
[270] J. Yang, T. Zhao, L. Liu, Y. Zhou, G. Li, E. Zhou, X. Chen, others, Isothermal crystallization behavior of the poly (L-lactide) block in poly (L-lactide)-poly (ethylene glycol) diblock copolymers: Influence of the PEG block as a diluted solvent, Polym. J. 38 (2006) 1251–1257.
[271] S. Huang, S. Jiang, L. An, X. Chen, Crystallization and morphology of poly (ethylene oxide-b-lactide) crystalline–crystalline diblock copolymers, J. Polym. Sci. Part B Polym. Phys. 46 (2008) 1400–1411.
[272] Y. Shi, L. Shao, J. Yang, T. Huang, Y. Wang, N. Zhang, Y. Wang, Highly improved crystallization behavior of poly (L-lactide) induced by a novel nucleating agent: substituted-aryl phosphate salts, Polym. Adv. Technol. 24 (2013) 42–50.
[273] S. Wang, C. Han, J. Bian, L. Han, X. Wang, L. Dong, Morphology, crystallization and enzymatic hydrolysis of poly (L-lactide) nucleated using layered metal phosphonates, Polym. Int. 60 (2011) 284–295.
[274] H.-Y. Yin, X.-F. Wei, R.-Y. Bao, Q.-X. Dong, Z.-Y. Liu, W. Yang, B.-H. Xie, M.-B. Yang, High-melting-point crystals of poly (l-lactic acid)(PLLA): the most efficient nucleating agent to enhance the crystallization of PLLA, CrystEngComm. 17 (2015) 2310–2320.
[275] A.T. Lorenzo, M.L. Arnal, J. Albuerne, A.J. Müller, DSC isothermal polymer crystallization kinetics measurements and the use of the Avrami equation to fit the data: guidelines to avoid common problems, Polym. Test. 26 (2007) 222–231.
[276] Silvestre, C., Di Lorenzo M. L., Di pace, E., Chapter 9, in: Vasile, C. (Ed.), Handb. Polyolefins, Marcel Dekker Inc., 2002.
[277] Y. He, Z. Fan, Y. Hu, T. Wu, J. Wei, S. Li, DSC analysis of isothermal melt-crystallization, glass transition and melting behavior of poly (l-lactide) with different molecular weights, Eur. Polym. J. 43 (2007) 4431–4439.
[278] Caroline Abler, Talc in Green Plastics, in: Barcelona, 2011. http://www.imerystalc.com/content/bu/Plastics/News_and_publications/Technical_publications/index.php.
[279] T. Miyata, T. Masuko, Crystallization behaviour of poly (L-lactide), Polymer. 39 (1998) 5515–5521.

[280] Y. Aoyagi, K. Yamashita, Y. Doi, Thermal degradation of poly [(R)-3-hydroxybutyrate], poly [ε-caprolactone], and poly [(S)-lactide], Polym. Degrad. Stab. 76 (2002) 53–59.
[281] F.-D. Kopinke, M. Remmler, K. Mackenzie, M. Möder, O. Wachsen, Thermal decomposition of biodegradable polyesters—II. Poly (lactic acid), Polym. Degrad. Stab. 53 (1996) 329–342.
[282] O. Wachsen, K. Platkowski, K.-H. Reichert, Thermal degradation of poly-L-lactide—studies on kinetics, modelling and melt stabilisation, Polym. Degrad. Stab. 57 (1997) 87–94.
[283] M. Hakkarainen, A.-C. Albertsson, S. Karlsson, Weight losses and molecular weight changes correlated with the evolution of hydroxyacids in simulated in vivo degradation of homo-and copolymers of PLA and PGA, Polym. Degrad. Stab. 52 (1996) 283–291.
[284] S. Li, S. McCarthy, Further investigations on the hydrolytic degradation of poly (DL-lactide), Biomaterials. 20 (1999) 35–44.
[285] X. Zhang, M. Espiritu, A. Bilyk, L. Kurniawan, Morphological behaviour of poly (lactic acid) during hydrolytic degradation, Polym. Degrad. Stab. 93 (2008) 1964–1970.
[286] D. Rasselet, A. Ruellan, A. Guinault, G. Miquelard-Garnier, C. Sollogoub, B. Fayolle, Oxidative degradation of polylactide (PLA) and its effects on physical and mechanical properties, Eur. Polym. J. 50 (2014) 109–116.
[287] A. Copinet, C. Bertrand, S. Govindin, V. Coma, Y. Couturier, Effects of ultraviolet light (315 nm), temperature and relative humidity on the degradation of polylactic acid plastic films, Chemosphere. 55 (2004) 763–773.
[288] H. Tsuji, Y. Echizen, Y. Nishimura, Photodegradation of biodegradable polyesters: A comprehensive study on poly (l-lactide) and poly (ε-caprolactone), Polym. Degrad. Stab. 91 (2006) 1128–1137.
[289] L. Zaidi, M. Kaci, S. Bruzaud, A. Bourmaud, Y. Grohens, Effect of natural weather on the structure and properties of polylactide/Cloisite 30B nanocomposites, Polym. Degrad. Stab. 95 (2010) 1751–1758.
[290] J.D. Badia, E. Strömberg, A. Ribes-Greus, S. Karlsson, Assessing the MALDI-TOF MS sample preparation procedure to analyze the influence of thermo-oxidative ageing and thermo-mechanical degradation on poly (Lactide), Eur. Polym. J. 47 (2011) 1416–1428.
[291] Q. Zhou, M. Xanthos, Nanosize and microsize clay effects on the kinetics of the thermal degradation of polylactides, Polym. Degrad. Stab. 94 (2009) 327–338.
[292] M. Sepe, The Problem of Confounded Mechanisms in Accelerated Testing Protocols, (2015). http://knowledge.ulprospector.com/3262/pe-the-problem-of-confounded-mechanisms-in-accelerated-testing-protocols-presented-by-michael-sepe/.
[293] K.T. Gillen, M. Celina, R.L. Clough, J. Wise, Extrapolation of accelerated aging data: Arrhenius or erroneous?, Trends Polym. Sci. 5 (1997) 250–257.
[294] M.C. Gupta, V.G. Deshmukh, Thermal oxidative degradation of poly-lactic acid, Colloid Polym. Sci. 260 (1982) 514–517.
[295] I.C. McNeill, H.A. Leiper, Degradation studies of some polyesters and polycarbonates—1. Polylactide: General features of the degradation under programmed heating conditions, Polym. Degrad. Stab. 11 (1985) 267–285. doi:10.1016/0141-3910(85)90050-3.
[296] I.C. McNeill, H.A. Leiper, Degradation studies of some polyesters and polycarbonates—2. Polylactide: Degradation under isothermal conditions, thermal degradation mechanism and photolysis of the polymer, Polym. Degrad. Stab. 11 (1985) 309–326. doi:10.1016/0141-3910(85)90035-7.
[297] A. Babanalbandi, D.J.T. Hill, D.S. Hunter, L. Kettle, Thermal stability of poly(lactic acid) before and after γ-radiolysis, Polym. Int. 48 (1999) 980–984. doi:10.1002/(SICI)1097-0126(199910)48:10<980::AID-PI257>3.0.CO;2-B.
[298] X. Liu, Y. Zou, W. Li, G. Cao, W. Chen, Kinetics of thermo-oxidative and thermal degradation of poly(d,l-lactide) (PDLLA) at processing temperature, Polym. Degrad. Stab. 91 (2006) 3259–3265. doi:10.1016/j.polymdegradstab.2006.07.004.
[299] R. Bernstein, D.K. Derzon, K.T. Gillen, Nylon 6.6 accelerated aging studies: thermal–oxidative degradation and its interaction with hydrolysis, Polym. Degrad. Stab. 88 (2005) 480–488.
[300] E.M. Hoàng, D. Lowe, Lifetime prediction of a blue PE100 water pipe, Polym. Degrad. Stab. 93 (2008) 1496–1503.
[301] ISO 2578:1993 - Plastics -- Determination of time-temperature limits after prolonged exposure to heat, ISO. (n.d.). http://www.iso.org/iso/home/store/catalogue_ics/catalogue_detail_ics.htm?csnumber=7547 (accessed June 13, 2016).
[302] S. Kahlen, G.M. Wallner, R.W. Lang, Aging behavior and lifetime modeling for polycarbonate, Sol. Energy. 84 (2010) 755–762.

Euskal Herriko Unibertsitatea **Leartiker S. Coop.**